

# Proceedings



18<sup>th</sup> European Conference On Non-Linear Optical Spectroscopy, the annual meeting devoted to diverse topics in the field of nonlinear optical spectroscopy, including coherent Raman scattering, novel laser sources, microscopy, imaging, combustion, ultrafast and vibrational spectroscopy.

The conference main topics of this edition will be highlighted by recognized scientific speakers who agreed to deliver to ECONOS attendants pedagogic lectures.



In the tradition of recent years, a special issue 'ECONOS/ECW' of the Journal of Raman spectroscopy for the Proceedings of the conference is planned. Author information regarding the preparation of manuscripts can be found on JRS webpage



## COMMITTEES

### Steering committee :

- Brigitte Attal-Tretout (Chair) – ONERA (Palaiseau, France)
- Per-Erik Bengtsson – Lund University (Sweden)
- Dionisio Bermejo – Instituto de Estructura de la Materia (Madrid, Spain)
- Pierre Joubert – Institut Utinam (Besançon, France)
- Johannes Kiefer – University of Bremen (Germany)
- Alexander Kouzov – Saint Petersburg State University (Russia)
- Dmitry Kozlov – Russian Academy of Sciences (Moscow, Russia)
- Bruno Lavorel – Institut Carnot de Bourgogne (Dijon, France)
- Michele Marrocco – ENEA (Roma, Italia)
- Arnulf Materny – University of Bremen (Germany)
- Julian Moger – University of Exeter (England)
- Herman Offerhaus – University of Twente (Enschede, Netherlands)
- Dario Polli – Politecnico di Milano (Italy)
- Peter Radi – University of Berne (Swiss)
- Monika Ritsch-Marte – Medical Faculty of the University of Innsbruck (Austria)
- Maarten Roeffaers – University of Leuven (Belgium)
- Michael Schmitt – Friedrich-Schiller University (Jena, Germany)
- Thomas Seeger – University of Siegen (Germany)
- Aleksei Zheltikov – Moscow State University (Russia)

### 2019 Organising committee

**Co-Chairs** : Prof. Frédéric GRISCH & Dr Benoît BARVIAU, CORIA-UMR 6614 (Rouen, France),  
Brigitte ATTAL-TRETOUT, ONERA (Palaiseau, France)

**Organiser** : Christophe LETAILLEUR, CORIA-UMR 6614 (Rouen, France).

**Secretary** : Florence FRADET, CORIA-UMR 6614 (Rouen, France).

**Staff** : Cédric CHAMBRELAN (IT manager), Saïd IDLAHCEN, Sylvain LEGROS, Bruno MILLE,  
Pradip XAVIER, CORIA-UMR 6614 (Rouen, France).



## **ECONOS History, 37 years of history**

Former 17 editions of the ECONOS Meetings:

- ECONOS 2018, Milan, Italy, April 8-11
- ECONOS 2017, Jena, Germany, April 2-5
- ECONOS 2016, Göteborg, Sweden, April 24-27
- ECONOS 2015, Leuven, Belgium, April 12-15
- ECONOS 2014, Dole, France, May 11-14
- ECONOS 2013, Exeter, UK, April 22-24
- ECONOS 2012, Aberdeen, UK, July 8-11
- ECONOS 2011, Enschede, Netherlands, May 23-25
- ECONOS 2010, Bremen, Germany, Jun 21-23
- ECONOS 2009, Frascati, Italy, May 25-27
- ECONOS 2008, Igls, Austria, May 25-27
- ECONOS 2007, St. Petersburg, Russia, May 12-15
- ECONOS 2006, Smolenice, Slovak Republik, April 9-11
- ECONOS 2005, Oxford, United Kingdom, April 10-12
- ECONOS 2004, Erlangen, Germany, April 4-6
- ECONOS 2003, Besançon, France, March 30,31 and April 1
- ECONOS 2002, Villigen, Switzerland, March 18-19

That is not all the story, indeed, the conference is named ECONOS since 2002, and was previously called European CARS workshop, starting in 1982 !

2001, Lund, Sweden - 2000, Moscow, Russia - 1999, Frascati, Italy - 1998, Besançon, France - 1997, Heidelberg, Germany - 1996, Sheffield, United Kingdom - 1995, Madrid, Spain - 1994, Gif sur Yvette, France - 1993, Villigen, Swiss - 1992, Florence, Italy - 1991, Garching, Germany - 1990, Dijon, France - 1989, Oxford, United Kingdom - 1988, Pisa, Italy - 1987, Stuttgart, Germany - 1986, Lund, Sweden - 1985, Rouen, France - 1984, Harwell, United Kingdom - 1983, Chatillon, France - 1982, Harwell, United Kingdom



## Institutional partners



Fonds Européen  
de Développement  
Régional



**NORMANDY  
Region**



**National Institute of Applied  
Sciences, Normandy, Rouen.**



**National Centre  
for Scientific  
Research**



energy materials &  
clean combustion center



**Sciences & Techniques Faculty**



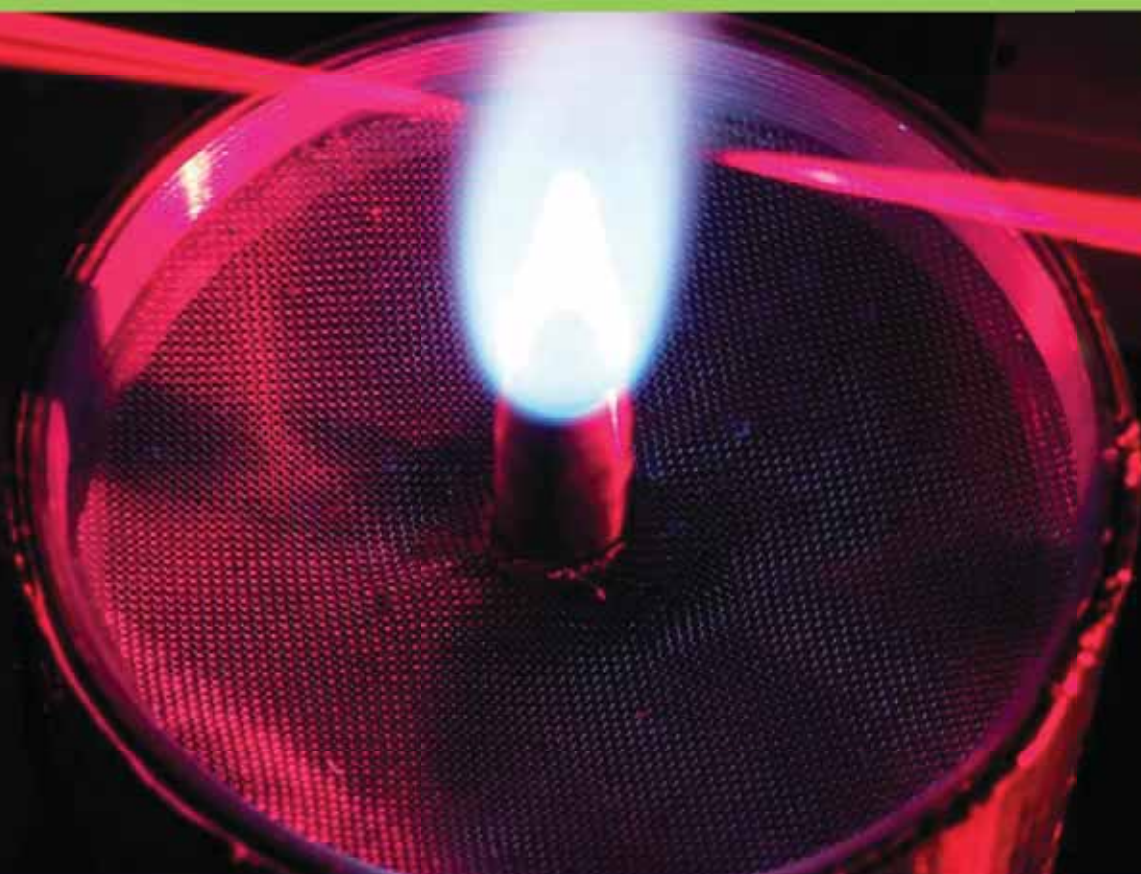
Industrial partners





**ECONOS**

2019, April 7-10  
CORIA, Rouen, France



# Program

**coRia**  
UMR 6614



## Sunday April 7th, 2019.

16:00 Welcome in the tourist office of Rouen

16:40 Opening of ECONOS 2019 by **B. Barviau & F. Grisch**

17:00 **Keynote**  
**Eric Potma**, University of California Irvine  
*Nonlinear optical microscopy in the mid-infrared*

18:00 Cocktail dinner

19:00 Cathedral carillons concert by Mr Latour

## Monday April 8th, 2019.

8:00 Registration

8:30 Speeches by institutional representatives

9:00 **Invited speaker**  
**Joakim Bood**, Lund University  
*Backward lasing for range-resolved detection of atomic species*

9:40 **Ali Hosseinnia**, Lund University  
*Single-shot Raman linewidth measurements using time-resolved hybrid femtosecond/nanosecond rotational CARS*

10:00 **Michael Scherman**, ONERA Palaiseau  
*Amplified laser architecture for ultrafast ro-vibrational fs/ps-CARS thermometry in flames*

10:20 COFFEE BREAK & POSTER SESSION



11:00 **Michele Marrocco**, ENEA Rome  
*Chirp effects in CARS signals generated by femtosecond laser pulses under strong chirp regime of the probe*

11:20 **Sylvain Legros**, CORIA Rouen  
*Single-Shot 1 kHz CPP fs CARS: Temperature Measurements From Atmospheric to High-Pressure Environments*

11:40 **Yang Ran**, Friedrich-Schiller-Universität Jena  
*Collision-free two-beam ultrabroadband coherent anti-stokes Raman scattering spectroscopy for high pressure thermometry*

12:00 **Alexis Bohlin**, Delft University of Technology  
*Single-shot CARS imaging of near-wall turbulent reacting flows*

12:20 LUNCH

13:50 **Invited speaker**  
**Emmanuel Beurepaire**, LOB Palaiseau  
*Multicolor multiphoton microscopy of developing and nervous tissues*

14:30 **Sandro Heuke**, Institut Fresnel, Marseille  
*Coherent anti-Stokes Raman Fourier Ptychography Microscopy*

14:50 **Tiago Buckup**, Universität Heidelberg  
*Time-Resolved Coherent Raman Spectroscopy of Wild Type and Mutated Anabaena Sensory Rhodopsin*

15:10 COFFEE BREAK & POSTER SESSION

15:50 **Invited speaker**  
**Ahmed Abdelmonem**, Karlsruhe Institute of Technology  
*Molecular level characterization of atmospheric aerosol – water – ice interactions using nonlinear optical spectroscopy, mainly SHG and SFG*

16:30 **Maximilian Brinkmann**, University of Muenster  
*Live Multi-Color Coherent Raman Imaging Enabled by a Compact and Robust Light Source*

16:50 **Alejandro De la Cadena**, Politecnico di Milano  
*Broadband Stimulated Raman Scattering Microscopy with In-Line Balanced-Detection*

17:10 **Dario Polli**, Politecnico di Milano  
*Retrieving the complex vibrational susceptibility with interferometric stimulated Raman scattering (iSRS)*

18:30 **Historial Jeanne d'Arc**  
Cocktail dinner and enjoy a place steeped in history

## Tuesday April 9th, 2019.

8:30 **Invited speaker**

**Waruna Kulatilaka**, Texas A&M University

*Ultrashort-Pulse Multi-Photon Multi-Species Imaging Techniques for Combustion Diagnostics*

9:10 **Pengji Ding**, Lund University

*Femtosecond Two-Photon Absorption Laser-Induced Fluorescence Imaging of Atomic Hydrogen and Oxygen in a Plasma-Assisted Methane/Air Flame*

9:30 **Konstantin A. Vereshchagin**, Federal State Institution of Science A.M. Prokhorov General Physics Institute

*Generation of Parametric Superfluorescence by Picosecond Pulses under Low Frequency Pump in KTP Crystal*

9:50 COFFEE BREAK & POSTER SESSION

10:30 **Ali Hosseinnia**, Lund University

*Pure rotational coherent anti-Stokes Raman spectroscopy of ethylene-nitrogen mixtures, Experiments and modelling*

10:50 **Thomas Würthwein**, University of Münster

*Suppression of Stimulated Raman Scattering via Photon Depletion in a Two-Color Three-Beam Setup*

11:10 **Malik Nafa**, CNR/INO & LENS

*THz-QCL sources for precision spectroscopy*

11:30 **David Sedarsky**, Chalmers University of Technology

*Time-gated back-scatter imaging in turbid media*

11:50 LUNCH



13:20 **Invited speaker**

**Elena Obratsova**, Institute of Russian academy of Sciences, Moscow  
*Modified single-wall carbon nanotubes and graphene for saturable absorbers in solid state lasers*

14:00 **Angela Vella**, GPM Rouen

*Study of strain sensitivity and symmetry of color center in diamond nanoscale needles by contactless optical piezo-spectroscopy*

14:20 **Michele Marrocco**, ENEA Rome

*Classical Representation of Non-Linear Response Functions and their Connections to Quantum-Mechanical Graphic Representations Based on Double-Sided Feynman Diagrams and Liouville Space Coupling Scheme*

14:40 **Industrial session**

ACAL BFI, AMPLITUDE, A.P.E., COHERENT, FEMTO EASY, HORIBA, MKS NEWPORT, NOVAE, OPTON LASER, TELEDYNE PRINCETON, THORLABS.

15:40 COFFEE BREAK & POSTER SESSION

16:00 **Peter Radi**, Paul Scherrer Institute

*Experimental Determination of the Potential Energy Function of the Copper Dimer Ground State*

16:20 **Haisu Zhang**, Université de Bourgogne Franche Comté

*Rotational echoes: a versatile tool for investigating ultrafast dissipation*

16:40 **Iryna Gozhyk**, UMR 125 CNRS / Saint-Gobain

*Correction of plasma emission in reflectivity spectroscopy during sputtering deposition*

17:30 *Rouen pedestrian guided tour*

19:00 *Conference dinner in "La halle aux toiles" of Rouen*



## Wednesday April 10th, 2019.

9:00 **Invited speaker**

**Caterina Merla**, ENEA Roma

*Wide field CARS microspectroscopy and real-time follow-up of hydration changes induced by electropulsation of liposomes*

9:40 **Luis Mir**, CNRS Villejuif

*Confocal Raman Microspectroscopy to Investigate the Consequences of the Delivery of Electric Pulses to Live Cells*

10:00 **Vikas KUMAR**, University of Duisburg Essen

*Time –and polarization-resolved CARS spectroscopy of  $\alpha$ -DNBP (2-(2,4-dinitrobenzyl)pyridine) in the electronic ground state*

10:20 COFFEE BREAK

11:00 **Pierre Gilliot**, PCMS Strasbourg

Structured illumination experiments with vortex beams

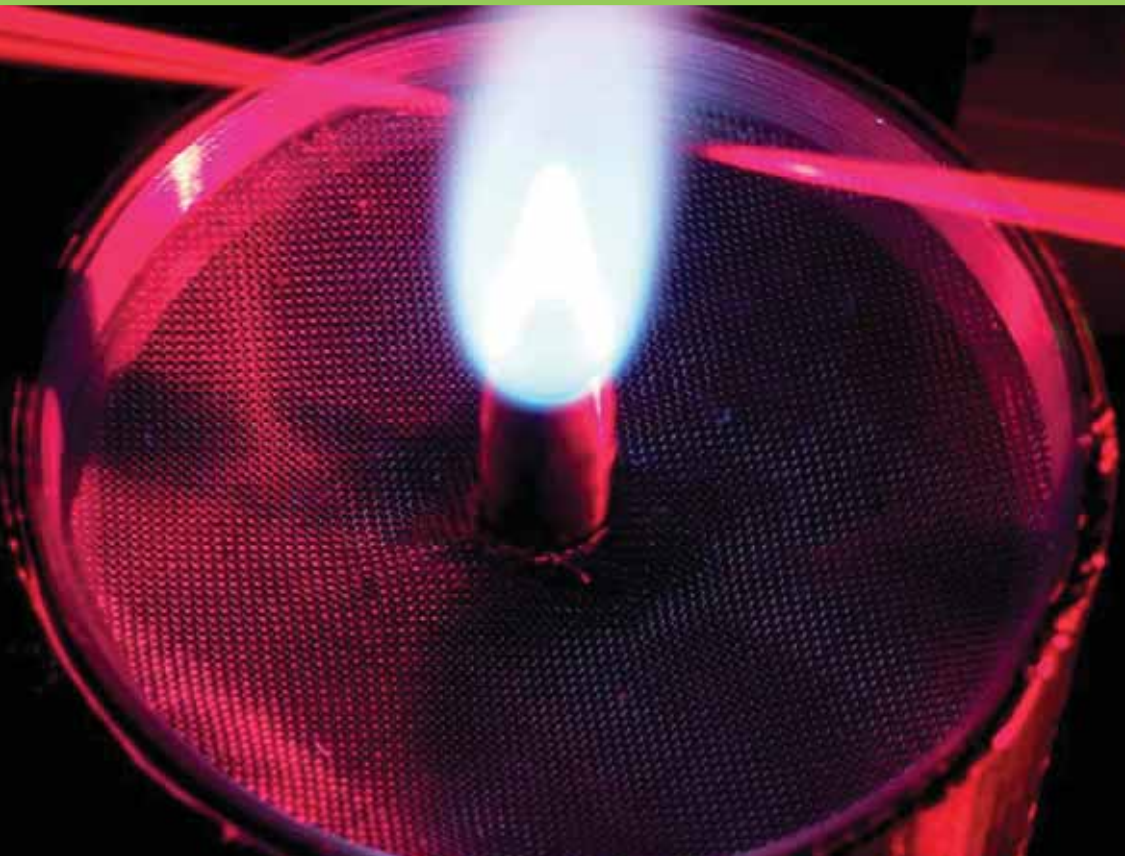
11:20 **Thomas Godin**, CORIA Rouen

*Photonic time-stretch: applications to ultrafast spectroscopy and real-time imaging*

11:40 Closing & intro. to ECONOS2020

12:00 LUNCH

14:00 **CORIA Lab tour**, Saint Etienne du Rouvray, Subscription needed



## Social events



## Social Events

Sunday, april 7<sup>th</sup> from 4 pm - Welcome reception in the tourist office (in front of the cathedral)



Settled in this Renaissance mansion, from February to mid-April 1892 and 1893 it was here that Claude Monet painted his famous series of thirty paintings of the western facade of Notre Dame Cathedral. Claude Monet's studio, a prestigious room at the heart of Rouen...



7pm : Carillon concert of the cathedral



**Monday, april 8<sup>th</sup> ,6:30 pm**

**Cocktail in the “Jeanne d’Arc historial”**



**Tuesday, april 9<sup>th</sup>**

**5:30 pm : Rouen guided tour**



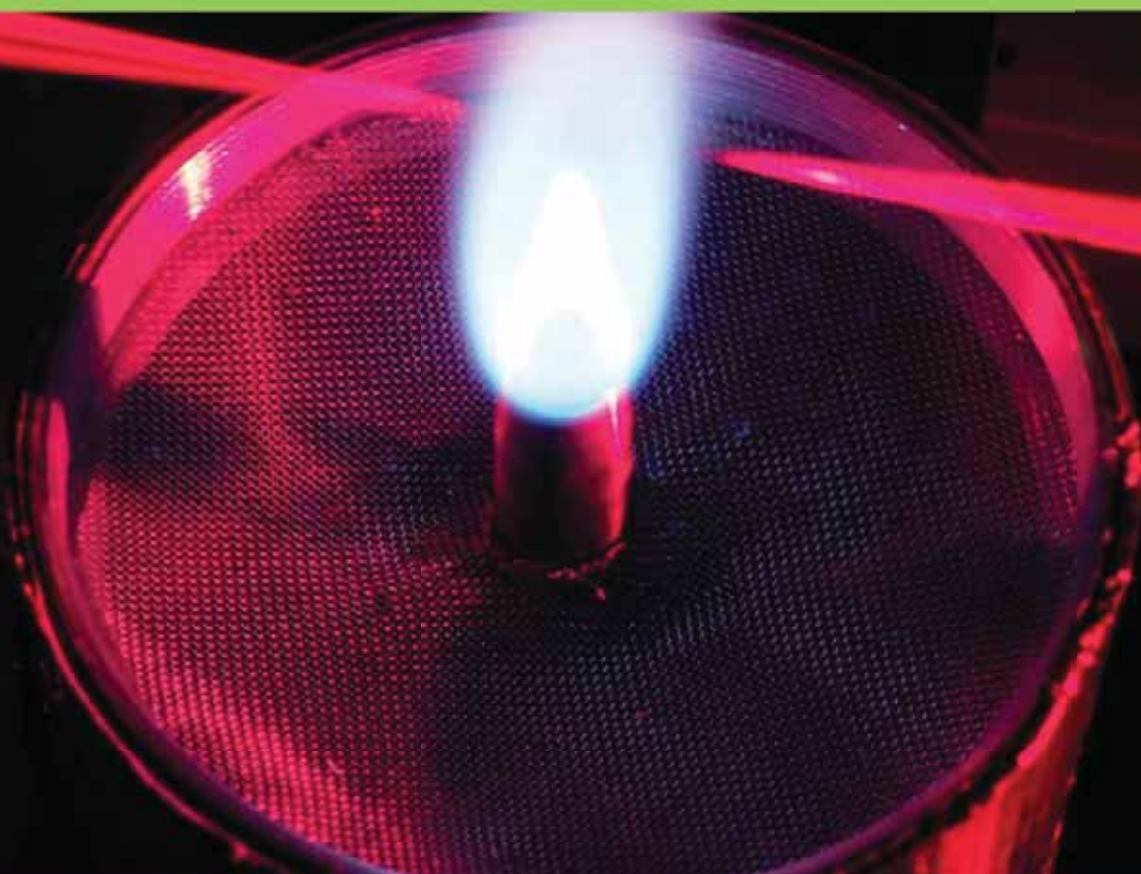
**7:00 pm : ECONOS Dinner in the “Halle aux toiles” of Rouen.**





**ECONOS**

2019, April 7-10  
CORIA, Rouen, France



# Contributions

**coRia**  
UMR 6614





## Invited Speaker - Sunday Keynote



**Prof. Eric Potma**

**University of California Irvine**

### Nonlinear optical microscopy in the mid-infrared

Born and raised in the Netherlands, Eric Potma got his Masters at the University of Groningen in 1996. He stayed five more years for his graduate research, which he completed in 2001. While working in the ultrafast spectroscopy group of Prof. Douwe Wiersma, Eric focused his research on the development of laser sources for microscopy and the application of nonlinear methods to optical imaging. In 2001, Potma joined the group of Prof. Sunney Xie at Harvard University as a postdoctoral fellow. During this time, he was been involved with projects on synchronizing mode-locked lasers, visualizing lipid bilayers with CARS microscopy and vibrational imaging of tissue *in vivo* at video rate. In 2005, Eric joined the Department of Chemistry at the University of California in Irvine, where he currently is a Professor of Chemistry. His group focuses on the characterization of nano-structured materials and biological tissues with the aid of new optical imaging techniques.

# Nonlinear optical microscopy in the mid-infrared

Eric O. Potma

*Department of Chemistry and Beckman Laser Institute, University of California, Irvine, CA 92697, USA*

Microscopy with vibrational spectroscopic contrast is one of the most successful forms of chemical mapping. The strongest light-matter interaction that facilitates the probing of molecular vibrations is the absorption of an IR-photon by the molecule, which leads to the resonant excitation of a given vibrational mode. This principle is used in IR-based spectroscopy, a popular technique for detecting and analyzing molecular samples, especially in the form of Fourier transform IR (FTIR) spectroscopy.[1] When incorporated in a microscope, the IR spectroscopy technique can be used to produce images with genuine spectroscopic contrast, allowing label free imaging of a wide range of samples.[2]

Despite the proven utility of FTIR microspectroscopy, the technique exhibits several disadvantages. First, the detector technology in the IR is more expensive and less efficient than detection strategies in the visible range of the spectrum. Although the focal plane array (FPA) has made FTIR microspectroscopy possible and practical, the detection efficiencies are significantly worse compared to inexpensive visible photodetectors. Second, since the spatial resolution is dictated by the IR-diffraction limit, the achievable resolution is about an order of magnitude less than what is common for microscopes that operate in the visible. This lower resolution implies that IR-based microscopy overlooks smaller details and precludes its application to samples with important sub-micrometer features.

The imaging properties of IR-based microscopy can be improved if information about the IR molecular transition is converted into a visible signal. This can be accomplished through nonlinear upconversion. Several strategies have been used to upconvert the IR signal through a sum-frequency generation (SFG) process in a nonlinear crystal. Here we seek an alternative to upconverting the IR light outside of the sample. Instead, we aim to accomplish the upconversion step directly in sample, using the nonlinear optical properties of the target molecules. Using collinear excitation schemes, we have been able to use the SFG process for probing biological structures with noncentrosymmetry based on chemical selective IR-transitions. This allows for rapid laser-scanning SFG microscopy of collagen fibers, cellulose granules and microcrystals of chiral biomolecular compounds. We have recently expanded the SFG modality, which probes the second-order optical properties of the sample, with a third-order sum-frequency generation (TSFG) modality. This new technique probes the third-order optical properties of the specimen and its contrast is thus not limited to noncentrosymmetric structures. Like coherent anti-Stokes Raman scattering (CARS) microscopy, TSFG microscopy generates images with vibrational spectroscopic contrast without symmetry restrictions. Compared to CARS, which is sensitive to Raman-active modes, TSFG probes molecules based on IR-active modes.

Both SFG and TSFG microscopy feature a high spatial resolution. Because the resolution is largely dictated by the upconversion step that occurs with visible/NIR light, the resolution at which the IR contrast is probed is on the order of 0.5 microns. This is about an order of magnitude better than what can be achieved with FTIR microscopy. In addition, the detection step is greatly simplified because standard photomultiplier tubes can be used instead of dedicated IR detectors. Moreover, the SFG and TSFG modalities can be integrated on a conventional laser-scanning multiphoton microscope, greatly facilitating its routine use. We expect that these advances introduce IR-based imaging to a larger set of applications.

In this contribution, we will provide an overview of the nonlinear approach to IR-based imaging, discuss the features of the SFG/TSFG microscope, and highlight various biological imaging applications.

## Example References

[1] Smith, B. C., *Fundamentals of Fourier Transform Infrared Spectroscopy*. CRC Press: Boca Raton, FL, 2011.

[2] Wetzel, D. L.; LeVine, S. M., Imaging Molecular Chemistry with Infrared Microscopy. *Science* **1999**, 285 (5431), 1224..



## Invited speaker



**Prof. Joakim Bood**

***Div . of Combustion Physics, Lund University (Lund, Sweden)***

**Backward lasing for range-resolved detection of atoms in flames**

Prof. Bood received his MSc and PhD degrees in Physics from Lund University, Sweden. His PhD project concerned development and application of Coherent anti-Stokes Raman spectroscopy (CARS) for thermometry and species concentration measurements. He was then a postdoctoral fellow at Sandia National Laboratories, California, USA, working on development of cavity-enhanced frequency-modulation spectroscopy (NICE-OHMS) for ultrasensitive detection. Prof. Bood is currently full professor at Lund University, where he is running a research program focused on short-pulse (ps/fs) spectroscopy, applied molecular spectroscopy, and laser/optical remote sensing. He has coauthored more than 80 scientific articles, including a number of review papers and book chapters. Since 2015, Prof. Bood is Deputy Director of the Lund Laser Centre.

## Backward lasing for range-resolved detection of atomic species

Pengji Ding, Maria Ruchkina, Marcus Aldén, and Joakim Bood

*Div. of Combustion Physics, Lund University, Lund, Sweden  
joakim.bood@forbrf.lth.se*

There is a strong need for sensitive methods able to measure at remote locations, i.e. remote sensing techniques. Such techniques are important not only in research, for example in atmospheric science, plasma and combustion chemistry, but also in many industrial applications as well as for fire safety and national security. The present talk concerns development of optical remote sensing concepts based on backward lasing, i.e. a mirror-less remote laser with a constituent of the ambient gas as the active medium. Lasing is accomplished in both the forward and backward direction through deep-UV multi-photon pumping of atoms using femtosecond (fs) laser pulses, as shown in Fig. 1. The focus of the talk is on spatially-resolved detection of atomic hydrogen in flames, yielding 656-nm lasing in the backward direction upon 2-photon pumping with 205-nm fs laser pulses. Spatial resolution is achieved by temporally-resolved detection of the backward lasing using a streak camera. The method is demonstrated in  $\text{CH}_4/\text{O}_2$  flames; both in a setup consisting of two flames, with variable spacing between the flames, and in a single flame. Although, the results demonstrate that the backward lasing technique is capable of detecting occurrences of hydrogen atoms in flames, further investigations are needed in order to extract quantitative concentrations. As a first step towards a deeper understanding of the signal generation mechanism, the gain of the hydrogen lasing has been studied.

It is evident that backward lasing could potentially revolutionize the remote-sensing field, as it might allow for a dramatic improvement of the detection sensitivity compared to traditional light detection and ranging (LIDAR), which is based on the detection of the nearly isotropic scattering induced by a forward-propagating laser beam. In addition, the high directionality of the backward lasing signal also opens up for measurements inside devices providing only one optical port. Besides detection of atoms and molecules in flames, the method also has potential for remote detection of atmospheric pollutants, gas leakage from pipelines, and the presence of explosives and hazardous materials.

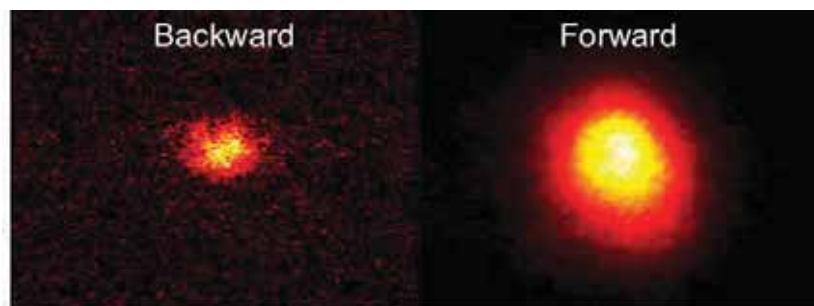


**Fig. 1** Backward and forward lasing at 656 nm from hydrogen atoms in a flame induced by femtosecond 2-photon pumping at 205 nm.

# Amplified laser architecture for ultrafast ro-vibrational fs/ps-CARS thermometry in flames

Michael Scherman<sup>1</sup>, Rosa Santagata<sup>1</sup>, Alexandre Bresson and Brigitte Tretout<sup>1</sup>

<sup>1</sup> ONERA, Chemin de la Lumière, BP80100, 91123 Palaiseau Cedex, France

Hybrid fs/ps-CARS spectroscopy has proven to be a standard for thermometry in reactive media such as combustion [1,2]. Ro-vibrational resolved spectra are of great interest for the fine characterization of molecular gases and complex environment such as non-equilibrium media [1]. However, in conventional single laser hybrid fs/ps-CARS setup, the spectral resolution is obtained at the expense of laser energy since a filtering stage is used to generate the picosecond probe [2,3].

To go beyond this limitation, new laser architecture is proposed and implemented. In this setup, the 3 hybrid fs/ps-CARS laser beams, pump, Stokes and probe, are produced out of a single compact femtosecond laser with moderate output pulse energy (1 mJ). On the probe path, a custom Yb:YAG crystalline fiber [4] amplifier (Fibercryst) is used in combination with an ultra-narrow filtering stage (volume Bragg grating [3]). Starting from a 100 cm<sup>-1</sup> wideband, 150 fs laser pulse at 1030 nm with 100 μJ energy, this design allows generating a 0.37 cm<sup>-1</sup> narrowband, 60 ps probe pulse with 100 μJ energy at 515 nm.

This arrangement is used to acquire single shot CARS spectra in flames with good enough signal to noise ratio to perform 1 kHz temperature measurements. The setup was tested on ambient air (Fig. 1 (a)), a premixed stoichiometric CH<sub>4</sub>/air flame (Fig. 1 (b)) and a C<sub>2</sub>H<sub>2</sub>/O<sub>2</sub> torch (Fig. 1 (c)). Experimental spectra were compared to simulations in order to estimate the temperature. Mean temperatures of 295 K, 2150 K and 3126 K were measured in these media with respective standard deviations of 9 K (1 %), 22 k (1 %) and 105 K (3.3%). State of the art precision in the range 300-3000 K is obtained. The influence of probe delay and polarization is also investigated to provide efficient nonresonant background rejection. We believe this new optical design to be of great interest for application of high speed CARS spectroscopy in media where high spectral resolution is required such as non-equilibrium environment or complex molecular mixtures.

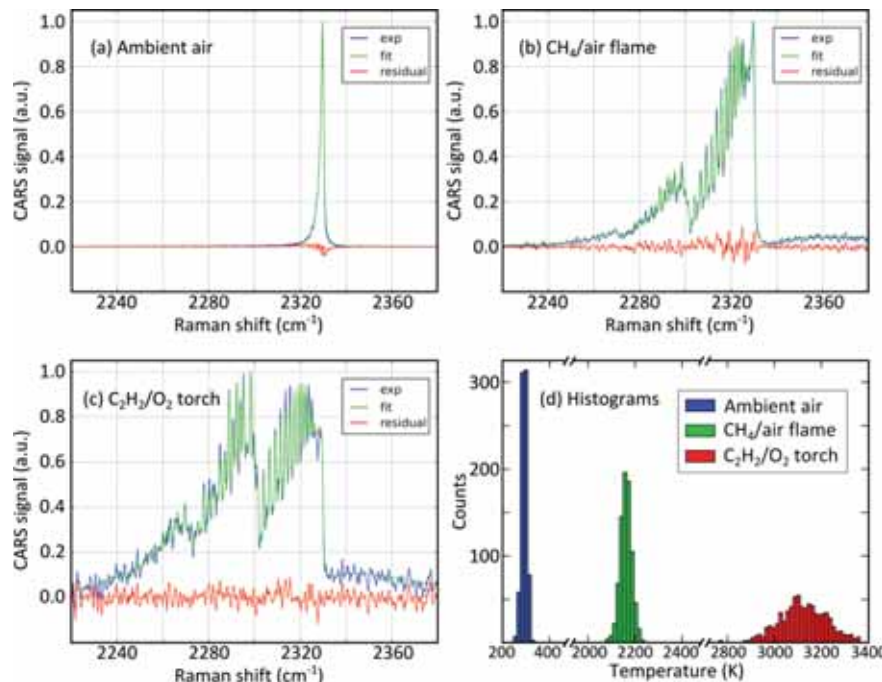


**Fig. 1** Typical single shot experimental spectra (blue line), best fit (green line) and residual (black line) obtained (a) in ambient air, (b) in a premixed stoichiometric CH<sub>4</sub>/air flame, and (c) in a turbulent C<sub>2</sub>H<sub>2</sub>/O<sub>2</sub> torch (3 points rolling average). (d) Histograms of temperature measured on 1000 successive laser shots at 1 kHz.

## References

- [1] A. K. Patnaik, I. Adamovich, J. R. Gord, and S. Roy, "Recent advances in ultrafast-laser-based spectroscopy and imaging for reacting plasmas and flames," *Plasma Sources Science and Technology* **26**, 103001 (2017).
- [2] H.U. Stauffer, S. Roy and J.R. Gord D.R. Richardson, "Comparison of chirped-probe-pulse and hybrid femtosecond/picosecond coherent anti-Stokes Raman scattering for combustion thermometry," *Applied Optics* **56**, 37649 (2017).
- [3] M. Scherman, M. Nafa, T. Schmid, A. Godard, A. Bresson, B. Attal-Tretout, and P. Joubert, "Rovibrational hybrid fs/ps CARS using a volume Bragg grating for N<sub>2</sub> thermometry," *Opt. Lett.* **41**, 488 (2016).
- [4] I. Martial, F. Balembois, J. Didierjean, and P. Georges, "Nd:YAG single-crystal fiber as high peak power amplifier of pulses below one nanosecond", *Opt. Express* **19**, 11667 (2011)

# Chirp Effects in CARS Signals Generated by Femtosecond Laser Pulses Under Strong Chirp Regime of the Probe

Michele Marrocco

ENEA, CR-Casaccia, via Anguillarese 301, IT-00123 Rome, Italy

Chirp in ultrafast optics defines the variation of the instantaneous frequency of the traveling electric field as a function of time. Understandably, such a dependence is fundamental to the description of phase effects taking place during the interaction between femtosecond (fs) laser pulses and matter. Here, such phase effects are considered in the spectral domain resulting from the mixing of three laser pulses necessary to generate fs coherent anti-Stokes Raman scattering (fs-CARS) for thermometric purposes. In this context, the typical experimental configuration involves simultaneous and slightly chirped pump and Stokes pulses for Raman preparation while probing occurs at later times by means of a strongly chirped pulse [1-3].

At the theoretical level, the problem was solved numerically a few years ago [1], but recent research shows that numerical methods provide inaccurate and unstable fit values for the optical parameters associated with best fits of the experimental spectra [2]. As a direct consequence, much care is needed to improve the statistical reliability of the numerical approach [3].

Unlike these attempts, the current work discusses an effort to tackle the same problem with analytical tools. The research is a follow-up of the analytical CARS model developed for linearly chirped CARS [4]. The extension to the case of non-linear or strong chirp is made under some reasonable assumptions about the spectral phase (regularity, perturbative cubic term). The assumptions reduce the complications arising in the theoretical handling of the CARS signal and the whole problem becomes treatable as long as the assumptions are used for suitable approximations about the phase dependences. It is found that stability in the fit parameters can be improved without giving up thermometric reliability. Comparisons with the numerical approach are examined and two examples are shown in Fig. 1.

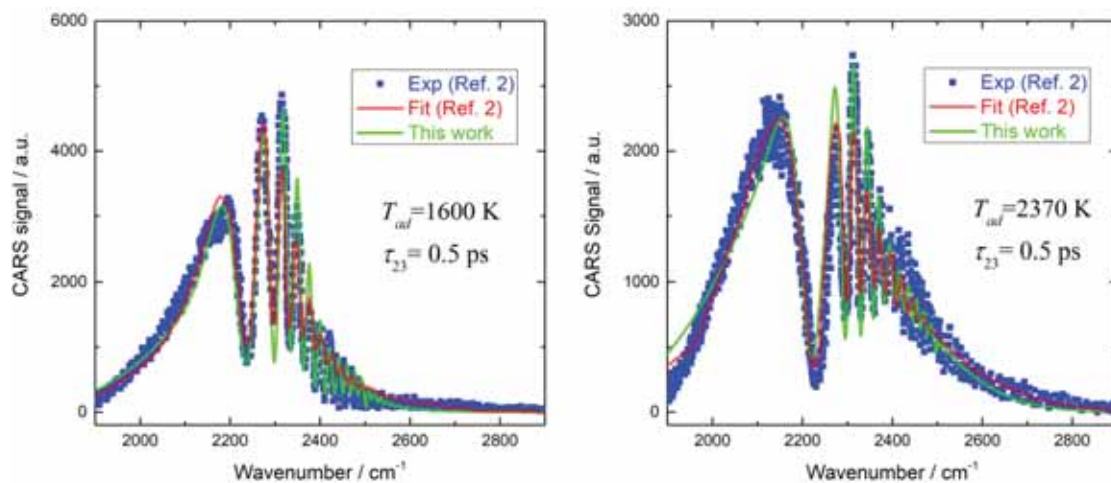


**Fig. 1** Comparison between the simulations of this work (green curves) with the numerical best fits (red curves) and single-laser-shot experimental spectra (blue symbols) of Richardson et al. [2]. The best fits and experimental spectra have been digitally extracted from Fig. 5 of Ref. [2] to ease the visual contrast between this work and the numerical fits. The plots refer to the reported adiabatic temperatures when the common probe delay is 0.5 ps. The numerical best fits are obtained in Ref. [2] for unphysical values of the optical parameters whereas the spectra of this work are obtained for realistic values of the relevant parameters.

## References

- [1] D. R. Richardson, R. P. Lucht, W. D. Kulatilaka, S. Roy, and J. R. Gord, "Theoretical Modeling of Single-Laser-Shot, Chirped-Probe-Pulse Femtosecond Coherent Anti-Stokes Raman Scattering Thermometry" *Appl. Phys. B* **104**, 699 (2011).
- [2] D. R. Richardson, H. U. Stauffer, S. Roy, and J. R. Gord, "Comparison of Chirped-Probe-Pulse and Hybrid Femtosecond/Picosecond Coherent Anti-Stokes Raman Scattering for Combustion Thermometry," *Appl. Opt.* **56**, E37 (2017).
- [3] L. M. Thomas, A. Satija, and R. P. Lucht, "Technique Developments and Performance Analysis of Chirped-Probe-Pulse Femtosecond Coherent Anti-Stokes Raman Scattering Combustion Thermometry," *Appl. Opt.* **56**, 8797 (2017).
- [4] M. Marrocco, "Simple Model of Coherent Anti-Stokes Raman Scattering Signals Generated by Means of Linearly Chirped Ultrashort Gaussian Laser Pulses," *J. Raman Spectrosc.* **49**, 1109 (2018).

# Single-Shot 1 kHz CPP fs CARS: Temperature Measurements From Atmospheric to High-Pressure Environments

Sylvain Legros<sup>1,2</sup>, Benoît Barvau<sup>2</sup>, Frédéric Grisch<sup>2</sup>

1. SAFRAN TECH, 78117, Châteaufort, France

2. CORIA & INSA de Rouen Normandie, 76801, Saint Etienne du Rouvray, France

Increased air traffic and growing awareness of its climatic impact result in harsh regulation standards (ACARE recommendations) to reduce pollutant emission. A scientific cooperation between the French motorist SAFRAN and the CORIA laboratory was recently established (Industrial Chair PERCEVAL) to address these problematic. The objective of this research is to investigate and improve experimental combustors simultaneously with the numerical modeling of the underlying chemical mechanisms. In particular, validation of the numerical simulations requires accurate experimental data in relevant high-pressure and high-temperature conditions. Among attractive optical diagnostics, Coherent anti-Stokes Raman Scattering (CARS) is developed to measure temperature in reactive flows. A renew interest for CARS has recently arisen with the availability of femtosecond laser sources [1]. High laser pulse energy delivered by the femtosecond laser makes single-shot measurements accessible. Taking interest of a repetition rate up to 10 kHz, thousand times larger than in the nanosecond regime, it also offers investigations of time-temporal physical processes [2].

In the current study, temperature is measured with the Chirped Probe Pulse (CPP)-CARS strategy. This one is applied to the excitation of  $N_2$  rovibrational Raman transitions thanks to a Legend Elite Laser source (Coherent) completed by a TOPAS prime plus (Light Conversion).  $N_2$  CARS excitation is performed with two 100 fs pulses, a 675 nm pump and a 800 nm Stokes pulses. A delayed 675 nm probe pulse temporally stretched in a 30 cm glass rod interrogates the gas temperature state in a folded BOXCARS configuration. Collection and detection are finally carried out with a spectrograph equipped with an EmCCD camera (Roper scientific).

To perform CARS measurements on real combustion chambers, a robust and reproducible measurement method completed by a reliable numerical algorithm has been initially developed to measure temperature. Validation of this experimental approach was performed through the temporal record of temperatures in an atmospheric buoyant  $H_2$ /air diffusion flame with a good accuracy ( $\sim 1\%$ ). To extend such measurements in high-pressure environments, measurements were performed in a high-pressure cell, for various pressures (up to 30 bar) and temperatures (300 – 600 K). Despite the “commonly” accepted idea according that femtosecond CARS spectra show a slight variation with pressure [3], strong variations of the CARS spectra recorded at various pressures were observed (fig.1).

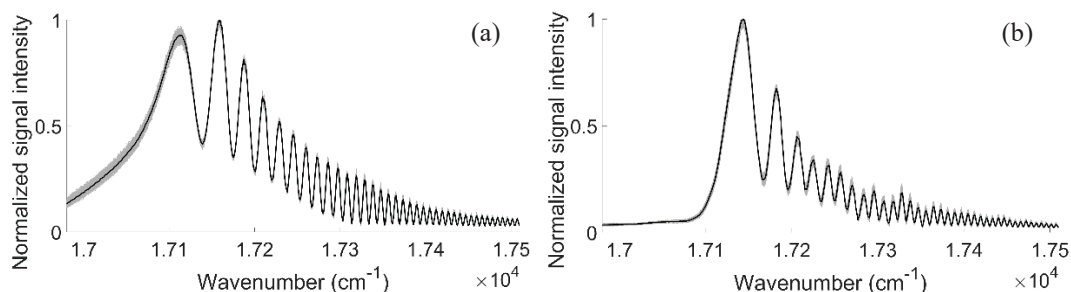


Fig 1: Mean spectrum (black line) superimposed on 1000 instantaneous single-shot spectra recorded at atmospheric pressure (a) and in 25.6 bar of air (b).

This unexpected result may originate from distortions of the time and spectral shapes of the excitation femtosecond pulses (Stokes and pump pulses) because of their focusing in the pressurized gas (Kerr effect, multiphotonic ionization, tunnel ionization). To infer this explanation, record of the spectral shapes of the pulse lasers before and after the passage of the optical cell was performed for various conditions of focus and for different incident energies. Additional experiments were also performed with pressurized argon in the test cell. Processing of data measurements led to the assertion that the use of focused femtosecond pulses with high irradiance could notably modify the femtosecond pulse propagation as well as the CARS signature.

**Acknowledgements:** The authors are grateful for the support of the French motorist SAFRAN, National Research Agency (ANR) and Labex EMC3 (Energy Materials and Clean Combustion Center).

## References

- [1] S. Roy, J.R. Gord, A.K. Patnaik, “Recent advances in coherent anti-Stokes Raman scattering spectroscopy: Fundamental developments and applications in reacting flows”, *Progress in Energy and Combustion Science*, 2010, 36, 280-306.
- [2] C.N. Dennis, A. Satija, R.P. Lucht, “High dynamic range thermometry at 5kHz in hydrogen/air diffusion flame using chirped-probe-pulse femtosecond coherent anti-stokes Raman scattering”, *Journal of Raman Spectroscopy*, 2016, 47, 177-188
- [3] R.P Lucht, P.J Kinnius, S. Roy, J.R Gord, “Theory of femtosecond coherent Anti-Stokes Raman scattering spectroscopy of gas-phase transitions”, *The Journal of Chemical Physics* 127, 044316 (2007).

# Collision-free Two-beam Ultrabroadband Coherent Anti-Stokes Raman Scattering Spectroscopy for High Pressure Thermometry

Yang Ran<sup>1</sup>, Stefan Nolte<sup>1,2</sup>, Andreas Tünnermann<sup>1,2</sup>, Roland Ackermann<sup>1</sup>

1. Institute of Applied Physics, Abbe Center of Photonics, Friedrich-Schiller-Universität Jena, Albert-Einstein-Straße 15, 07745 Jena, Germany

2. Fraunhofer Institute for Applied Optics and Precision Engineering, Albert-Einstein-Straße 7, 07745 Jena, Germany

Gas thermometry under high temperature and high pressure is of great importance for applications in gasification or combustion. Femtosecond coherent anti-Stokes Raman scattering (fs-CARS) has been proved to be an ideal approach for non-invasive temperature measurements [1, 2]. Miller et al. (2011) presented a hybrid fs/ps RCARS with obvious N<sub>2</sub> collisional decay observed from 1 bar to 20 bar by using a ~ 100 fs pump/Stokes pulse and an 8.1 ps probe pulse [3]. Wrzesinski et al. (2013) implemented a three-beam fs-CARS scheme with all beams generated from an 85-fs Ti:Sapphire amplifier, resulting in time-resolved CARS signals independence of system pressure up to 50 bar in the 1-3 ps probe delay range [4]. In the present study, the thermometry is implemented from the recorded CO<sub>2</sub> CARS spectrum avoiding temporal scan [5]. In order to ensure sufficient CARS spectral resolution for accurate temperature measurements and also to get rid of the influence of collision under high pressures, a ~ probe pulse with ~ 1.6 ps duration is chosen. In addition, a ~ 7 fs ultrabroadband pulse (~ 650 nm – 1100 nm) is used as the pump/Stokes pulse to achieve the ultrabroadband excitation for multiple molecules. The modelling for the two-beam ultrabroadband CARS gas temperature determination is described in detail in [6]. We present that our two-beam ultrabroadband CARS system is collision-free from 1.7 bar to 20 bar. The temperature measurements are implemented with high accuracy at temperatures up to 1000 K and pressures up to 20 bar.

The time-resolved N<sub>2</sub> CARS signals are measured in the first place at elevated pressures to check the collision influence on our system. Fig. 1 (a) shows the time-resolved N<sub>2</sub> CARS signals with almost the same decay behaviour at 1.7 bar, 10 bar and 20 bar at 295 K, indicating that the measurements are independent of collisional decay up to 20 bar in the delay range from -1 ps to 12 ps. Accordingly, the temperature measurements based on CO<sub>2</sub> CARS spectra without considering collisions at 1.7 bar, 10 bar and 20 bar are shown in Fig. 1 (b). At 1.7 bar, the temperatures are measured up to 1000 K with accuracy and precision of 2.7 % and 1.4 %. At 10 bar and 20 bar, the temperatures are measured up to 500 K with accuracy of 1.7 % and 0.7 %, respectively, of the set temperature. For temperatures from 295 K to 1000 K and pressures from 1.7 bar to 20 bar, the precision is found to be within 0.3 % to 1.8 % of the averaged measured temperatures.

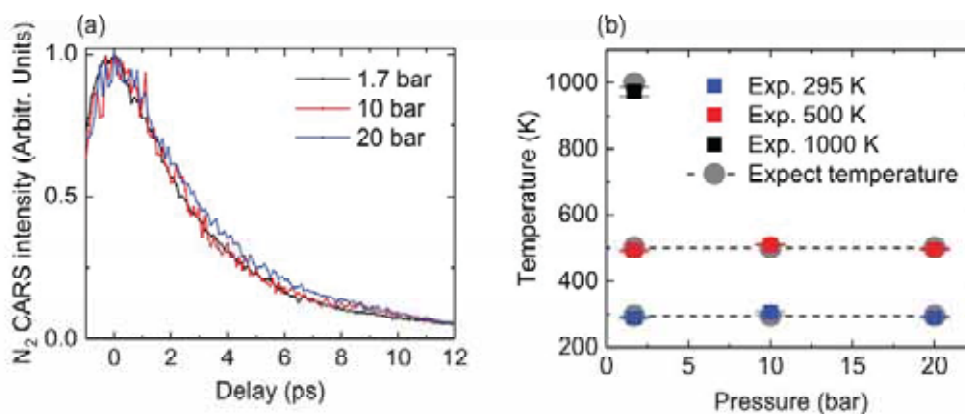


**Fig. 1** (a) Time-resolved N<sub>2</sub> CARS signals over -1 ps to 12 ps range at room temperature and pressures of 1.7 bar, 10 bar and 20 bar in a CO<sub>2</sub>/N<sub>2</sub>/H<sub>2</sub> gas mixture. (b) Temperature measurement results based on the spectra of the two-beam ultrabroadband CARS of CO<sub>2</sub> at 1.7 bar, 10 bar and 20 bar. The data points show the averaged temperatures from 12 CARS spectra in 1-3 ps range with error bars showing the standard deviations.

## References

- [1] R. P. Lucht, S. Roy, T. R. Meyer, and J. R. Gord, "Femtosecond coherent anti-Stokes Raman scattering measurement of gas temperatures from frequency-spread dephasing of the Raman coherence," *Appl. Phys. Lett.* **89**, 251112 (2006).
- [2] S. Roy, J. R. Gord, and A. K. Patnaik, "Recent advances in coherent anti-Stokes Raman scattering spectroscopy: Fundamental developments and applications in reacting flows," *Prog. Energy Combust. Sci.* **36**, 280-306 (2010).
- [3] J. D. Miller, S. Roy, J. R. Gord, and T. R. Meyer, "Communication: Time-domain measurement of high-pressure N<sub>2</sub> and O<sub>2</sub> self-broadened linewidths using hybrid femtosecond/picosecond coherent anti-Stokes Raman scattering," *J. Chem. Phys.* **135**, 201104 (2011).
- [4] P. J. Wrzesinski, H. U. Stauffer, W. D. Kulatilaka, J. R. Gord, and S. Roy, "Time-resolved femtosecond CARS from 10 to 50 Bar: collisional sensitivity," *J. Raman Spectrosc.* **44**, 1344-1348 (2013).
- [5] M. Kerstan, I. Makos, S. Nolte, A. Tünnermann, and R. Ackermann, "Two-beam femtosecond coherent anti-Stokes Raman scattering for thermometry on CO<sub>2</sub>," *Appl. Phys. Lett.* **110**, 021116 (2017).
- [6] G. Matthäus, S. Demmler, M. Lebugle, F. Küster, J. Limpert, A. Tünnermann, S. Nolte, and R. Ackermann, "Ultra-broadband two beam CARS using femtosecond laser pulses," *Vib. Spectrosc.* **85**, 128-133 (2016).



# Single-shot CARS Imaging of Near-Wall Turbulent Reacting Flows

Alexis Bohlin<sup>1</sup>, Karim El Sioufy<sup>1</sup>

Christopher Jainski<sup>2</sup>, Andreas Dreizler<sup>2</sup>

Brian D. Patterson<sup>3</sup>, Christopher J. Klierwer<sup>3</sup>

1. Faculty of Aerospace Engineering, Delft University of Technology, Kluyverweg 1, 2629 HS Delft, The Netherlands

2. Institute of Reactive Flows and Diagnostics (RSM), Technische Universität Darmstadt, 64287 Darmstadt, Germany

3. Combustion Research Facility, Sandia National Laboratories, Livermore, CA 94551, USA

In practical combustion devices featuring high power densities, the interaction between flames and walls may have a significant impact on the thermodynamic efficiency and the formation of pollutants (e.g. unburned hydrocarbons and carbon monoxide). The common understanding is that at the region near the wall  $\sim 1$  mm, where the solid metal surface is generally much cooler than the impinging flames, steep temperature gradients exist which may result in incomplete combustion and local quenching of the flame. This has been investigated experimentally, by CARS monitoring of temperature- and major species profiles from premixed methane/air flames impinging against a cooled steel side-wall, performed at well-characterized quasi-stationary laminar conditions [1].

In these new experiments, we have employed the same generic burner and CARS imaging system [2], but now operating at significantly enhanced turbulence intensities induced by a turbulence generator grid (blockage ratio 45%, turbulence level  $u'/\bar{u} = 6-7\%$ ). The complex interplay between the laser diagnostic and the turbulent reacting flow in the near-wall region has been overcome, for instance, with the balanced detection between CARS signals originating from unreacted- and reacted mixtures imaged on the same detector frame, the removal of the laser beams reflecting from the surface, and the suppression of background flame luminosity within the clear aperture of the coherent imaging system. A quick-fitting routine enabling rapid convergence of two-beam femtosecond/picosecond CARS signal analysis has been developed. Correlated statistics have been produced, for instance, on the instantaneous temperature gradients near the wall (position with magnitude). This temperature data supports the recent findings of velocity measurements [3], and adds to the database on this burner system which can be used as a benchmark to improve the fidelity of numerical simulation on near-wall turbulent reacting flows.

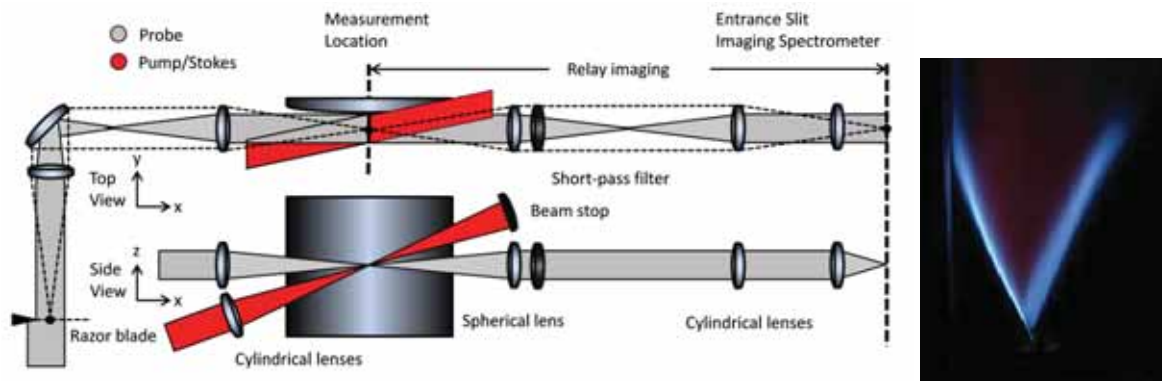


**Fig. 1.** (left) The single-shot CARS imaging system employed for direct temperature contour analysis of premixed methane/air turbulent flames impinging on a cooled steel side-wall. The probe and pump/Stokes beams originating from separate picosecond- and femtosecond regenerative amplifier laser systems, respectively, are combined at the measurement location utilizing a two-beam CARS phase-matching scheme. (right) The V-flame supported by the side-wall quenching burner, is operated in the wrinkled flamelet regime at some distance from the wall.

## References

- [1] A. Bohlin, C. Jainski, B.D. Patterson, A. Dreizler, C.J. Klierwer, "Multiparameter spatio-thermochemical probing of flame-wall interactions advanced with coherent Raman imaging", *Proc. Combust. Inst.* **36**, 4557–4564 (2017).
- [2] A. Bohlin, B.D. Patterson, C.J. Klierwer, "Communication: Simplified two-beam rotational CARS signal generation demonstrated in 1D", *J. Chem. Phys.* **138**, 081102 (2013)
- [3] C. Jainski, M. Reißmann, S. Jakirlic, B. Böhm, A. Dreizler, "Quenching of Premixed Flames at Cold Walls: Effects on the Local Flow Field", *Flow Turbul. Combust.* **100**, 177-196 (2018)



## Invited speaker



**Dr. Emmanuel Beaurepaire**

**Lab for optics and biosciences – Ecole Polytechnique (Palaiseau, France)**

Multicolor multiphoton microscopy of developing and nervous tissues

Emmanuel Beaurepaire is a specialist of multiphoton microscopy of tissues. He works at the Laboratory for Optics and Biosciences at Ecole polytechnique (Palaiseau, France), where he is appointed as a Research Director by the CNRS.

# Multicolor multiphoton microscopy of developing and nervous tissues

*Emmanuel Beaurepaire*

*Laboratory for Optics and Biosciences, Ecole Polytechnique, CNRS, INSERM, Institut Polytechnique de Paris, France*

[www.lob.polytechnique.fr](http://www.lob.polytechnique.fr)

Many questions in developmental (neuro)biology require tissue-scale measurements of multiple cell parameters. Recent progress in large-scale microscopy approaches are transforming brain imaging, but generally lack efficient color contrast modalities. The talk will discuss ongoing work aiming at augmenting the information content of multiphoton microscopy of tissues.

First, we developed chromatic multiphoton serial (ChroMS) microscopy [1], an approach combining trichromatic multiphoton excitation through wavelength mixing and microtome-based serial block-face image acquisition to image neural tissue expressing multiple fluorescent proteins. This approach provides micrometric color imaging with constant resolution and sub-micron channel registration over the entire imaged volume. We demonstrate continuous 3D imaging over several cubic millimeters of neural tissue, and brain-wide imaging by serial 2D acquisition. We illustrate the potential of ChroMS for several types of measurements, such as color-based morphological, clonal and connectivity analyses.

Second, we report on the development of a novel infrared OPA emitting simultaneously at 1.3 and 1.7  $\mu\text{m}$  with characteristics optimized for in-depth dual-color three-photon microscopy of tissues [2].

## References

- [1] Abdeladim et al, Nat Comm (2019), <https://doi.org/10.1038/s41467-019-09552-9>
- [2] Guesmi, Abdeladim et al, Light Sci App (2018), <https://doi.org/10.1038/s41377-018-0012-2>

## Coherent anti-Stokes Raman Fourier Ptychography Microscopy

Sandro Heuke<sup>1</sup>, Kevin Unger, Samira Khadir<sup>1</sup>, Patrick C. Chaume<sup>1</sup>, Anne Sentenac<sup>1</sup>, Hervé Rigneault<sup>1\*</sup>

<sup>1</sup>. Aix Marseille Univ, CNRS, Centrale Marseille, Institut Fresnel, Marseille, France.

\* Corresponding author: herve.rigneault@fresnel.fr

For most of the applications CARS imaging is performed point-wise using laser scanning technology. Exploiting its nonlinearity, intrinsic confocal images are obtained allowing for 3D sectioning of thick samples. For thin samples, i.e. with an axial extent of only a few micrometers (e.g.  $<10\ \mu\text{m}$ ), the confocality may lose its relevance in favor of the image acquisition rate. To improve the latter, multiple wide-field CARS implementations were developed from which in particular the emerging histo-pathological application branch of coherent Raman microscopy could fundamentally benefit in the future.

Here, we present a numerical study of coherent anti-Stokes Raman scattering Fourier ptychography microscopy (CARS FPM) [1], a scheme that has not been considered so far in the previously reported CARS wide-field imaging schemes. We show that CARS FPM allows the reconstruction of both real and imaginary parts of the complex third order susceptibility, the latter giving access to the Raman information. Further advantages are anticipated due to the low NA of the objective lens used to collect the anti-Stokes radiation, namely, an extended field of view (FOV) within the range of millimeters, long working distances as well as the reduced prices for their purchase.

First, we introduce a full vectorial model for an efficient computation of CARS far-field images based on the angular spectrum representation of the dyadic green function. Second, the concept of the Ewald's sphere is extended to apply for wide-field CARS microscopy in order to visualize phase-matching as well as the corresponding object transfer in the k-space. Third, we demonstrate numerically how wide-field CARS images acquired under different illumination angles can be used to reconstruct the complex scatterer distribution applying the intensity-based diffractive tomography (IDT) algorithm [2]. If the pump instead of the Stokes beam is angle-scanned, super-resolved images are obtained by the reconstruction procedure. Finally, we suggest a possible experimental setup that allows CARS FPM and we discuss the relevance of the recently developed laser sources in this context.

[1] S. Heuke et al. "Coherent anti-Stokes Raman Fourier ptychography" (2019) submitted.

[2] K. D. Unger et al. "Three-dimensional vectorial phaseless optical diffractive tomography inversion," submitted.

# **Time-Resolved Coherent Raman Spectroscopy of Wild Type and Mutated Anabaena Sensory Rhodopsin**

*Partha Pratim Roy*<sup>1</sup>, *Rei Abe-Yoshizum*<sup>2</sup>, *Yoshitaka Kato*<sup>2</sup>, *Hideki Kandori*<sup>2</sup>, *Tiago Buckup*<sup>1</sup>

*1. Physikalisch-Chemisches Institut, Ruprecht-Karls Universität Heidelberg, D-69120, Heidelberg, Germany*

*2. Department of Life Science and Applied Chemistry, Nagoya Institute of Technology, Showa-ku, Nagoya 466-8555, Japan*



## Invited speaker



**Dr. Ahmed Abdelmonem**

***Karlsruhe Institute of Technology (KIT) (Karlsruhe, Germany)***

Molecular level characterization of atmospheric aerosol – water – ice interactions using nonlinear optical spectroscopy, mainly SHG and SFG

Dr. Ahmed Abdelmonem is a project leader of an independent research program funded by the German Research Foundation (DFG). His expertise includes 1) physical chemistry and molecular level characterization of surfaces and interfaces using linear and nonlinear optical spectroscopy, 2) studying ice- and water-mineral interactions under atmospheric and environmental conditions, 3) the development and application of airborne optical instruments for in-situ climate research (received an R&D award from the KIT in 2013). In 2014, he established a new research line at the KIT, "Atmospheric Surface Science", to study physics and chemistry of the atmosphere on the molecular level using NLO spectroscopy (mainly SHG and SFG).

## Molecular level characterization of atmospheric aerosol – water – ice interactions using nonlinear optical spectroscopy, mainly SHG and SFG

*Ahmed Abdelmonem<sup>1\*</sup>, Johannes Luetzenkirchen<sup>1</sup> and Sanduni Ratnayake<sup>1</sup>*

1. *Karlsruhe Institute of Technology (KIT) – Germany*

2. *Invited Speaker*

Atmospheric aerosol-cloud-climate interactions (e.g. particle oxidation and photosensitization, heterogeneous ice nucleation ...) are fundamental processes in the atmosphere. Despite the importance of these processes in energy transfer, cloud dynamics, precipitation formation, and hence climate change, little is known about the molecular mechanism and the respective contribution of different surface properties of the atmospheric aerosols and ice nuclei controlling these processes in the atmosphere. Nonlinear optical spectroscopy, particularly second-harmonic generation (SHG) and sum-frequency generation (SFG) are powerful surface spectroscopic techniques that are capable of characterizing interactions next to surfaces and interfaces. This talk will focus on a novel supercooled SHG/SFG setup to probe aerosol–water–ice interactions on the molecular level and present recent findings on the potential changes in ice nucleation ability of silica, as a relevant atmospheric aerosol surface, under aging inside acidic clouds.

## Live Multi-Color Coherent Raman Imaging Enabled by a Compact and Robust Light Source

Maximilian Brinkmann<sup>1,2</sup>, Tim Hellwig<sup>1,2</sup>, and Carsten Fallnich<sup>1,2,3</sup>

<sup>1</sup>Institute of Applied Physics, University of Münster, Corrensstraße 2, 48149 Münster, Germany

<sup>2</sup>Refined Laser Systems, University of Münster, Corrensstraße 2, 48149 Münster, Germany

<sup>3</sup>Cells-in-Motion Cluster of Excellence (EXC 1003 CiM), Münster, Germany

E-mail: [brinkmannmax@wwu.de](mailto:brinkmannmax@wwu.de)

We present multi-color coherent Raman imaging (CRI) with a frame rate of 8 Hz and rapid wavelength tuning within only 5 ms between successive images, enabled by a novel fiber optical parametric oscillator (FOPO). In CRI the limited tuning speed of conventional laser systems ( $>1$  s) prevents the acquisition of successive images per second at more than one vibrational (Raman) resonance and is considered as a bottleneck for multi-color assessments of rapidly evolving samples. Recent approaches to CRI with wavelength switching on a timescale of (sub-)milliseconds were based on tunable laser amplifiers [1] or spectral focusing techniques [2], both with a limited tuning bandwidth of less than  $300\text{ cm}^{-1}$ , or two synchronized oscillators [3], being limited to two resonances. In contrast, the energy difference of the pump and Stokes pulses, emitted by the here presented FOPO, is tunable across the wide spectral range between  $865$  and  $3050\text{ cm}^{-1}$  within only 5 ms. Furthermore, tuning can be done in discrete steps, enabling to specifically target a pre-programmed set of key Raman resonances. Assuming an equal time span for tuning and acquisition, up to 100 user-selectable Raman resonances could be imaged per second, when imaging with 100 frame/s. The rapid tuning was achieved by a novel tuning concept for optical parametric oscillators, based on the dispersive matching of the repetition frequency change of the pump pulses to the associated repetition frequency change of the resonant signal pulses in the FOPO. No alteration of the FOPO, e.g., via a mechanical delay line, was required for tuning the signal wavelength, and the light source could be composed of all-spliced fiber components. Compared to previously presented FOPOs, the system runs at a high repetition rate of 40 MHz. The pump and Stokes pulses exhibit equal durations of 7 ps and an average power of 500 and 200 mW, respectively. As a first proof-of-concept of the CRI capabilities, Fig. 1 shows three images of a sample consisting of oil and beads of PMMA and PS, taken successively with an acquisition time of 125 ms for each frame, limited only by the sampling rate of our detection setup. The energy difference was tuned in a frame-by-frame manner between  $2850$ ,  $2950$ , and  $3050\text{ cm}^{-1}$  in a time of 5 ms, a negligible time span compared to the acquisition time.

In order to promote the non-stationary application of CRI, e.g., for diagnostic bed-side imaging, we fitted the all-fiber setup in a portable, passively cooled housing with a compact footprint below  $50\times 40\times 15\text{ cm}^3$ . We will demonstrate a reliable operation of the system under non-laboratory conditions, e.g., after mechanical shocks of more than  $25\text{ m/s}^2$ .

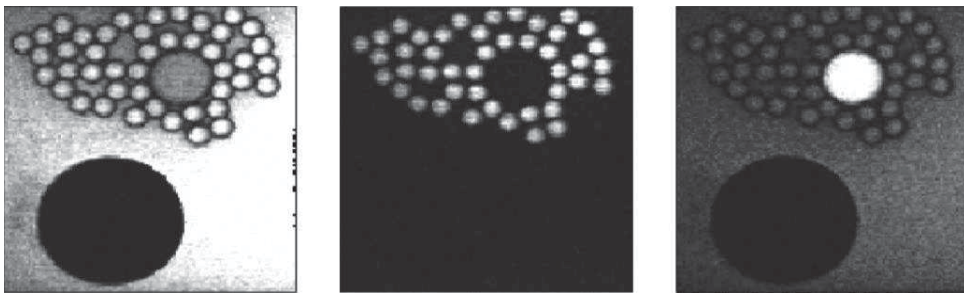


Fig. 1: CRI images of a sample consisting of oil and beads of PMMA and PS, each taken with an acquisition time of 125 ms. The energy difference of the excitation pulses was tuned in a frame-by-frame manner within 5 ms to (a)  $2850\text{ cm}^{-1}$ , highlighting oil, (b)  $2950\text{ cm}^{-1}$ , highlighting PMMA, (c)  $3050\text{ cm}^{-1}$ , highlighting PS.

### References:

- [1] Y. Ozeki, T. Asai, J. Shou and H. Yoshimi, "Multicolor Stimulated Raman Scattering Microscopy With Fast Wavelength-Tunable Yb Fiber Laser," *IEEE Journal of Selected Topics in Quantum Electronics*, **25**, 1-11 (2019).
- [2] M. Alshaykh, C. Liao, O. Sandoval, G. Gitzinger, N. Forget, D. Leaird, J. Cheng, A. Weiner, "High-speed stimulated hyperspectral Raman imaging using rapid acousto-optic delay lines," *Opt. Lett.*, **42**, 1548–1551 (2017).
- [3] S. Heuke, B. Sarri, X. Audier, and H. Rigneault, "Simultaneous dual-channel stimulated Raman scattering microscopy demultiplexed at distinct modulation frequencies," *Opt. Lett.*, **43**, 3582-3585 (2018).



## Broadband Stimulated Raman Scattering Microscopy with In-Line Balanced-Detection

Alejandro De la Cadena, Andrea Ragni, Giuseppe Sciortino, Giorgio Ferrari, Marco Sampietro, Giulio Cerullo and Dario Polli

Politecnico di Milano, Piazza L. da Vinci 32, 20133 Milano (Italy)

Stimulated Raman scattering (SRS) is an increasingly employed technique in optical nonlinear microscopy, as it is capable of identifying different chemical species and their concentration in a sample. It exploits the third-order nonlinear optical response of the specimen to ultrashort pump and Stokes pulses, by setting up and detecting a vibrational coherence within the ensemble of molecules inside the laser focus. In its broadband modality, SRS excites a manifold of molecular vibrational bands, thus providing more information about the chemical composition of the sample compared to the narrowband version. It therefore opens up the possibility to discriminate chemical species with overlapping Raman signatures.

We report here on an innovative broadband SRS setup capable of high-speed imaging in the C-H stretching region ( $2800\text{-}3050\text{ cm}^{-1}$ ). It is based on a homemade optical parametric oscillator at 80-MHz repetition rate [1]. It delivers broadband pump pulses in the 780-810 nm region and narrowband ( $\approx 10\text{ cm}^{-1}$ ) Stokes pulses at 1040-nm, modulated at  $\approx 7\text{ MHz}$  frequency, in order to detect the stimulated Raman loss (SRL) of the pump. To increase the signal-to-noise ratio, which is typically limited by the relative intensity noise fluctuations of the laser source, we take advantage of the in-line balanced detection scheme [2] (see Fig. 1(a)). A birefringent plate is placed before the sample in the broadband pump branch, to generate two replicas with orthogonal polarization, one serving as the pump pulse for SRS and the second as a reference for balancing purposes. Both replicas interact with the sample, although only one temporally coincides with the narrowband Stokes beam and undergoes SRL. In this way, the reference pulse experiences the same local attenuation, due to spatially varying sample transmission, but it does not bear any modulation transfer due to SRS. After the sample, a spectral filter rejects the Stokes while the pump/reference pulses are dispersed with a transmission grating in Littrow configuration, separated with a polarizing beam splitter and sent to different photodiodes for the pump and the reference beams. Their intensities are electronically subtracted before demodulation, thus reaching close to shot-noise-limited detection.

SRS detection can be performed in two modalities. In the first (IBD-G, see left inset of Fig. 1(a)), an off-the-shelf balanced photodiode with two single-pixel detectors is employed, whose output is connected to a standard single-channel lock-in amplifier, employed at maximum speed ( $1.8\text{-}\mu\text{s}$  integration time). Retrieval of the vibrational spectrum is performed by varying the detected pump wavelength after the sample by means of a single-axis galvanometric scanning mirror. Figures 1(b-c) report imaging results on a test sample made of dispersed PMMA ( $6\text{-}\mu\text{m}$  diameter, see red spheres in panel (c) at  $2956\text{ cm}^{-1}$ ) and polystyrene ( $3\text{-}\mu\text{m}$  diameter, see blue spheres in panel (d) at  $3066\text{ cm}^{-1}$ ) beads. Panel (d) shows the image collected at  $3005\text{ cm}^{-1}$ , in which both specimens are visible due to overlapping vibrational features. Fig. 1(e) reports exemplary SRS spectra of PS and PMMA. In the second detection modality, a home-made multi-channel lock-in amplifier (M-LIA, see right inset of Fig. 1(a)) [3] is employed with 4 parallel channels and  $10\text{-}\mu\text{s}$  integration time constant, thus allowing very fast SRS imaging at 4 distinct frequencies. In the future, the system will be upgraded to a 32-channel M-LIA.

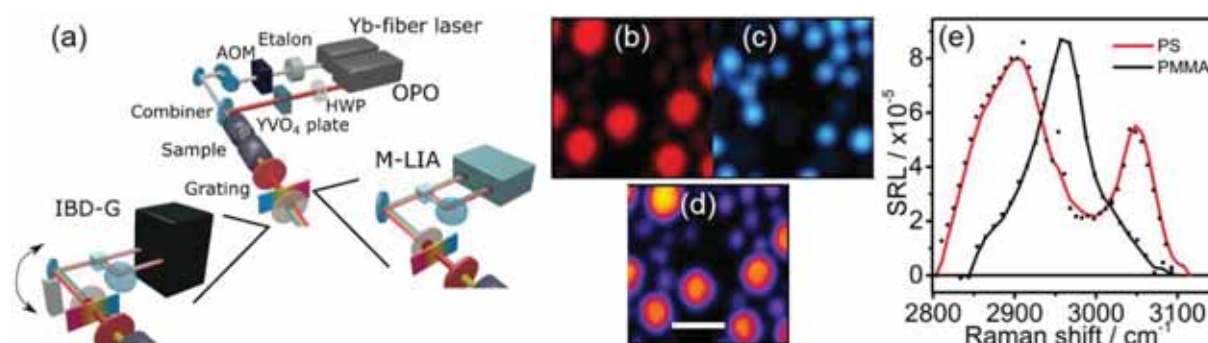


**Fig. 1** (a) Scheme of the experimental set-up, showing the two possible detection schemes employing either a galvanometric scanner (IBD-G, on the left) or a multi-channel lock-in amplifier (M-LIA, on the right). (b-c-d) SRS imaging of PMMA and PS beads at  $2956\text{ cm}^{-1}$  (c),  $3066\text{ cm}^{-1}$  (d) and  $3005\text{ cm}^{-1}$  (e) Raman shift. Scalebar:  $10\text{ }\mu\text{m}$ . (e) Raman spectra of the two components.

[1] N. Coluccelli, D. Viola, V. Kumar, A. Perri, M. Marangoni, G. Cerullo, and D. Polli, "Tunable 30 fs light pulses at 1 W power level from a Yb-pumped optical parametric oscillator", *Opt. Lett.* **42**, 4545 (2017).

[2] F. Crisafi, V. Kumar, T. Scopigno, M. Marangoni, G. Cerullo, and D. Polli, "In-line balanced detection stimulated Raman scattering microscopy", *Sci. Rep.* **7**, 10745 (2017).

[3] A. Ragni, G. Sciortino, M. Sampietro, G. Ferrari, and D. Polli, "Lock-In Based Differential Front-End for Raman Spectroscopy Applications", *14<sup>th</sup> Conference on Ph.D. Research in Microelectronics and Electronics (PRIME)* **1**, 221–224 (2018).

# Retrieving the complex vibrational susceptibility with interferometric stimulated Raman scattering (iSRS)

Carlo Michele Valensise<sup>1</sup>, Vikas Kumar<sup>2</sup>, Sandro De Silvestri<sup>1</sup>, Giulio Cerullo<sup>1</sup> and Dario Polli<sup>1</sup>

1. IFN-CNR, Dipartimento di Fisica, Politecnico di Milano, Piazza Leonardo da Vinci 32, I -20133 Milano, Italy  
2. Universität Duisburg-Essen, Fakultät für Chemie (PC), Universitätsstr. 5 45141 Essen, Germany

Coherent Raman Scattering (CRS) [1] is a class of third-order optical processes, which drive a nonlinear polarization in the sample, proportional to the third order nonlinear vibrational susceptibility  $\chi^{(3)}(\omega)=\chi_R^{(3)}(\omega)+\chi_{NR}^{(3)}$ . This is a mixture of a complex resonant term, associated to the different vibrational transitions, and a purely real and frequency-independent non-resonant term. The two most common CRS techniques, in their standard implementation, do not allow the retrieval of the full complex  $\chi^{(3)}$  signal: the CARS signal is a mixture of its real and imaginary parts, while SRS only retrieves the imaginary part. Measurement of the complex  $\chi^{(3)}$  signal would offer instead a richer spectroscopic information to be used, e.g., to distinguish molecules with similar amplitude response but different spectral phase [2]. Numerical methods [3] can be used to reconstruct the full vibrational  $\chi^{(3)}$ , but their main limitation is the requirement of the entire vibrational spectrum, which often cannot be acquired at high speed. Interferometric techniques can overcome this limitation and have been demonstrated for CARS [4].

In this work, we introduce single-frequency interferometric SRS (iSRS), thanks to a simple modification of a standard SRS setup, which allows to measure the full complex  $\chi^{(3)}$ . The Stokes arm is equipped with a common-path interferometer, similar to that employed by Orrit and coworkers [5], but based on an ultra-stable birefringent common-path interferometer (GEMINI by NIREOS S.R.L). It simply requires the addition of a birefringent plate before the sample, creating two replicas of the Stokes beam with perpendicular polarization, and two birefringent wedges after the sample, to bring the pulses back to zero time delay. Finally, the combination of a quarter-wave plate and a linear polarizer set at a proper angle before the photodiode allows us to disentangle and independently measure the real and imaginary components of  $\chi^{(3)}$ . Figure 1 shows imaging results on PMMA and PS beads (with 6 and 3- $\mu\text{m}$  diameter, respectively) at 3000  $\text{cm}^{-1}$  vibrational frequency. While PMMA displays a strong signal in the imaginary component (see Fig. 1(a)), as expected at this Raman shift, its real counterpart almost vanishes (see Fig. 1(b)). The opposite behavior is seen for PS, so that the two specimens can be distinguished and quantified without the need for scanning the frequency detuning between pump and Stokes. Even more strikingly, the phase image (Fig. 1(c)) enables us to distinguish the two components clearly even at their thin borders, demonstrating that it provides a more robust discrimination criterion than the Raman amplitude.

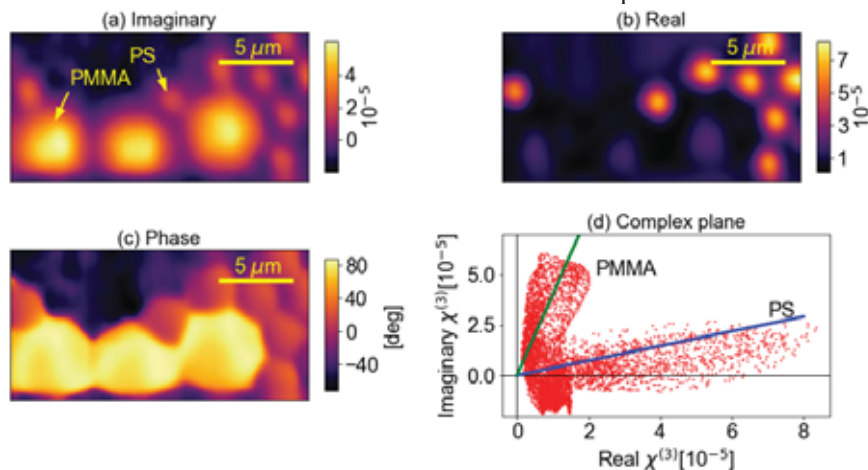


**Fig. 1** iSRS images of a mixture of PS and PMMA beads measured at 3000  $\text{cm}^{-1}$ . Imaginary (a) and real (b) parts of the vibrational response are measured, thus allowing the reconstruction of a phase image (c) and the representation of chemicals into the complex plane (d), simplifying the distinction of species with similar vibrational features.

## References

- [1] D. Polli, V. Kumar, C. M. Valensise, M. Marangoni, and G. Cerullo, "Broadband Coherent Raman Scattering Microscopy", *Laser Photonics Rev.* 1800020 (2018).
- [2] M. Jurna, E. T. Garbacik, J. P. Korterik, J. L. Herek, C. Otto, and H. L. Offerhaus, "Visualizing Resonances in the Complex Plane with Vibrational Phase Contrast Coherent Anti-Stokes Raman Scattering", *Anal. Chem.*, **82**, 7656–7659 (2010).
- [3] Y. Liu, Y. J. Lee, M. T. Cicerone, "Broadband CARS spectral phase retrieval using a time-domain Kramers–Kronig transform", *Opt. Lett.*, **34**, 1363 (2009). E. M. Vartiainen, "Phase retrieval approach for coherent anti-Stokes Raman scattering spectrum analysis" *J. Opt. Soc. Am. B*, **9**, 1209 (1992).
- [4] M. Jurna, J. P. Korterik, C. Otto, J. L. Herek, and H. L. Offerhaus, "Vibrational Phase Contrast Microscopy by Use of Coherent Anti-Stokes Raman Scattering" *Phys. Rev. Lett.*, **103**,4 (2009).
- [5] M. A. van Dijk, M. Lippitz, D. Stolwijk, and M. Orrit, "A common-path interferometer for time-resolved and shot-noise-limited detection of single nanoparticles" *Opt. Express* **15** (2007).



## Invited speaker



**Dr. Waruna Kulatilaka**

***Associate Professor, Texas A&M University, (Texas, USA)***

### Ultrashort-Pulse Multi-Photon Multi-Species Imaging Techniques for Combustion Diagnostics

Dr. Waruna Kulatilaka is an Associate Professor and Morris E. Foster Faculty Fellow I in the J. Mike Walker '66 Department of Mechanical Engineering at Texas A&M University. He also holds a joint courtesy appointment in the Department of Aerospace Engineering. Dr. Kulatilaka's research activities are centered on the development and application of advanced optical and laser-based diagnostics for combustion, propulsion and fluid dynamics studies. In recent years, he has made significant contributions to the development ultrashort-pulse multi-photon imaging techniques for highly reactive atomic species such as H and O. His work is reported in over 50 peer-reviewed journal articles and numerous conference publications and presentations. Prior to the current appointment, Dr. Kulatilaka was a Senior Research Scientist/On-Site Contractor at the Air Force Research Laboratory at Wright-Patterson Air Force Base, OH (AFRL/RQTC), and also completed a postdoctoral research term at the Combustion Research Facility (CRF) at the Sandi National Laboratories, CA. He is active in numerous professional organizations, including ASME (Fellow), AIAA (Associate Fellow), OSA (Senior Member), the Combustion Institute (Board Member–Central States Section), and has also won several significant awards.

# Ultrashort-Pulse Multi-Photon Multi-Species Imaging Techniques for Combustion Diagnostics

*Waruna Kulatilaka*

*Associate Professor in Mechanical Engineering (also, Aerospace Engineering by courtesy)  
Texas A&M University, College Station, TX 77843, USA*

Reactive minor species play a crucial role in turbulent chemistry, and complex flow-flame interactions in combustion and plasma systems, yet quantitative two- and three-dimensional imaging diagnostics of these atomic and molecular species are extremely challenging in practical operating conditions relevant to those devices. In combustion systems, the efficiency, heat release rate, and formation pathways of various pollutants such as  $\text{NO}_x$ , CO, and soot are directly related to reaction pathways involving atomic species such as hydrogen (H), oxygen (O), and nitrogen (N), as well as molecular species of hydroxyl (OH) and carbon monoxide (CO). Similarly, some of these intermediate species are also involved in rate-determining steps non-equilibrium chemistry of low-temperature plasmas. Therefore, simultaneous, time-resolved, multi-dimensional imaging diagnostics relevant chemical species are of vital importance for better understanding of the fundamental reaction chemistry, computational model validations, as well as designing next-generation efficient combustion and plasma systems.

In this talk, we discuss novel approaches for utilizing ultrashort, femtosecond (fs) duration laser pulses for kilohertz (kHz)-rate imaging of key atomic and molecular species such as H, O, CO, and OH in flames. H and O play a critical role in ignition/extinction and heat release processes in hydrocarbon flames. OH is a prominent marker of the reaction zone, while CO is a harmful byproduct of incomplete fuel oxidation. Femtosecond, two-photon laser-induced fluorescence (fs-TPLIF) of H and O are facilitated by deep-UV fs pulses followed by fluorescence detection in the visible or near-infrared wavelengths. The first part of the talk I will outline some recent advances of fs-TPLIF for photolytic-interference-free, kHz-rate, two-dimensional imaging of H, O, and N in flames and plasmas. Subsequently, fs-TPLIF of CO imaging diagnostics are discussed by using 230.1-nm excitation of the  $\text{B}^1\Sigma^+ \leftarrow \text{X}^1\Sigma^+$  electronic transition of CO. Specific temporal and spectral filtering approaches are implemented for minimizing interferences in challenging flame conditions such as in sooting ethylene air flames. This diagnostic scheme is subsequently applied for CO formation studies in piloted, liquid-fuel-spray flames stabilized over a flat-flame McKenna burner fitted with a direct-injection high-efficiency nebulizer. The second part of the talk highlights the utilization of fs-duration laser pulses for kHz-rate imaging of OH in flames. Approximately 283-nm wavelength, broadband, 80-fs-duration laser pulses are used for excitation of a large number of rovibrational transitions in the  $\text{A}^2\Sigma^+ \leftarrow \text{X}^2\Pi(1, 0)$  band of OH radical, followed by LIF imaging from (0, 0) and (1, 1) vibrational manifolds. The single-laser-shot 2D OH-PLIF imaging is demonstrated at a 1-kHz repetition rate in a turbulent  $\text{CH}_4/\text{H}_2/\text{air}$  diffusion flame. Advantages of fs excitation for imaging molecular species such as OH at elevated-pressure conditions are also discussed.

The broad spectral bandwidth present in ultrashort, fs-duration laser pulses can be challenging for species-specific excitation in some situations, yet provide distinct opportunities for simultaneous multi-species imaging, which can be a significant advantage for better characterizing the complex chemistry in many practical systems. Several recent approaches in simultaneous excitation of several species using broadband fs laser pulse are outlined, along with a future outlook for implementation of ultrashort pulse laser diagnostics for multi-species imaging.

Tuesday

Morning

# Femtosecond Two-Photon Absorption Laser-Induced Fluorescence Imaging of Atomic Hydrogen and Oxygen in a Plasma-Assisted Methane/Air Flame

Davide Del Cont-Bernard<sup>1</sup>, Maria Ruchkina<sup>2</sup>, Pengji Ding<sup>2,\*</sup>, Joakim Bood<sup>2</sup>, Andreas Ehn<sup>2</sup>, Deanna A. Lacoste<sup>1</sup>

1. Clean Combustion Research Center, King Abdullah University of Science and Technology, Thuwal, 23955-6900, Saudi Arabia  
2. Division of Combustion Physics, Department of Physics, Lund University, Box 118, Lund SE-221 00, Sweden

Corresponding author: [pengji.ding@forbrf.lth.se](mailto:pengji.ding@forbrf.lth.se)

In the last decades, non-equilibrium plasmas produced by nanosecond repetitively pulsed (NRP) discharges have shown promising ability for combustion enhancement [1]. For example, significant reduction of ignition delay time and lean-flammability limit, as well as control of flame dynamics, can be achieved with the aid of NRP discharges [2]. Measurements of spatial distribution and temporal evolution of key intermediate species, including ions, neutral meta-stables, and particularly neutral atoms, are vital to the understanding of the physicochemical mechanisms of the NRP discharge action on the flame behavior. Femtosecond two-photon absorption laser-induced fluorescence (fs-TALIF) has been applied for detection of atomic species, such as O and H, and molecules, such as OH, NO, and CO, in laminar flames and low-pressure or atmospheric plasma [3]. Compared to using nanosecond laser, femtosecond lasers have shown apparent superiority for TALIF due to high peak power while the pulse energy is still modest, which allows efficient multi-photon excitation with minimal photolytic interference. In this work, we report on fs-TALIF 2-D imaging of atomic hydrogen and oxygen in a plasma-assisted laminar CH<sub>4</sub>/air flame at atmospheric pressure. The objective is to evaluate the impact of plasma actuation on the flame in terms of the spatial distribution of H and O atoms, providing a valuable dataset for assessing the chemical impact of non-equilibrium plasma discharge on the combustion chemistry.

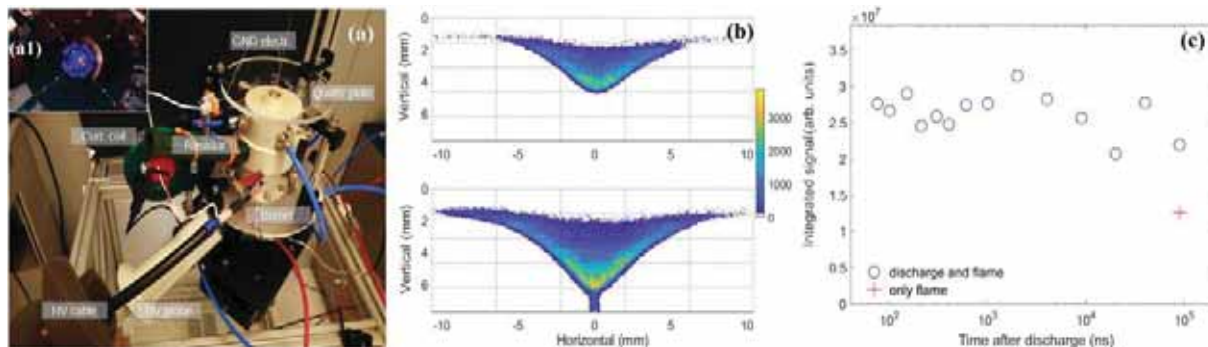


**Fig. 1** (a) The burner that produces a V-type methane/air flame, with a pin-to-pin discharge penetrating through the flame along its central symmetry line. The inlet (a1) shows a top-down view of the V-type flame. (b) Images of 656-nm fluorescence from hydrogen without discharge (upper panel) and 1  $\mu$ s after 8.3 kV-discharge events at 10 kHz repetition rate (lower panel). (c) Integrated hydrogen fluorescence signal as a function of the time delay between the discharge onset and the LIF measurement.

In these experiments, the femtosecond laser system delivers 125-fs laser pulses at 205 nm (for H detection) or 226 nm (for O detection), which are focused by a cylindrical lens into the flame to excite H or O atoms. Fluorescence occurs at 656 nm for H and 845 nm for O, which is detected with an intensified CCD camera from the side. The plasma-assisted combustion (PAC) burner, as shown in Fig. 1(a), consists of a laminar stagnation plate burner, equipped with a NRP discharge generator. A lean V-type methane-air flame with a nitrogen co-flow is established. Plasma is actuated between two pin electrodes. One electrode is located on the central axis of the burner nozzle, while the other is located in the quartz plate, so that a plasma channel is formed in a 9-mm gap, crossing the flame and developing in both the cold and hot gases.

As an example of results, Fig. 1(b) shows fs-TALIF images of H atoms recorded without discharge (upper panel) and 1  $\mu$ s after 8.3-kV glow discharge at 10 kHz repetition rate (lower panel). It can be noticed that the discharge plasma has a clear impact on the distribution of H atoms. The flame front is forced to move towards the cathode electrodes, and an elevated concentration of H atoms is formed in the vicinity of the tip of the flame. The overall concentration of H has been enhanced by approximately 100%. Figure 1(c) shows the integrated H-TALIF signal over the whole image as a function of the time delay between of the discharge onset and the LIF measurement, showing a pretty constant hydrogen concentration over a discharge cycle of 100  $\mu$ s. Data analysis is currently ongoing and more results will be presented and discussed at the conference.

## References

- [1] Y. Ju, and W. Sun, "Plasma assisted combustion: Dynamics and Chemistry", *Prog. Energy Combust. Sci.* **48**, 21 (2015).
- [2] D. A. Lacoste, D. A. Xu, J. P. Moeck, and C. O. Laux, "Dynamic response of a weakly turbulent lean-premixed flame to nanosecond repetitively pulsed discharges", *Proc. Combust. Inst.* **34**, 3259 (2013).
- [3] A. K. Patnaik, I. Adamovich, J. R. Gord, and S. Roy, "Recent advances in ultrafast-laser-based spectroscopy and imaging for reacting plasma and flames", *Plasma Sources Sci. Technol.* **26**, 103001 (2017).

# Generation of Parametric Superfluorescence by Picosecond Pulses under Low Frequency Pump in KTP Crystal

K.A. Vereshchagin<sup>1,2</sup>, A. K. Vereshchagin<sup>1,2</sup>, V.B. Morozov<sup>2</sup>, V.G. Tunkin<sup>2</sup>

1. Federal State Institution of Science A.M. Prokhorov General Physics Institute, Russian Academy of Sciences, Vavilov Str.38, 119991, Moscow, Russia;

2. International Laser Center and Faculty of Physics of M.V. Lomonosov Moscow State University, Leninskie Gori,1, 119991, Moscow, Russia

The nature of cubic and cascaded quadratic nonlinear responses [1] in the KTiOPO<sub>4</sub> crystal under picosecond pump is studied. The main attention is paid to determination of the origin and properties of the blue radiation accompanying the red light amplification process (the central wavelength ~685 nm, bandwidth ~20 nm) in a noncollinear optical parametric amplifier (NOPA) pumped by the second-harmonic radiation of the picosecond Nd:YAG laser (532 nm, 60 ps). In NOPA, the amplified seed radiation ( $\omega_s$ ) becomes so intense that it can participate in nonlinear three-wave interaction and also can play the role of the Stokes wave in the coherent anti-Stokes Raman scattering-process in which powerful pump radiation ( $\omega_p$ ) of the main parametric process serves both as the pump and the probe waves. Possible causes of the blue light emanating from the KTP crystal and the mechanisms for their realization are analysed. We interpret the ring of blue light around the axis located between the directions of propagation of the green pump beam and the red beam of the amplified seed radiation, as the emission of amplified parametric fluorescence (signal wave) under low-frequency pump [2].

We found that there is the only possible cause of this blue ring ("blue light"), namely it is the quadratic cascaded process:  $\omega_p^{(o)} = \omega_s^{(e)} + \omega_i^{(o)} \rightarrow \omega_{SFG}^{(o)} = \omega_p^{(o)} + \omega_s^{(e)} \rightarrow \omega_{SFG}^{(o)} = \omega_{aS}^{(o)} + \omega_{idler2}^{(e)}$ .

In the first process, the pump photons  $\omega_p^{(o)}$  break up into signal  $\omega_s^{(e)}$  and idle  $\omega_i^{(o)}$  photons. The second process is the sum-frequency generation (SFG), when the summation of the pump wave and the signal wave generates a new wave with frequency  $\omega_{SFG}^{(o)} = [2\omega_p - \omega_i]$  ("UV-light"). In the third process, the "new pump" photon  $\omega_{SFG}^{(o)}$  breaks up into a "new signal"  $\omega_{aS}^{(o)}$  and a "new idler"  $\omega_{idler2}^{(e)}$  photons. The last process in the cascade creates a new wave with a frequency  $\omega_{aS}^{(o)} = 2\omega_p - (\omega_i + \omega_{idler2})$ , which coincides with the frequency of the "blue light". The polarization of the "new signal" wave is vertical, which is the same as for the "blue light". The "blue light" cone axis is oriented in the direction of the wavevector of the "UV-light" ( $\omega_{SFG}^{(o)}$ ), while the radius of "blue ring" seems to correspond to the non-collinearity angle for cascaded process discussed.

The peculiarity of the final stage of the cascaded processes is that pumping wave for this process has the wavelength of ~300 nm, which is strongly absorbed in KTP crystal. The absorption coefficient at the wavelength of 300 nm is  $\gg 10 \text{ cm}^{-1}$  [3], and so the pumping wave for the final stage parametric process has been not observed at the crystal output. This means that the energy of the pump wave ( $\omega_p$ ) can be converted into the energy of the SFG-wave only at a short distance  $L_{abs} \sim 1/\alpha_{SFG}$ , where  $\alpha_{SFG}$  is the absorptance of the "UV light". At this distance, both phase matched and phase mismatched types of interactions can coexist. Due to strong absorption, the inequality  $L_{abs} \ll l_{coh}$  is fulfilled, and despite the non-zero wavevector mismatch the shift ( $\Delta\varphi \sim \Delta k \cdot L_{abs}$ ) between phases of oscillations of the electric field vectors of interacting waves can be neglected with respect to  $\pi$ .

The fact that "UV light" is obtained with a phase mismatch does not matter, since the "carrier of the phase" now is the pair "pump( $\omega_p$ )&signal( $\omega_s$ )", which generates at each point of each thin layer  $L_{abs}$  a "new pump" wave with regular phase, that leads to constructive interference of "blue light" waves along path length. In some sense it looks like a quasi-phase-matched process with spatial modulation of the nonlinearity: every thin layer  $L_{abs}$  works as a short nonlinear crystal with a "new pump" wave ("UV-light",  $\lambda_{UV} \sim 300 \text{ nm}$ ) at the input and with a "new signal" ("blue light",  $\lambda_{aS} \sim 460 \text{ nm}$ ) together with a "new idler" ("idler2",  $\lambda_{idler2} \sim 870 \text{ nm}$ ) waves at the output. The last proof of the correctness of our interpretation of the "blue light" is the presence at the NOPA output of NIR emission: we managed to register the spectra in the region of 860-890 nm, and we attribute them to the emission of the "new idler" wave.

Hence, effective broadband noncollinear optical parametric amplification under low-frequency picosecond pump (NOPA-LFPP) was realized as a quasi-phase matched process in a spatially homogeneous nonlinear KTP crystal.

## References

- [1]. G. Assanto, in *Beam Shaping and Control with Nonlinear Optics*, vol 369, (Eds: F. Kajzar, R. Reinisch), NATO Science Series B: (Advanced Science Institutes Series), (Springer, Boston, MA 2002).
- [2]. E. Y. Morozov, A. S. Chirkin, "Consecutive parametric interactions of light waves with aliquant frequencies", *J. Opt. A: Pure Appl. Opt.*, **5**, 233 (2003)
- [3]. G. Hansson, H. Karlsson, S. Wang, F. Laurell, "Transmission measurements in KTP and isomorphic compounds", *Appl. Opt.*, **39**, 5058 (2000).

# Pure rotational coherent anti-Stokes Raman spectroscopy of ethylene-nitrogen mixtures

## Experiments and modelling

Ali Hosseinnia, Christian Brackmann, Per-Erik Bengtsson

Combustion Physics, Department of Physics, Lund University, P.O. Box 118, SE-221 00 Lund, Sweden

Rotational coherent anti-Stokes Raman spectroscopy (CARS) is an established diagnostic technique for temperature and concentration measurements in combustion-related experiments. The evaluation is conventionally made in the spectral domain by forming a library of theoretical spectra at different temperatures and species molar fractions, followed by least-square fittings to find the best fit for the experimentally recorded spectrum among the theoretical spectra interpolated from this library. This method works if all molecular information is at hand for successful modeling. Therefore, CARS has mainly been applied on di- and tri-atomics with linear molecular symmetry, for which good agreement is achieved between experimental and theoretical spectra. Hydrocarbons have so far been less attractive for rotational CARS studies, partly because of their complex molecular symmetries making it challenging to obtain molecular parameters necessary for a successful modeling. Nevertheless, in this work we have studied the asymmetric top molecule ethylene ( $C_2H_4$ ) using rotational CARS through experiments and theoretical modelling. Experimental spectra have been recorded at temperatures between 293 K and 804 K, and theoretical spectra have been calculated with a novel method for which the crucial temperature-dependent linewidth parameters were estimated by comparison of experimental and theoretically calculated spectra. Line-mixing effects and temperature dependence of the isolated linewidths were studied using a semi-classical approach considering an exponential gap law and a scaling law.

Subsequently, in a more combustion-relevant experiment, several rotational CARS spectra of  $C_2H_4-N_2$  mixtures were recorded at different temperatures and molar fractions. The information achieved at the first stage of the project for pure ethylene was used to develop a theoretical model that can predict spectra of nitrogen-ethylene mixtures. Figure 1(a) shows an experimental rotational CARS spectrum of a mixture of 60% ethylene in nitrogen at 506 K and atmospheric pressure, together with the difference spectrum between the experimental and corresponding best-fit theoretical spectrum shown separately in Fig. 1(b). Obviously, the agreement between the experimental data and the model is very good. Remaining differences between theoretical and experimental spectra may at least partly be due to uncertainties in the collisional broadening effects between the two molecules.

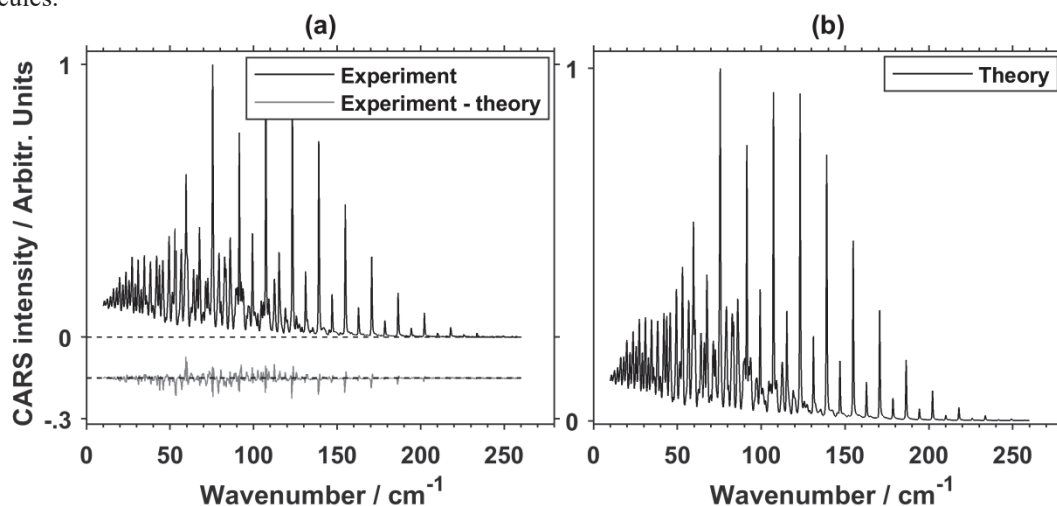


Fig. 1 Experimental rotational CARS spectra of ethylene (black left plot) and the difference (grey) between spectra and the corresponding best-fit theoretical spectra (black right plot) at atmospheric pressure and temperatures of  $T = 506$  K with ethylene molar fraction of 60 %.

The developed method was applied in rotational CARS measurements at different vertical and radial positions of an ethylene diffusion flame on a Gülder burner. These flame spectra are currently analyzed using the developed theoretical model for thermometry and concentration measurements. In conclusion, this work not only investigates the potential of using rotational CARS on ethylene for diagnostic purposes, but also expands the applicability of the technique to a whole new class of molecules with asymmetric-top molecular symmetry.

# Suppression of Stimulated Raman Scattering via Photon Depletion in a Two-Color Three-Beam Setup

Thomas Würthwein<sup>1</sup>, Niels Irwin<sup>1</sup>, Carsten Fallnich<sup>1,2,3</sup>

1. Institute of Applied Physics, University of Münster, Correnstr. 2, 48149 Münster, Germany

2. MESA+ Institute of Nanotechnology, University of Twente, Enschede 7500 AE, The Netherlands

3. Cells-in-Motion Cluster of Excellence (EXC 1003 CiM), Münster, Germany

Sub-diffraction limited imaging schemes have become widely used in fluorescence microscopy [1]. However, the need for labeling with fluorescent dyes remains a major downside of fluorescence microscopy. The size, availability, toxicity as well as photo-bleaching of the used dyes can complicate measurements [2]. In contrast, Raman imaging is inherently label-free. Unfortunately, the super-resolution schemes used in fluorescence microscopy are currently not transferable to Raman microscopy. This paper presents the development of a scheme for the suppression of coherent Raman scattering through the depletion of probe photons, inspired by the work of M. Cho et al. [3, 4], who showed the suppression of coherent Raman scattering using two Raman resonances and laser pulses at three different colors.

In our case, probe depletion is achieved by saturated femtosecond stimulated Raman scattering (FSRS) addressing a single Raman resonance in a three-beam setup with only two colors involved. Fig. 1 (a) and (b) present the working principle: in the unsuppressed case, the simultaneous irradiation of the sample with pump and probe pulses induces stimulated Raman loss (SRL<sub>P</sub>) of the probe and stimulated Raman gain (SRG<sub>P</sub>) of the pump. In the suppressed case a second strong pump pulse, working as the depletion pulse, depletes the probe pulse via stimulated Raman scattering (SRL<sub>D</sub>) and induces a shortage of probe photons at the Raman resonances. Thus, if SRL<sub>P</sub> is detected while the depletion beam is turned on, only a small amount of additional SRL<sub>Sup</sub> < SRL<sub>P</sub> induced by the pump can be measured. The energy transferred via the FSRS process is visualized for the (weak) pump and the (strong) depletion by the red and blue arrows, respectively.

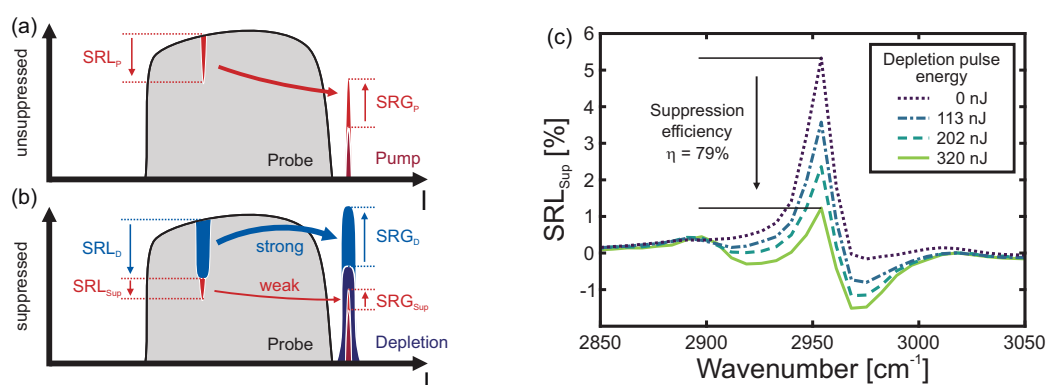


**Fig. 1** (a) Scheme for stimulated Raman loss (SRL<sub>P</sub>) and gain (SRG<sub>P</sub>) induced by the pump in the unsuppressed case. In (b) the suppression of SRL<sub>Sup</sub> by photon depletion is shown. The arrows visualize the energy transferred via the Raman process. (c) Raman spectra in the CH-stretch region of acetonitrile for different depletion pulse energies. For details see text.

This method enables the suppression of a Raman signal by stimulated Raman scattering without the need for a second Raman resonance and further, no a priori information about the molecular spectrum is necessary in contrast to reference [4]. Fig. 1 (c) shows the stimulated Raman spectra of the CH-stretch region of acetonitrile for a depletion pulse energy of 0 nJ, 113 nJ, 202 nJ and 320 nJ and a constant pump pulse energy of 60 nJ. A reduction of the Raman signal at the resonance of up to 79 %, calculated by the suppression efficiency  $\eta = 1 - \text{SRL}_{\text{Sup}} / \text{SRL}$ , for a depletion pulse energy of 320 nJ could be measured.

The developed suppression technique has the potential to enable resolution enhancement in coherent Raman microscopy similar to stimulated emission depletion (STED, [5]), a super-resolution scheme used in fluorescence microscopy. Thus, the work presented here opens up a simplified pathway towards label-free and sub-diffraction limited imaging in comparison to the work of M. Cho et al. [3, 4].

## References

- [1] B. Huang, M. Bates and X. Zhuang, "Super resolution fluorescence microscopy," *Annu. Rev. Biochem.* **78**,993-1016 (2006).
- [2] R. Alford, H. M. Simpson, J. Duberman, G. C. Hill, M. Ogawa, C. Regino, H. Kobayashi and P. L. Choyke, "Toxicity of Organic Fluorophores Used in Molecular Imaging: Literature Review," *Mol. Imaging* **8**, 341-354 (2009).
- [3] M. Cho, "Three-beam double stimulated Raman scatterings," *J. Chem. Phys.* **148**, 014201 (2018).
- [4] D. Kim, D.S. Choi, J. Kwon, S.-H. Shim, H. Rhee and M. Cho, "Selective Suppression of Stimulated Raman Scattering with Another Competing Stimulated Raman Scattering," *J. Phys. Chem. Lett.* **8**, 6118-6123 (2017).
- [5] S. W. Hell and J. Wichmann, "Breaking the diffraction resolution limit by stimulated emission: stimulated emission-depletion fluorescence microscopy," *Opt. Lett.* **19**, 780-782 (1994).



# THz-QCL sources for precision spectroscopy

Malik Nafa<sup>1</sup>, Luigi Consolino<sup>1</sup>, Michele De Regis<sup>1</sup>, Miriam Vitiello<sup>2</sup>, Paolo De Natale<sup>1</sup>, Saverio Bartalini<sup>1,3</sup>

1. CNR-Istituto Nazionale di Ottica and LENS, Via N. Carrara 1, 50019 Sesto Fiorentino (FI), Italy

2. NEST, CNR - Istituto Nanoscienze and Scuola Normale Superiore, Piazza S. Silvestro 12, 56127, Pisa, Italy

3. ppqSense Srl, Via Gattinella 20, 50013 Campi Bisenzio FI, Italy

The terahertz (THz) domain, ranging from 0.1 to 10 THz has been for a long time a hard-to-access and thus underexploited spectral region. Different spectrometers have been developed to explore molecular transitions in this region, mostly based on second order frequency conversion setups. A major inconvenient of these beams is the low optical power (around 1  $\mu$ W) available for spectroscopy. This issue has been overcome by THz Quantum Cascade Lasers (QCLs), semiconductor-based laser sources allowing ad-hoc tailoring of their emission frequency, which optical power in continuous wave operation is in the mW range [1], [2].

THz QCLs have shown a very narrow intrinsic linewidth (in the order of  $\sim$ 100 Hz) [3], [4] that can be exploited for high precision spectroscopy by phase-locking the device emission to a spectrally pure local oscillator. One technique is to phase-lock the QCL emission to a free-standing THz frequency comb, generated by optical rectification of a fs-laser. The heterodyne detection is performed through a Hot Electron Bolometer (HEB), allowing efficient detection of the down-converted radio-frequency beatnote between a few percents of the QCL emission and one mode of the THz comb. This phase-locking procedure is illustrated in Fig. 1(b). With this experimental setup, almost all the QCL optical power is available for absorption spectroscopy, allowing accurate characterization of transitions, as for example the linecenter and pressure shift of a CH<sub>3</sub>OH rotational transition [5]. In order to overcome the  $4 \cdot 10^{-9}$  accuracy limit of this setup, imposed by the Doppler limited spectroscopy scheme, the Lamb-dip spectroscopy setup depicted on Fig. 1(a) has been built.

The optical system, composed by a quarter-waveplate and two orthogonal wire-grid polarizers (WGP), not only splits the QCL emission into pump and probe beams, but also minimizes their optical feedback on the laser, and allows their simultaneous detection with two room-temperature pyroelectric detectors. A 1:1 telescope, composed by two parabolic mirrors, is set around the gas cell, increasing the pump intensity to saturate the molecular transition. With this optical setup and phase-locked QCL, direct absorption signals have already been obtained, whereas Lamb-dip signals are soon expected to deliver an accuracy around  $10^{-10}$  on the molecular transition linecenters. Such an accuracy would enable studying the contributions of Zeeman, AC-Stark (Autler-Townes), and blackbody shifts that are difficult to observe, and that are expected around this uncertainty levels.

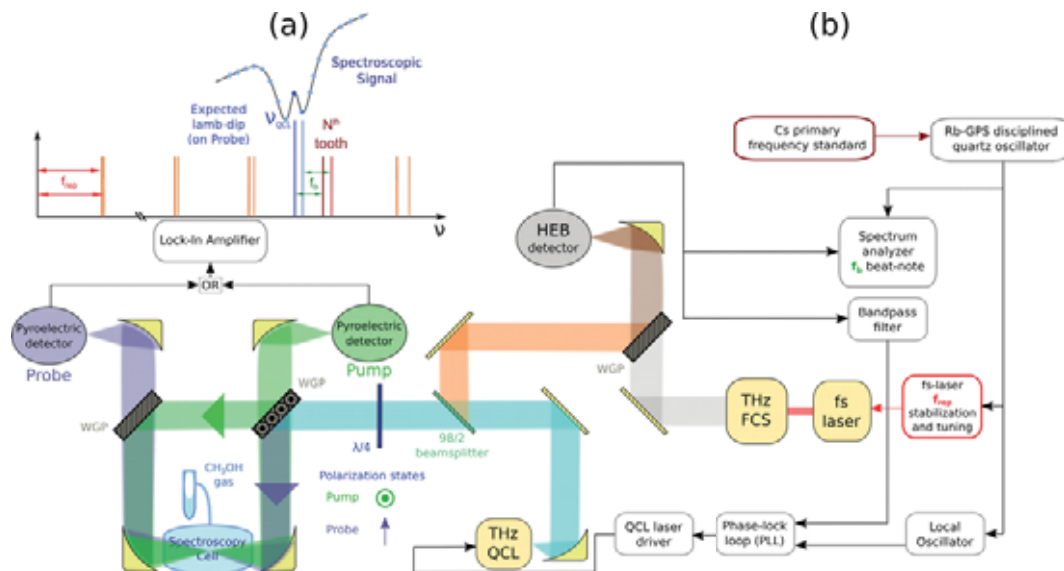


**Fig. 1** (a) Illustration of the Lamb-dip spectroscopy setup, the frequency of the phase-locked QCL can be tuned by changing the THz comb repetition rate ( $f_{rep}$ ). (b) The QCL emission linewidth is narrowed by the phase-locking to a free-standing THz frequency comb.

## References

- [1] J. Faist, F. Capasso, D. Sivco, C. Sirtori, A. Hutchinson, and A. Cho, "Quantum Cascade Laser," *Science*, vol. 264, p. 4, 1994.
- [2] M. S. Vitiello, G. Scalari, B. Williams, and P. De Natale, "Quantum cascade lasers: 20 years of challenges," *Opt. Express*, vol. 23, no. 4, p. 5167, Feb. 2015.
- [3] M. S. Vitiello *et al.*, "Quantum-limited frequency fluctuations in a terahertz laser," *Nat. Photonics*, vol. 6, no. 8, pp. 525–528, Jul. 2012.
- [4] M. Ravaro *et al.*, "Measurement of the intrinsic linewidth of terahertz quantum cascade lasers using a near-infrared frequency comb," *Opt. Express*, vol. 20, no. 23, p. 25654, Nov. 2012.
- [5] S. Bartalini *et al.*, "Frequency-Comb-Assisted Terahertz Quantum Cascade Laser Spectroscopy," *Phys. Rev. X*, vol. 4, no. 2, Apr. 2014.

# Time-gated back-scatter imaging in turbid media

David Sedarsky

Chalmers University of Technology

Highly scattering environments such as fuel injection sprays and turbid fluids present challenges to imaging diagnostics due to signal attenuation and multiple scattering that tends to obscure fluid structures and forces active in flow dynamics [1]. This underlying structural information is often important for understanding and correcting flow anomalies in such systems, e.g. primary breakup in high-pressure fuel injection sprays.

A series of three regeneratively amplified pulses  $\sim 100$  fs ultrafast pulses which can be positioned arbitrarily in time is used as input source light for back-scatter imaging. Detection and interpretation of the back-scatter signal is accomplished through the application of an optical Kerr-effect time-gate which filters the backscattered imaging light. Here the arrival time and delay-tuning of the detection can be used to spatially resolve the scattered light signal within the turbid measurement volume [2].

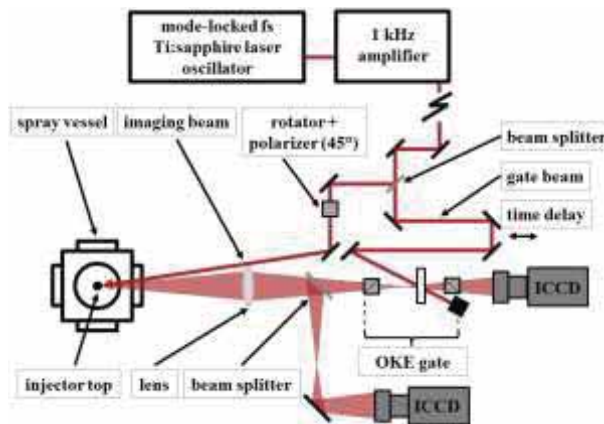


Fig. 1 Source light and gating setup for a single imaging pulse arrangement capturing backscatter and time-gated signal.

## References

- [1] W. Drexler and J.G. Fujimoto, *Optical coherence tomography*, 3rd. ed., (Springer, 2008).
- [2] M. P. Silverman, and W. Strange, "Object delineation within turbid media by backscattering of phase-modulated light," *Opt. Comm.* **144**, 7-11 (1997).



## Invited speaker



**Dr. Elena Obratsova**

### **Nanomaterials Spectroscopy Laboratory of A.M. Prokhorov General Physics Institute of Russian academy of Sciences (Moscow, Russia)**

Modified single-wall carbon nanotubes and graphene for saturable absorbers in solid state lasers

Elena Obratsova was graduated from the quantum radiophysics chair of the Physics Department of M.V. Lomonosov Moscow State University (MSU) in 1981. She got her PhD in optics at MSU in 1990. Since 1992, she worked at A.M. Prokhorov General Physics Institute of Russian Academy of Sciences (GPI RAS), heading the Nanomaterials spectroscopy laboratory since 2001. Since 2018 she is also a Head of Nanocarbon materials laboratory in Moscow Institute of Physics and Technology (MIPT), formed as a joint laboratory of Russian Academy of Sciences and MIPT. Her scientific interests concern synthesis, optical spectroscopy and applications of low-dimensional materials. Last years, she was involved in studies of different forms of nanocarbon. An important cycle of works on laser applications of carbon nanotubes and graphene was performed. She is a coauthor of more than 270 papers in reviewed journals. Her Hirsh factor is 32. She was a supervisor of 13 PhD theses defended. She is a coordinator of several national and international research projects and a member of the editorial advisory board of 2 international scientific journals: Carbon and Laser Physics Letters. 3 times she was a Guest editor of specials issues of "Journal of Nanoelectronics and Optoelectronics".

# Modified Single-Wall Carbon Nanotubes and Graphene for Saturable Absorbers in Solid State Lasers

Elena D. Obraztsova<sup>1,2</sup>

<sup>1</sup>A.M. Prokhorov General Physics Institute, RAS, Moscow, Russia

<sup>2</sup>Moscow Institute of Physics and Technology, Dolgoprudny, Moscow Region, Russia

In this work the progress achieved during last 10 years in application of carbon nanotube- and graphene-based saturable absorbers for solid state lasers is demonstrated.

Single-wall carbon nanotubes have many advantages for using as ultra-fast stable saturable absorbers: a wide working spectral range (0.7-3.0  $\mu\text{m}$ ), a femtosecond relaxation time of electronic excitations, a high thermal stability, a low threshold of “switching on” the mode locking regime. These advantages have been demonstrated for a wide class of solid state lasers (including fiber ones) with working wavelengths 0.7-2.0  $\mu\text{m}$  [1-4] (Fig.1a). The elements in different forms (aqueous suspensions, polymer composites with embedded nanotubes, coatings on mirrors, thin films for fiber laser connectors, etc. (Fig 1b)). Today the accent in research is shifted to the lasers working in spectral range of 2-3  $\mu\text{m}$  [5]. Such lasers are important for laser medicine and atmosphere diagnostics. The nanotubes of big diameter and specific functionalizations are needed to solve this task.

Another approach is graphene utilization. Graphene is a two-dimensional hexagonal carbon network with unique physical and chemical properties [6]. Multi-layer graphene is efficiently used for saturable absorbers. One layer of graphene absorbs 2.3 % of incident light. Due to the linear character of electron energy dispersion the working spectral range of graphene is practically unlimited. The results for CO<sub>2</sub> laser (with wavelength of 10  $\mu\text{m}$ ) are demonstrated [7].



Fig. 1. a) The working spectral range of solid state lasers for whose the mode locking regime has been realized with saturable absorbers based on single-wall carbon nanotubes;  
b) different forms of saturable absorbers based on single-wall carbon nanotubes  
(from left to right: aqueous suspension, polymer composite with embedded nanotubes, coatings on mirrors, thin film on the fiber cross-section in fiber laser connector).

The work was supported by RFBR projects 18-42-130001 and 18-29-19113.

## References

- [1] N.N. Il'ichev, E.D. Obraztsova, S.V. Garnov, S.E. Mosaleva “1.54 mm nonlinear transmission of single-wall carbon nanotube suspension in D<sub>2</sub>O; realization of self-mode-locking regime in Er<sup>3+</sup>-glass laser with nanotube-based Q-switcher”, *Quantum Electronics* **34**, 572(2004).
- [2] M.A. Solodyankin, E.D. Obraztsova, A.S. Lobach, A.I. Chernov, A.V. Tausenev, V.I. Konov, E.M. Dianov “1.93 mm mode-locked thulium fiber laser with a carbon nanotube absorber”, *Optics Letters* **33**,1336 (2008).
- [3] M. Zhang, E.J.R. Kelleher, A.S. Pozharov, E.D. Obraztsova, S.V. Popov, and J.R. Taylor “Passive synchronization of all-fiber lasers through a common saturable absorber”, *Optics Letters* **36**, 3984(2011).
- [4] A.A. Krylov, D.S. Chernykh, E.D. Obraztsova “Gyroscopic effect detection in the colliding-pulse hybridly mode-locked erbium-doped all-fiber ring soliton laser”, *Optics Letters* **42**,2439(2017).
- [5] S.A. Filatova, V.A. Kamynin, N.R. Arutyunyan, A.S. Pozharov, A.I. Trikshev, I.V. Zhlyuktova, I.O. Zolotovskii, E.D. Obraztsova, V.B. Tsvetkov “Hybrid mode-locking of an all-fiber holmium laser”, *JOSA B* **35**, 3122 (2018).
- [6] P.A. Obraztsov, M.G. Rybin, A.V. Tyurnina, S.V. Garnov, E.D. Obraztsova, A.N. Obraztsov and Yu.P. Svirko “Broadband Light-Induced Absorbance Change in Multilayer Graphene”, *NanoLetters* **11**, 1540 (2011).
- [7] V.R. Sorochenko, E.D. Obraztsova, P.S. Rusakov, M.G. Rybin, “Nonlinear transmission of CO<sub>2</sub>-laser radiation by graphene”, *Quantum Electronics* **42**, 907 (2012).

# Study of strain sensitivity and symmetry of color center in diamond nanoscale needles by contactless optical piezo-spectroscopy .

A.Vella, L. Rigutti, L. Venturi<sup>1</sup>, J. Houard<sup>1</sup>, A. Normand<sup>1</sup>, I. Blum, S.A. Malykhin<sup>2,3</sup>, A.N. Obraztsov<sup>2,3</sup>.

<sup>1</sup> Normandie Univ, UNIROUEN, INSA Rouen, CNRS, Groupe de Physique des Matériaux, 76000 Rouen, France.

<sup>2</sup> University of Eastern Finland, Department of Physics and Mathematics, Joensuu 80101, Finland

<sup>3</sup> M V Lomonosov Moscow State University, Department of Physics, Moscow 119991, Russia

In this work we report a method to perform optical piezo-spectroscopy of nanoscale systems by electrostatic field regulation.

The nanoscale systems studied are diamond needles containing color centers, that have been investigated since two decades, e.g., for the implementation of qubits in quantum informatics protocols [1]. Color centers in diamond have also unique applications as nanoscale field sensors. In particular, in the case of strain field, they are key components for the realization of strain-coupled hybrid spin-oscillator systems.

The photoemission of these centers is studied using a micro-photoluminescence ( $\mu$ -PL) system. The application of a high electrostatic field at the apex of monocrystalline diamond nanoscale needles induces an energy splitting of the photoluminescence lines of color centers [2].

The capabilities and unicity of our experimental set-up are presented by the study of the well-known  $NV^0$  color center in diamond. After that, the strain sensitivity of the color center emitting at 2.65 eV is studied. We compare the strain sensitivity of this center with that of the well-known neutral nitrogen-vacancy ( $NV^0$ ) center. We show that the 2.65 eV center has a higher strain sensitivity than the  $NV^0$  center and can be explored as strain sensor and/or for strain-coupled systems. Moreover, we perform polarization-resolved photoluminescence (PL) spectroscopy under a high uniaxial tensile stress and the polar behavior reported for the 2.65 eV center points out to a defect symmetry which is different from that of  $NV^0$  center.

We also discuss recent results obtained by multiphoton excitation of the  $\mu$ -PL signal of  $NV^0$  color center.

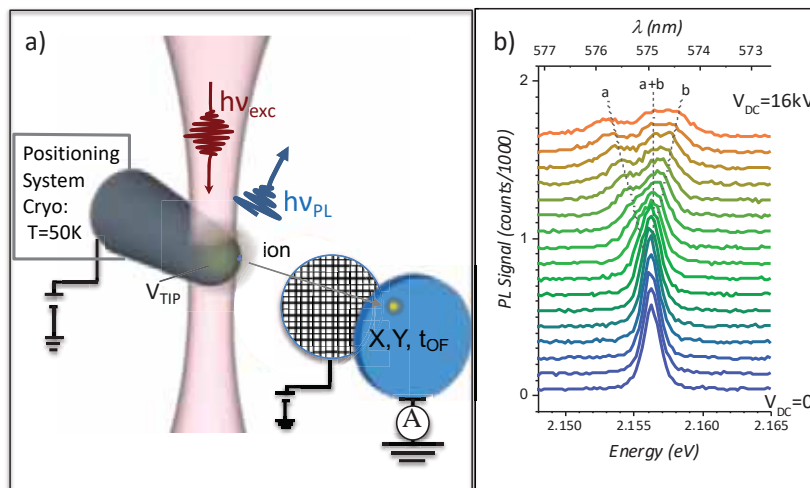


**Fig. 1** The needle specimen is inserted in a vacuum chamber equipped with an in situ photoluminescence bench, an ion spectrometer and a position and time sensitive detector. The high voltage applied to the tip leads to an intense electric field at the specimen's apex, which allows field evaporation of ions. Moreover, laser pulses can trigger ion evaporation and photon emission. (b) The photoluminescent signal of the  $NV^0$  center acquired for different values of the applied voltage.

## References

[1] Kurtsiefer et al., *Stable Solid-State Source of Single Photons*. *Phys. Rev. Lett.* **2000**, 85 (2), 290–293.

[2] L. Rigutti, et al., *Optical Contactless Measurement of Electric Field-Induced Tensile Stress in Diamond Nanoscale Needles*. *Nano Lett., ACS Pub.*, **2017**.

# Classical Representation of Non-Linear Response Functions and their Connections to Quantum-Mechanical Graphic Representations Based on Double-Sided Feynman Diagrams and Liouville Space Coupling Scheme

Michele Marrocco

ENEA, CR-Casaccia, via Anguillarese 301, IT-00123 Rome, Italy

The non-linear dielectric susceptibility represents the material response function that is at the core of the quantum-mechanical description of non-linear optical interactions [1]. These, according to the most advanced treatment (Liouville-von Neumann equation for the density operator), are summarized by either the pictorial language of the double-sided Feynman diagrams or the schematic interpretation emerging from the Liouville space pathways.

In addition to such complex syntheses of wave mixing, optical non-linearity can also be introduced at a very basic level within the classical context of damped anharmonic oscillators (Lorentz model) as taught by the founders of non-linear optics [2, 3]. However, it is known that the classical picture differs significantly from quantum-mechanical approaches. According to Boyd [3], the primary shortcoming of the classical model is the restriction to a single resonance frequency for each atom or molecule (for example, see the classical derivation of non-linear Raman scattering by Yariv [4]) and the recovery of quantum-mechanical results is thus limited to those cases in which all the optical frequencies lie well below the lowest atomic or molecular resonance.

Here, we present an attempt at a classical description that is free from the limitations of the traditional approach. The attempt is based on a perturbative method conceived in close analogy with the perturbative technique employed in the Schrödinger and density matrix representations of the response function. Taking inspiration from the propagation of light in crystals [5], bound electrons are pictured as attached to a set of fictitious elastic springs (under weak coupling regime) that emulate the quantum-mechanical resonances (Fig. 1a). In this manner, traveling electric fields interact with a set of oscillators (i.e., dipoles under electric-dipole approximation) whose partial displacements add up to form the final electron displacement that build up the optical response. It is finally shown that it is possible to establish a graphic correspondence between classical and density matrix representations of non-linear susceptibilities (Fig. 1b).

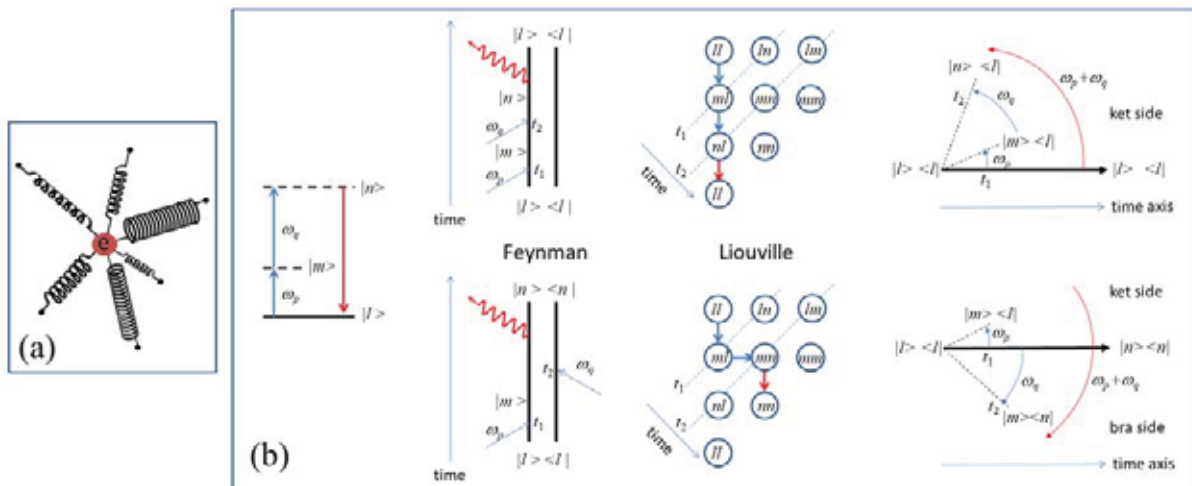


**Fig. 1** (a) A bound electron is pictured as attached to several springs whose oscillation frequencies correspond to the optical resonance frequencies. (b) Traditional energy level scheme (on the left) does not help to follow the time evolution of the atomic or molecular internal state and it might appear that the final state is always coincident with the initial state. Time evolution is instead considered in double-sided Feynman diagrams and Liouville space pathways for two terms among eight of the second-order susceptibility). In the upper Feynman diagram and upper Liouville scheme, the final state coincides with the initial state. In the lower Feynman diagram and lower Liouville scheme, the final state differs from the initial state. The classical counterparts of diagrammatic time evolution for these two different cases could be arranged as shown on the right side.

## References

- [1] S. Mukamel, *Principles of Nonlinear Optical Spectroscopy*, (Oxford University Press, New York, 1995).
- [2] N. Bloembergen, *Nonlinear Optics*, (W. A. Benjamin Inc., New York, 1965).
- [3] R. W. Boyd, *Nonlinear Optics*, 3rd ed., (Academic Press, San Diego, 2008).
- [4] A. Yariv, *Quantum Electronics*, 2nd ed., (John Wiley, New York, 1975).
- [5] G. R. Fowles, *Introduction to Modern Optics*, 2nd ed., (Dover, New York, 1989).

# Experimental Determination of the Potential Energy Function of the Copper Dimer Ground State

*Peter Bornhauser, Qiang Zhang, Martin Beck, Peter P. Radi*  
Paul Scherrer Institute, 5232 Villigen, Switzerland

The copper dimer has attracted much interest from both experimentalists and theorists owing to the relatively simple electronic configuration, the closed d shell and the filled orbital in its electronic ground state, which makes it a good starting point to understand bonding properties of electronically more complex transition metal dimers. In this talk, we present a spectroscopic study of dicopper aimed at mapping out its electronic ground state potential energy function at high precision. The  $\text{Cu}_2$  molecules are produced in a home-built laser vaporization source and cooled by a near supersonic expansion in a molecular beam environment. Rotationally resolved stimulated emission pumping (SEP) spectra have been recorded for both main isotopologues,  $^{63}\text{Cu}_2$  and  $^{65}\text{Cu}^{63}\text{Cu}$ , by applying non-linear two-color resonant four-waving mixing (TC-RFWM). Double-resonance schemes involving perturbation assisted excitations opened ways to access high-lying vibrational levels of the ground state. The determined energies and inertial rotational constants of  $v$  up to 103 are analyzed by using a near-dissociation equation taking into account the dominant long-range dispersion term. The applied iteration procedure yields an accurate RKR potential and refined molecular constants up to the dissociation asymptote. We report the determined dissociation energy and the vibrational quanta at the upper limit of the bonding. These experimental results extend our knowledge of the copper dimer bonding and provide a benchmark for assessing the accuracy of ab initio calculation.

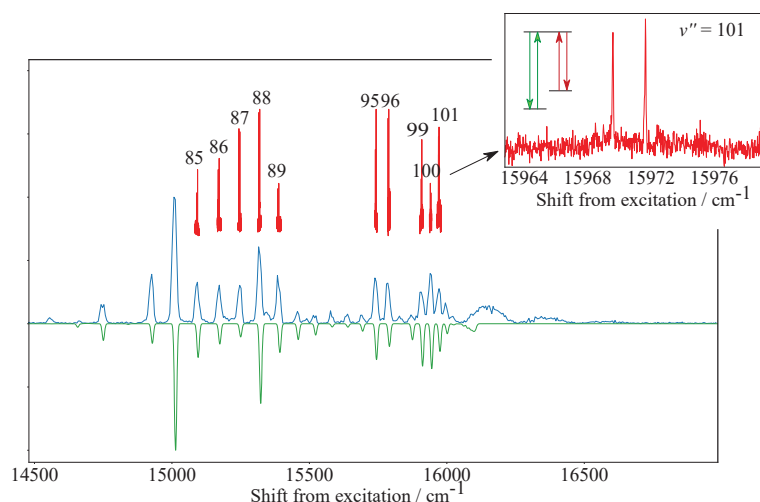


**Fig.1** Dispersed fluorescence and TC-RFWM spectra to high lying vibrational levels in the ground state  $X^1\Sigma_g^+(0_g^+)$  of  $^{65}\text{Cu}^{63}\text{Cu}$ . Fluorescence is excited by using the P(18) line of the  $G62 - X(v=0)$  transition. Significant emission is observed to levels up to  $v=101$  of the ground state (upper trace, blue). The inverted trace is a simulation taking into account the line positions and intensities determined in this work. The offset traces show separate SEP-type TC-RFWM scans of the PROBE laser. As for dispersed fluorescence, the PUMP lasers are tuned to P(18) of line of  $G62 - X(v=0)$ . The inset is an expanded representation of the four-wave mixing PROBE scan displaying the P(18) and R(16) branch of the excited  $J'=17$  level.

# Rotational echoes: a versatile tool for investigating ultrafast dissipation

Haisu Zhang<sup>1</sup>, Junyang Ma<sup>1,3</sup>, Bruno Lavorel<sup>1</sup>, Franck Billard<sup>1</sup>, Jean-Michel Hartmann<sup>2</sup>, Edouard Hertz<sup>1</sup>, Erez Gershnel<sup>4</sup>, Yehiam Prior<sup>4</sup>, Jian Wu<sup>3,†</sup>, Ilya Sh. Averbukh<sup>4,‡</sup>, and Olivier Faucher<sup>1,\*</sup>

<sup>1</sup>Laboratoire Interdisciplinaire Carnot de Bourgogne, UMR No. 6303, CNRS, Université Bourgogne Franche-Comté, 9 Avenue A. Savary, BP 47870, 21078 Dijon Cedex, France

<sup>2</sup>Laboratoire de Météorologie Dynamique/IPSL, CNRS, École polytechnique, Sorbonne Université, École Normale Supérieure, PSL Research University, F-91120 Palaiseau, France

<sup>3</sup>State Key Laboratory of Precision Spectroscopy, East China Normal University, Shanghai 200062, China

<sup>4</sup>Department of Chemical and Biological Physics, the Weizmann Institute of Science, Rehovot 76100, Israel

<sup>†</sup>[jwu@phy.ecnu.edu.cn](mailto:jwu@phy.ecnu.edu.cn)

<sup>‡</sup>[ilya.averbukh@weizmann.ac.il](mailto:ilya.averbukh@weizmann.ac.il)

<sup>\*</sup>[olivier.faucher@u-bourgogne.fr](mailto:olivier.faucher@u-bourgogne.fr)

The present work demonstrates the utilization of rotational echoes of molecular alignment for investigating ultrafast collisional dissipation of molecules. As the first step, the echo response of single CO<sub>2</sub> molecules, kicked by two non-resonant ultrashort laser pulses (denoted as  $P_1$  and  $P_2$ ) with parallel polarizations, is studied both experimentally and theoretically. The rotational echo manifests itself as a transient restoration of molecular alignment with respect to the polarization direction of the two pump pulses, at the instant of  $t=2\tau_{12}$ , with  $t$  the elapsed time after  $P_1$  and  $\tau_{12}$  the temporal delay between  $P_1$  and  $P_2$ . The strength of the rotational echo is found to oscillate when changing the delay  $\tau_{12}$  between  $P_1$  and  $P_2$ , which is in sharp contrast to the traditional spin [1] and photon [2] echoes observed in inhomogeneously broadened two-level systems. The latter echo response is conserved when scanning the delay between the two excitation pulses in decoherence-free conditions. Further analysis reveals the entangled effects of the intensity  $I_2$  and delay  $\tau_{12}$  of the rephasing pulse ( $P_2$ ) in rotational echoes. This behavior is also well predicted by the classical theory of rotational echo based on the kick-induced filamentation in the phase-space of 2D rigid-rotors [3-5].

The echo response of single molecules is quickly damped at increasing densities, due to the decoherence process incurred by frequent collisions with adjacent molecules. In order to get unambiguous access to the collisional dissipation of molecules, the echo response of single molecules is optimized to be relatively flat for a limited range of  $\tau_{12}$  by setting a compromised intensity of  $P_2$ . Then the flattened echo response is effectively employed to measure the collision-induced rotational relaxation of CO<sub>2</sub> molecules, at high pressure (large density) and/or diluted with large density He atoms, up to 50 bar where the quantum revival of molecular alignment induced by a single pump pulse is fully extinguished due to its long revival time. The decay time constant  $\tau_E$  for the rotational echo, extracted from the measurements of the collisional decay of echo conducted at a series of pressures, is found to be in good agreement with the decay time constant  $\tau_R$  obtained by measuring the collisional decay of alignment revivals [6], both in the CO<sub>2</sub>-He mixture and pure CO<sub>2</sub>. This important finding corroborates the dominance of inelastic collisions during the collisional dissipation of molecules. A natural and tempting extension of the present method would thus be to carry similar investigations in the liquid phase for which any rotational information or coherence imprinted in the system has vanished due to very quick thermalization at time scales of a few ps.

[1] E. L. Hahn, Phys. Rev. **80**, 580 (1950).

[2] N. A. Kurmit, I. D. Abella, and S. R. Hartmann, Phys. Rev. Lett. **13**, 567 (1964).

[3] G. Karras, E. Hertz, F. Billard, B. Lavorel, J. M. Hartmann, O. Faucher, E. Gershnel, Y. Prior, and I. Averbukh, Phys. Rev. Lett. **114**, 153601 (2015).

[4] G. Karras, E. Hertz, F. Billard, B. Lavorel, G. Siour, J. M. Hartmann, O. Faucher, E. Gershnel, Y. Prior, and I. S. Averbukh, Phys. Rev. A **94**, 033404 (2016).

[5] K. Lin, P. F. Lu, J. Y. Ma, X. C. Gong, Q. Y. Song, Q. Y. Ji, W. B. Zhang, H. P. Zeng, J. Wu, G. Karras, G. Siour, J. M. Hartmann, O. Faucher, E. Gershnel, Y. Prior, and I. S. Averbukh, Phys. Rev. X **6**, 041056 (2016).

[6] T. Vieillard, F. Chaussard, F. Billard, D. Sugny, O. Faucher, S. Ivanov, J. M. Hartmann, C. Boulet, and B. Lavorel, Phys. Rev. A **87**, 023409 (2013).





## Invited speaker

Dr. Caterina Merla

**ENEA, Division of Health Protection Technologies  
(Rome, Italia)**

Wide field CARS microspectroscopy and real-time follow-up of hydration changes induced by electropulsation of liposomes

Caterina Merla received her PhD in electronic engineering in 2008 on electromagnetic modelling of cells in the framework of bioelectromagnetic studies. Caterina Merla received the “Young Scientist Award” from the International Union of Radio-Science URSI, in 2008 at the General Assembly in Chigago, IL USA, for her work of thesis. Then, she worked as a post-doc from 2008 to 2012 at XLIM CNRS-University of Limoges France, and at the Inter-University Centre for the Study of Electromagnetic Fields and Biosystems (ICEmB, Univ. Genoa) Italy. She was researcher at Light University, Bethlehem PA USA, in 2012; since 2013 she is researcher at ENEA (National Italian Agency for Energy and New Technolgoies) CR Casaccia, Rome Italy.

In 2015, she was the recipient of a H2020 Marie Sklodwska Curie Action Individual-Fellowship (g.a. 661041 OPTIC-BIOEM) at CNRS UMR 8203, Institute Gustave Roussy, Villejuif France studing cell electropermeabilization mechanisms using non-linear optics. Now, Caterina Merla is co-PI for ENEA of a H2020-FETOPEN-2016-2017 action, g.a. 737164, – SUMCASTEC (Semiconductor-based Ultra-wideband Micromanipulation of CAncer STEm Cells).

Caterina Merla is author of 41 articles (H-index of 17) in the field bioelectromagnetics and bioelectrochemistry on international peer reviewed journals, and over 100 contributions to international conferences. C. Merla has been invited as speaker in different international conferences, she chaired and organized various sessions at international meetings, she has been member of scientific committees. She participates in editorial boards (Frontier in Public Health-Radiation and Health) and acts as reviewer for various international journals. C. Merla has numerous international collaborations both in EU and US.

# Correction of plasma emission in reflectivity spectroscopy during sputtering deposition

Iryna Gozhyk<sup>1</sup>, Letian Dai<sup>1</sup>, Quentin Hérault<sup>1</sup>, Ekaterina Burov<sup>1</sup>, Hervé Montigaud<sup>1</sup>, Rémi Lazzari<sup>2</sup> and Sergey Grachev<sup>1</sup>

1. Surface du Verre et Interfaces (SVI), UMR 125 CNRS/Saint-Gobain Recherche,  
39 quai Lucien Lefranc, 93303 Aubervilliers, France

2. CNRS UMR 7588, Sorbonne Université, Institut des NanoSciences de Paris, 4 place Jussieu,  
75005 Paris, France

Nowadays, magnetron sputtering is a standard and mostly used technique for deposition of thin inorganic films in coating industry. Unlike thermal evaporation, sputtering requires the generation of plasma to sputter off target material to the sample, resulting in a vaster range on materials that can be deposited (metals and also dielectrics). Moreover, the growth rate in sputter deposition is rather high compared to evaporation (up to  $\sim 10 \text{ nm} \cdot \text{s}^{-1}$ ), which together with the presence of energetic species impacts significantly the kinetics of the growth and microstructure of the films.

Due to harsh environment inside deposition chamber, there are few in situ and real-time monitoring tools applicable to sputtering: resistivity [1], stress measurement [2] or spectroscopic techniques [3]. The latter two allow monitoring the very first stages of growth, initial nucleation and growth of isolated islands in the case of Volmer–Weber growth. In particular, spectroscopic reflectivity measurements can be interpreted with the optical models on supported plasmonic nanoparticles [4], allowing for in-situ monitoring of the shapes of growing nanoparticles. This is crucial for understanding of how the physical and process parameters of deposition impact the microstructure of resulting thin films.

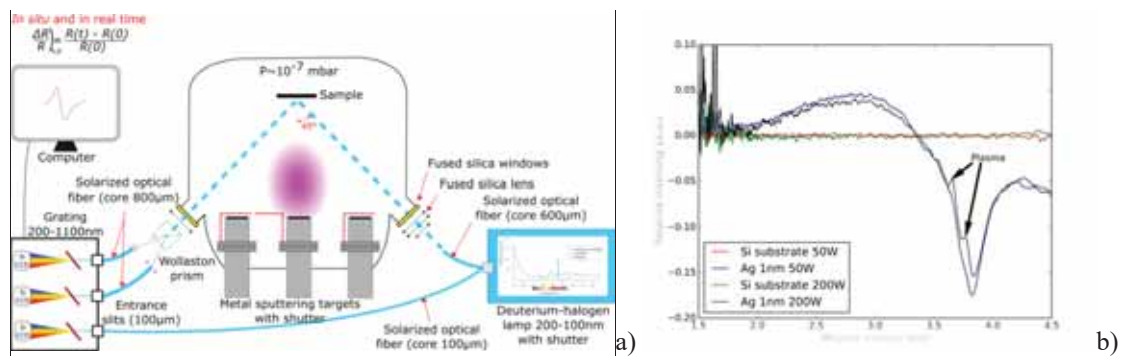


Fig. 1 SDRS setup II Surface differential reflectivity spectroscopy coupled to sputtering deposition chamber: a) schematic drawing; b) illustration of plasma impact on p-polarized SDRS spectra.

Surface differential reflectivity spectroscopy (SDRS, [3]) has already been successfully applied during the sputter deposition. Yet, in this case the recorded spectra contain not only the s- and p-polarized components of reflected probe light but also the spurious light originating from the optical emission of the plasma. For some deposition parameters this impact can significantly alter SDRS spectra (Fig.1) thus complicating their interpretation. In this work we provide a thorough study of the spurious plasma emission during sputtering deposition of thin silver film on silicon wafers. Two components of spurious emission are identified: (i) direct one, constant during the deposition and (ii) reflected from the sample surface, thus evolving during the deposition. Finally, we propose a measurement protocol of signal correction, which thanks to suitable measurements before and after the growth allow to get rid of the spurious plasma contribution in SDRS spectra.

## References

- [1] Fukuda K, Lim S H M and Anders A “Coalescence of magnetron-sputtered silver islands affected by transition metal seeding (Ni, Cr, Nb, Zr, Mo, W, Ta) and other parameters” *Thin Solid Films* **516**, 4546–52 (2008).
- [2] Abadias G, Simonot L, Colin J J, Michel A, Camelio S and Babonneau D “Volmer–Weber growth stages of polycrystalline metal films probed by in situ and real-time optical diagnostics” *Appl. Phys. Lett.* **107** 183105 (2015)
- [3] Chason E and Guduru P R “Tutorial: understanding residual stress in polycrystalline thin films through real-time measurements and physical models” *J. Appl. Phys.* **119** 191101 (2016)
- [4] Lazzari R and Simonsen I “GranFilm : a software for calculating thin-layer dielectric properties and Fresnel coefficients” *Thin Solid Films* **419** 124–36 (2002).

# Wide field CARS microspectroscopy and real-time follow-up of hydration changes induced by electropulsation of liposomes

C. Merla<sup>1,2</sup>, M. Nardoni<sup>3</sup>, M. Scherman<sup>4</sup>, S. Petralito<sup>3</sup>, F. Apollonio<sup>5</sup>, M. Liberti<sup>5</sup>, P. Paolicelli<sup>3</sup>, L. M. Mir<sup>1</sup>,  
Brigitte Attal-Tretout<sup>4</sup>

<sup>1</sup>Vectorology and Anticancer Therapies, UMR 8203, CNRS, Univ. Paris-Sud, Gustave Roussy, Université Paris-Saclay, 94805 Villejuif, France

<sup>2</sup>Division of Health Protection Technologies, ENEA National Italian Agency for Energy and New Technologies, 00123 Rome, Italy

<sup>3</sup>Department of Drug Chemistry and Technologies, Sapienza University of Rome, 00185 Rome, Italy

<sup>4</sup>ONERA, BP 80100, 91123 Palaiseau Cedex, France

<sup>5</sup>Department of Information Engineering Electronic and Telecommunication, Sapienza University of Rome, 00184 Rome, Italy

To deep more insight into basic phenomena occurring during and after electropulsation of biological membranes, a new experimental modality has been used combining a wide field Coherent Anti Stokes Raman Spectroscopy system [1] with a coplanar wave guide able to deliver nanosecond pulsed electric fields to different *in vitro* samples [2]. This setup allows to acquire CARS hyper-spectra at specific Raman bands from 2900 to 3500  $\text{cm}^{-1}$  (into the so called water vibration region) as well as to acquire in real time the CARS signature at specific wavelengths with a temporal resolution of few ns. This time scale is comparable to the duration of the electrical stimulation synchronised to the laser emission. As the biophysical and chemical bases of cells electropermeabilization are still debated, our setup allows the experimental assessment of the role of water molecules and phospholipid bilayers during the occurrence of this phenomenon which is used in various biotechnological, biological and medical applications.

Our experiments have been conducted on liposome suspensions placed between the central and lateral (ground) electrodes a grounded closed coplanar waveguide (GCCPW) [2], assuring the transmission of short electric pulses (10 ns) to the biological samples without distortions. Liposomes, that is lipid spherical unilamellar vesicles, were chosen as a suitable synthetic system to mimic phospholipid double layers as they are similar to the structure of real cell membranes. The GCCPW inter electrodes gap was fixed to 0.5  $\mu\text{m}$  in order to allow the pump and Stokes laser beams (diameters of about 100  $\mu\text{m}$ ) alignment and focusing into the liposomes suspension in a controlled way. The liposome suspension was contained in a PDMS holder with a total volume of 30  $\mu\text{L}$ . The illumination scheme of the CARS microscope followed a non-phase-matched geometry as suggested in [1]. The pump/probe laser axis was kept parallel to the microscope objective one, while the Stokes beam was tilted by 7° to efficiently attenuate the non-resonant signal. Spectra of liposomes suspensions were acquired immediately after electropulsation evidencing an increase of the vibrational modes around 3345  $\text{cm}^{-1}$  in the pulsed samples with respect to the non-pulsed one. Pulsed samples received 2000 pulses consecutively at 1 Hz and at an amplitude of 9 MV/m. This vibrational signature (3345  $\text{cm}^{-1}$ ) seems to be related to the so called lipid associated water molecules, representing a water structure in which the intermolecular OH bonds become weak (asymmetric OH stretch modes) leading to the interaction of single water molecules with lipids. This association makes the pulsed membrane more permeable due to this less organized and persistent structure of the water molecules. The appearance of this vibrational mode has been also verified during the exposure, in real-time specific experiments. Finally, the effective permeabilization of liposome suspensions after the electric pulses delivery was verified looking at the release of a fluorescent dye (5-6-carboxyfluorescein) included into the liposomes' core. Dynamic light scattering measurements (performed before and after the electric pulses exposure) demonstrated the maintenance of the vesicles integrity supporting the permanent hydration of the liposome membranes after electropulsation.

In summary, CARS, employing nanosecond lasers pulses and the properties of our wide field microscope and its intrinsic ability to sense complex interferences, has provided us with an appropriate diagnostic tool. Thanks to this setup, we were able to observe the spectra arising from interfacial and interstitial water molecules in liposome suspensions. The liposomes permeabilization was also confirmed by 5-(6) CF release after the exposure evidencing the interest of our results not only for the basic understanding of electropulsation mechanisms but also for their possible exploitation to smart drug delivery applications mediated by electric pulses. In a future, the underlined mechanism will be investigated on cells, hence taking into account recovery processes of cell membranes as well as the different interactions elicited by the application of longer  $\mu\text{s}$  electric pulses.

**Acknowledges:** Funding from European Union's Horizon 2020 Research and Innovation Program under Marie Skłodowska-Curie IF grant agreement No. 661041 OPTIC BIOEM are greatly acknowledged. This work was also supported by CNRS, Univ. Paris-Sud, Gustave Roussy, ITMO Plan Cancer ("Project Dynamo") and ONERA; it was also performed in the framework of the European Associated Laboratory (LEA) entitled "Pulsed Electric Fields Applications in Biology and Medicine" (EBAM), and the COST Action BM1609 EMF-Med (European network for innovative uses of electromagnetic fields in biomedical applications).

**References:**

- [1] A. Silve, N. Dorval, T. Schmid, L. M. Mir, and B. Attal-Trétout, A wide-field arrangement for single shot CARS imaging of living cells. *J. Raman Spectrosc*, 43, 644-650, 2012.
- [2] C. Merla, M. Liberti, P. Marracino, A. Muscat, A. Azan, F. Apollonio, L. M. Mir, A wide-band bio-chip for real-time optical detection of bioelectromagnetic interactions with cells. *Scientific Reports*, 8, 5044, 2018.

# Confocal Raman Microspectroscopy to Investigate the Consequences of the Delivery of Electric Pulses to Live Cells.

Antoine Azan<sup>1</sup>, Valérie Untereiner<sup>2,3</sup>, Cyril Gobinet<sup>2</sup>, Olivier Piot<sup>2,3</sup>, Marie Breton<sup>1</sup>, Guilhem Gallot<sup>4</sup>, Michael Scherman<sup>5</sup>, Brigitte Trétout-Attal<sup>5</sup> and Lluís M. Mir<sup>1</sup>

1. Vectorology and Anticancer Therapies, UMR 8203, CNRS, Univ. Paris-Sud, Gustave Roussy, Université Paris-Saclay, F-94805 Villejuif, France

2. BioSpecT, EA7506, University of Reims Champagne-Ardenne, Reims, France

3. Cellular and Tissular Imaging Platform PICT, Faculty of Pharmacy, University of Reims Champagne-Ardenne, Reims, France

4. Laboratoire d'Optique et Biosciences, Ecole Polytechnique, CNRS, INSERM, Route de Saclay, 91128 Palaiseau, France

5. ONERA, BP 80100, 91123 Palaiseau Cedex, France

Confocal Raman microspectroscopy [1] was used to study the effect of pulsed electric fields on live cells. This bioelectromagnetic interaction is known to induce the permeabilization of the plasma membrane [2] which is a long-lived state (several minutes at room temperature, and longer at lower temperatures). Electroporation has led to medical application such as electrochemotherapy, which combines tumor electroporation and specific chemotherapy.

Raman signatures of live human adipose-derived mesenchymal stem cells exposed or not to pulsed electric fields (8 pulses, 1 000 V/cm, 100  $\mu$ s, 1 Hz) were acquired at several cellular locations (nucleus and cytoplasm at cathodic, anodic and antipole places) and two spectral bands (600–1 800  $\text{cm}^{-1}$  and 2 800–3 100  $\text{cm}^{-1}$ ). During the spectra acquisition, the cells were maintained at 4°C since it is known that at this temperature cells remain permeable until temperature is increased again. No effect on cell viability was caused by this incubation, at least for one hour as respected in our spectra acquisitions.

The electroporation process causes modifications of the vibrational modes of proteins (phenylalanine and amide I) and lipids with a statistically significant difference. The relative magnitude of four phenylalanine peaks decreased in the spectra of the pulsed group. On the contrary, the relative magnitude of the amide I band at 1658  $\text{cm}^{-1}$  increased by 40% when comparing pulsed and control group. No difference was found between the control and the pulsed group in the high wavenumber spectral band. Our results reveal the modification of proteins in living cells exposed to pulsed electric fields by means of confocal Raman microspectroscopy.

We also acquired spectra of cells submitted to 8 pulses of 100  $\mu$ s at different field amplitudes. Unexpectedly significant differences were found between the spectra obtained from cells exposed to pulses leading to reversible electroporation or irreversible electroporation (as revealed by classical electroporation tests using the same cells under identical conditions). Reversibility of the spectral changes as a function of the incubation temperature during spectra acquisition was also analyzed.

These studies show the way in which confocal RAMAN microspectroscopy can contribute to the analysis of cell electroporation and reveal the complexity of the molecular changes occurring in the cells exposed to electroporation electric pulses.

## References

- [1] A. Downes, "Raman Microscopy and Associated Techniques for Label-Free Imaging of Cancer Tissue," *Appl. Spectrosc. Rev.*, 50, 8, July 2015, pp. 641–653, doi: 10.3390/s100301871.  
[2] C. Chen, S. W. W. Smye, M. P. P. Robinson, and J. A. A. Evans, "Membrane electroporation theories: a review.," *Med. Biol. Eng. Comput.*, 44, 1–2, March 2006, pp. 5–14, doi: 10.1007/s11517-005-0020-2.

# Time –and polarization-resolved CARS spectroscopy of $\alpha$ -DNBP (2-(2,4-dinitrobenzyl)pyridine) in the electronic ground state

Vikas Kumar, Sebastian Küpper, Sebastian Schlücker

Department of Chemistry, University of Duisburg-Essen, Universitaetsstr. 5, D-45141 Essen, Germany.

Investigating the photochromic molecule 2-(2,4-dinitrobenzyl)pyridine ( $\alpha$ -DNBP), a reversible light-driven intramolecular proton transfer system, has a long history due to potential technological applications in data storage (optical switch). UV irradiation (ca. 370-420 nm) converts  $\alpha$ -DNBP into a blue coloured tautomer [1]. Although the structure of this phototautomer is now considered as well known, the environment-dependent reaction mechanisms and reaction intermediates involved are still not fully understood. Coherent anti-Stokes Raman scattering (CARS) can be used as a spectroscopic tool to investigate these parameters by observing time lapses of  $\alpha$ -DNBP in ground state turning to excited state tautomers. Here we present our initial CARS results on the thermodynamically stable (ground state) tautomer of  $\alpha$ -DNBP. Since conventional CARS signal is limited by the inherently present nonresonant background (NRB), we incorporated ‘magic angle polarization’ [2] in folded-BOXCARS geometry for NRB-suppression in our CARS setup, while a ‘delayed probe’ provides time-resolved (TR) observation of dephasing of vibrational modes.

Our CARS setup is based on three optical parametric amplifiers (OPAs) synchronously pumped by a 6W-fs amplified Yb-laser. Each OPA provides 20kHz, 50-fs pulses tunable in the range 640-920 nm. The direct outputs of the first two OPAs provide femtosecond (fs) Raman-pump at 670nm and the tunable fs Stokes pulses respectively, while a part of the first OPA output is spectrally filtered to provide  $\sim$ 1 ps narrowband ( $\sim$ 15 $\text{cm}^{-1}$ ) probe pulses at 667.7 nm. The fs-pump/Stokes pulses generate broadband vibrational coherence in the sample, while ps-probe gives spectral resolution to CARS spectra. The third OPA output is frequency-doubled in a BBO crystal to synthesize a fs-tunable UV pump beam for excitation CARS. The Raman-pump, Stokes and probe pulses are spatially and temporally synchronized on the sample and generated CARS signal is collected through a grating-based spectrometer onto a CCD detector. Figure (1a) shows an acquired TR polarization CARS spectra of 2M  $\alpha$ -DNBP solution in chloroform at various probe pulse delays, while Fig (1d) such spectra but at time zero. Fig(1b) displays CARS intensity profile along probe-delay depicting decay times of different vibrational modes. Fig (1c) shows how presence of NRB without polarization geometry distorts CARS spectra at time zero.

In future studies we will perform UV pump/CARS probe experiments for investigating the reaction pathways of the ultrafast photo-excited intramolecular proton transfer in  $\alpha$ -DNBP.

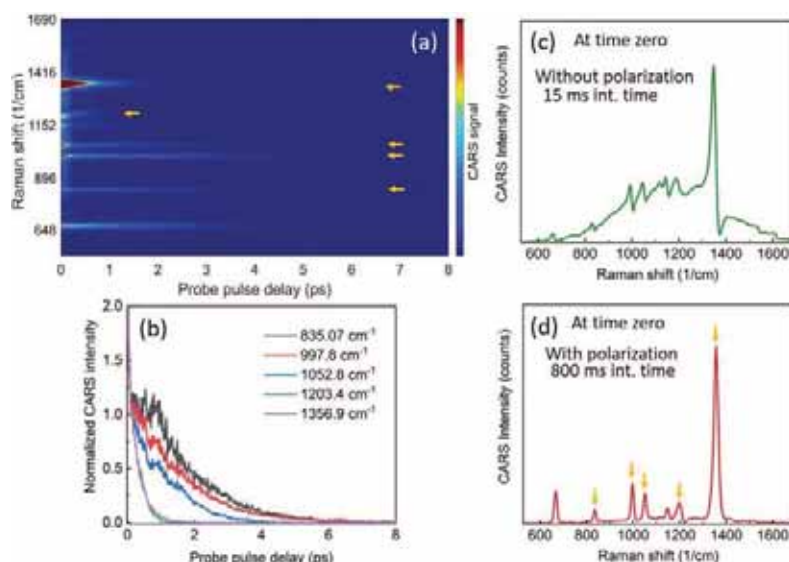


**Fig. 1** Broadband CARS spectra of  $\alpha$ -DNBP in chloroform (electronic ground state): (a) with probe pulse delay in TR polarization; (b) normalized CARS intensity profile along probe-delay depicting different decay times of the modes; at time zero (c) without and (d) with polarization geometry. Yellow arrows indicate vibrational Raman bands of  $\alpha$ -DNBP, other peaks are from the solvent chloroform.

## References

- [1] T. Nunes, Y Eichen, M Bastos, H D Burrows and H P Trommsdorff, J. Phys. D: Appl. Phys. **32**, 2108 (1999).
- [2] N. Kohles and A. Laubereau, Appl. Phys. B **39**,141-147 (1986).

# Structured illumination experiments with vortex beams

Marc Ziegler, Bernd Hönerlage, Mathieu Gallart, and Pierre Gilliot\*

<sup>1</sup>*Institut de physique et chimie des matériaux de Strasbourg  
UMR7504 CNRS- Strasbourg University,  
23, rue du Læss, B.P. 43, F-67034 STRASBOURG CEDEX, FRANCE*

\*Corresponding author: Pierre.gilliot@ipcms.unistra.fr

The optical properties of nanoobjects and nanostructures are a growing research subject. However, performing nonlinear (NL) or time-resolved (TR) spectroscopy experiments on a microscopic scale that goes beyond the sample spatial inhomogeneities, remains a challenge. Structured illumination methods allow for increased spatial resolution that can be further improved using nonlinearities [1]. This technique can then be transposed from photo-luminescence to Pump-and-Probe or Four-Wave Mixing (FWM) experiments that aim at measuring ultrafast dynamics.

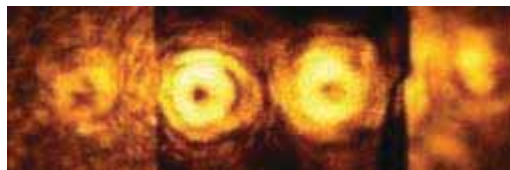


Figure 1: Beam profiles. Middle:  $\lambda_b=2$  and  $\lambda_a=1$  incident beams.  
Left:  $\lambda_{out}=2\lambda_b - \lambda_a=3$  and right  $\lambda_{out}=2\lambda_b - \lambda_a=0$  FWM signals

We have demonstrated through experiments on semiconductor quantum wells [2], that the use of light pulses with Laguerre-Gauss (LG) modes allows for the measurement of coherence times, i.e. that the optical angular momentum (OAM), (here labelled  $\lambda_i$  for the different beams “i”) is transferred to and then conserved by the electronic excitations, allowing time-resolved experiments. Our experiments show that it is possible to detect a FWM signal using its OAM conservation law given by  $\lambda_{out}=2\lambda_b - \lambda_a$  in a collinear configuration instead of the usual k-vector phase matching condition  $k_{out}=2k_b - k_a$ . This method presents an important advantage: the fact that one does not need anymore to have well-defined wave-vectors for the incident and signal beams allows for the use of LG beams with a very large numerical aperture (NA) in a collinear configuration. This will allow for a sharper focusing of the beams and give thus rise to a better spatial resolution of the experiment. This, in turn, leads to FWM experiments where the efficiency of the process as well as its time dynamics can be precisely mapped over an inhomogeneous sample.

We further present a method that develops products of 2D Hermite or Laguerre modes onto a sum of single modes that describe from the nonlinear mixing of exciting beams the generation of signals. Changing the superimposition of the incident pulses allows for configurations that extend the basic structured illumination method to Gaussian beams.

## References

- [1] Mats G. L. Gustafsson PNAS **102** (37) 13081-13086 (2005)
- [2] D. Persuy, M. Ziegler, O. Crégut, K. Kheng, M. Gallart, B. Hönerlage, and P. Gilliot, Phys. Rev. B **92**, 115312 (2015)

# Photonic time-stretch: applications to ultrafast spectroscopy and real-time imaging

Thomas Godin, Pierre-Henry Hanzard, Said Idlahcen, Claude Rozé, and Ammar Hideur

CORIA UMR 6614, Normandie Université, Université de Rouen Normandie - CNRS - INSA Rouen, 76800 Saint Etienne du Rouvray, France

The real-time measurement of ultrafast and non-repetitive events has been a major issue for decades in many scientific fields. Specifically in optical instrumentation and metrology, the performances of diagnostic systems have been hindered by the electronic limitations of CCD/CMOS sensors and by the classical trade-off between sensitivity and acquisition speed. On the one hand, best imagers to date provide sub- $\mu$ s temporal resolution and allow continuous data recording while, on the other hand, state-of-the-art burst imaging techniques reach remarkable sub-ps temporal resolution but are limited to a few tens of consecutive frames [1]. There is however a gap to fill between these two types of techniques, and many recent applications need for imaging techniques enabling both nanosecond time resolution and continuous recording. With this in mind, the so-called dispersive time-stretch imaging technique has been developed [2] and is, for now, mostly applied to microfluidics and flow cytometry [3]. Its principle is relatively straightforward and relies on two consecutive steps, as illustrated on the scheme in Fig. 1: (i) a space-to-wavelength mapping which consists in encoding an image onto the spectrum of spatially-dispersed broadband pulses and (ii) the conversion of the spectrally-encoded image into the time domain where high-speed digitizers are available. The wavelength-to-time mapping is achieved via a simple yet powerful ultrafast spectroscopy technique called dispersive Fourier transformation relying on space-time duality [4,5]. It consists in time-stretching the ultrashort pulses into a medium with chromatic dispersion (GVD): when the temporal equivalent of the far-field in diffraction is reached, i.e. for sufficient dispersion, the pulses' temporal shape then mimics their optical spectrum. Recording their waveform in the temporal domain with a fast photodetector thereby allows the real-time monitoring of pulse-to-pulse variations in the spectrum.

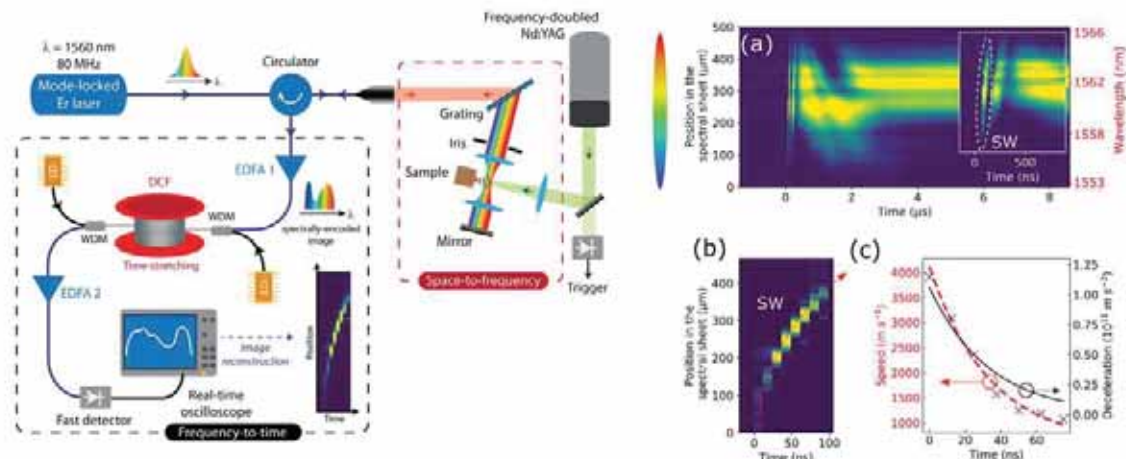


**Fig. 1** (Left) Experimental setup used for time-stretch imaging of shockwaves. (Right) (a) Capture of ultrafast events occurring after laser ablation, (b) close-up on a single shockwave, and (c) velocity measurement on a single shockwave.

As an illustration, we demonstrate the real-time tracking of single laser-induced shockwaves (SWs) with velocities exceeding a few km/s and show that time-stretch imaging allows to monitor their full dynamics, from their deceleration to the observation of the plasma contact wave and to easily acquire intensity and velocity statistics on large ensembles of SWs [6]. We also report the use of 1-D amplified time-stretch imaging to capture the rupture of liquid ligaments, which could bring new insights in two-phase flows physics. This study has then numerous potential applications in applied physics e.g. in the study of transient phenomena in pulsed laser-material interactions but also in plenty of related scientific fields involving fast non-repetitive events or processes with consequent shot-to-shot variations and low occurrence rate.

## References

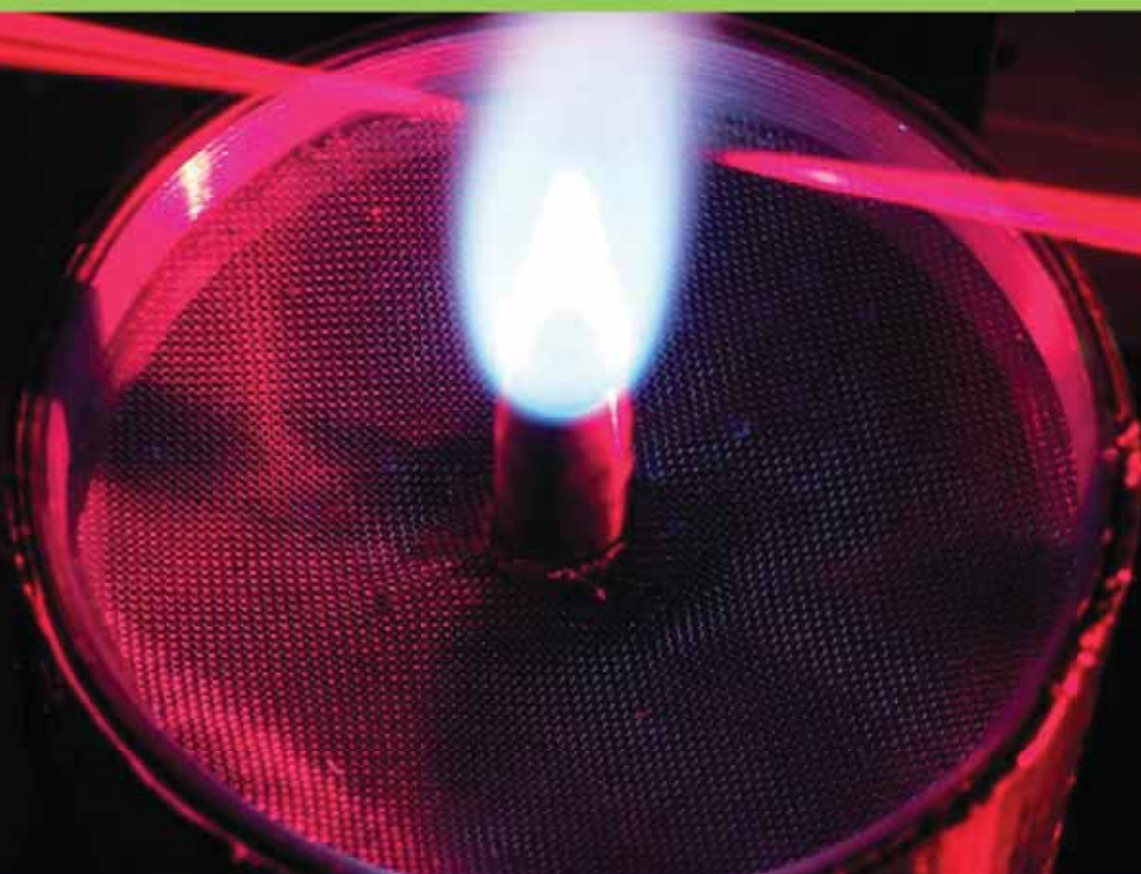
- [1] J. Liang, and L. V. Wang, "Single-shot ultrafast optical imaging," *Optica* **5**, 1113 (2018).
- [2] K. Goda, K.K. Tsia, and B. Jalali, "Serial time-encoded amplified imaging for real-time observation of fast dynamic phenomena," *Nature* **458**, 145 (2009).
- [3] A.K.S. Lau, H.C. Shum, K.K.Y. Wong, and, K.K. Tsia, "Optofluidic time-stretch imaging - an emerging tool for high-throughput imaging flow cytometry," *Lab Chip* **16**, 1743 (2016).
- [4] A. Mahjoubfar et al., "Time stretch and its applications," *Nat. Photonics* **11**, 341 (2017).
- [5] K. Goda and B. Jalali, "Dispersive Fourier transformation for fast continuous single-shot measurements," *Nat. Photonics* **7**, 102 (2013).
- [6] P.H. Hanzard, T. Godin, S. Idlahcen, C. Rozé, and A. Hideur, "Real-time tracking of single shockwaves via amplified time-stretch imaging," *Appl. Phys. Lett.* **112**, 161106 (2018).





**ECONOS**

2019, April 7-10  
CORIA, Rouen, France



# Exhibitors

**coRia**  
UMR 6614

# Photonique & Imagerie

## Créer la lumière



### Lasers Impulsionnels

- ns, ps, fs
- De l'UV à l'IR
- Accordables (OPO, OPCPA, OPA)
- Modules d'amplification YAG, YLF...
- Diodes laser ns forte puissance
- DPSS ns SLM ultracompact
- Applications : PV, LIDAR, marquage...



### Lasers continus

- Sources THz
- Combineurs LED sur mesure
- LEDs UV forte puissance
- Sources spectrales et accordables
- Corps noirs
- LEDs et lasers pour vision Industrielle
- Génération de motifs...

## Mettre en forme la lumière



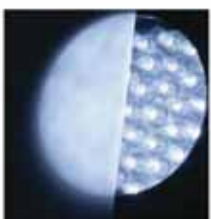
### Composants optiques

- De l'UV au THz
- Lentilles, miroirs et prismes
- Cristaux laser, cristaux non-linéaires
- Optiques polarisantes
- Filtres optiques et densités
- Isolateurs optiques
- Micro-composants optiques
- Sous-ensembles optomécaniques
- Polissage haute précision
- Traitements standards ou spécifiques
- Solutions en stock et sur mesure



### Scanners et modulateurs

- Modulateurs acousto-optiques
- Modulateurs électro-optiques
- Modulateurs photo-élastiques
- Scanners et galvanomètres
- Têtes de marquage



### Diffuseurs de lumière

- Films diffuseurs de lumière
- Films déviateurs de lumière



### Sécurité laser et accessoires

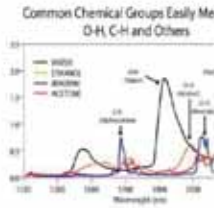
- Lunettes et masques de protection
- Rideaux, écrans et fenêtres de protection
- Colorants laser
- Shutters, obturateurs de sécurité
- Protection customisée

# Mesurer et analyser la lumière



## Analyses de faisceaux laser

- Joulemètres et puissancemètres laser
- Analyseurs de faisceaux
- Analyseurs de longueurs d'onde
- Analyseurs de spectre
- Profil spatial
- Photodétecteurs



## Mesures et analyses

- Process Analytical Technologies
- Imagerie multi et hyperspectrale
- Ultraviolet, visible, NIR, Raman
- Spectromètres ultracompacts
- Systèmes à LED
- Smart Industry, farming, homes



## Photométrie

- Spectrogoniomètres
  - Mesures CCT, IRC, TM30, SDCM, flux total
  - Génération fichiers IES et LDT en 30s
  - Contrôles qualité et R & D
- Spectroradiomètres
  - Mesures sur  $\mu\text{cd}/\text{m}^2$  au  $> 10 \text{ Mcd}/\text{m}^2$
  - Imagerie et contrôle d'homogénéité
  - Contrôle production displays



## Détecteurs

- De l'UV à  $16 \mu\text{m}$  et THz
- Photodiodes Si, InGaAs, GaAs, MCT
- Standards et customisés
- Sous-ensembles opto-électroniques complexes (détecteur+optiques+électro-nique+boltier)
- Photoconducteurs, photovoltaïques, jonctions multiples

# Visualiser



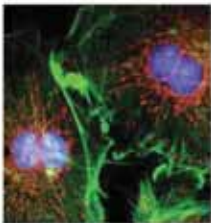
## Imagerie thermique

- Caméras thermiques
- Caméras thermographiques
- Caméras MWIR, SWIR
- Caméras scientifiques rapides
- Caméras large bande



## Machine Vision

- Capteurs CCD-CMOS
- Jusqu'à 29 MP
- $> 100 \text{ fps}$
- Interfaces USB et GigE



## Imagerie scientifique

- Caméras sCMOS refroidies
  - QE  $> 95\%$
  - 200 - 1100 nm
- Caméras rapides
  - Jusqu'à 3 MP
  - 12 742 fps @ 1080 px
  - Interface professionnelle et intuitive



## Traitement d'images

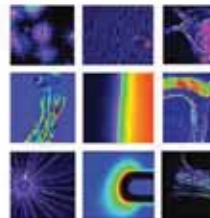
- Drones / PTZ
  - Compatibles caméras EO / IR
  - Stabilisation, détection, auto-tracking
  - Encodage 4k, fusion d'images
- Machine vision
  - Lecture codes-barres : 1D / 2D
  - Mesure de dimensions, coordonnées 3D

# Détecter et synchroniser



## Traitement et génération du signal

- Détection synchrone
- Analyseurs de spectre
- Générateurs de délais
- Oscillateurs
- Préamplificateurs
- Analyseurs de gaz résiduels
- Amplificateurs haute tension



## Mesure de biréfringence

- Substrats mesurés : verres, plastiques, cristaux, silicium...
- Dimensions : du  $\mu\text{m}$  à 1,85 m
- Formes : plaques, incurvées, boules, lingots...
- Retard : 0,005 à 3500 nm



# Ultrafast Lasers for Industrial, Medical and Scientific Applications

## Satsuma



- > Air-cooled up to 20 W
- > FemtoBurst™
- > Trigger on demand - FemtoTrig™
- > SuperSync Control

### Ideal for

- > Microelectronics
- > Multiphoton Imaging
- > Medical Device Manufacturing
- > Ophthalmology
- > And many more....

## Tangerine



- > Short Pulse option < 150 fs
- > FemtoBurst™
- > Trigger on demand - FemtoTrig™
- > SuperSync Control

### Ideal for

- > Microelectronics
- > Micromachining
- > Ultrafast Spectroscopy
- > High Harmonic Generation / Attoscience
- > And many more....

Our lasers are compatible with many options, and notably:  
SHG, THG, FHG, OPA, and our new pulse management module **Compress**.

More information at  
[amplitude-laser.com](http://amplitude-laser.com)

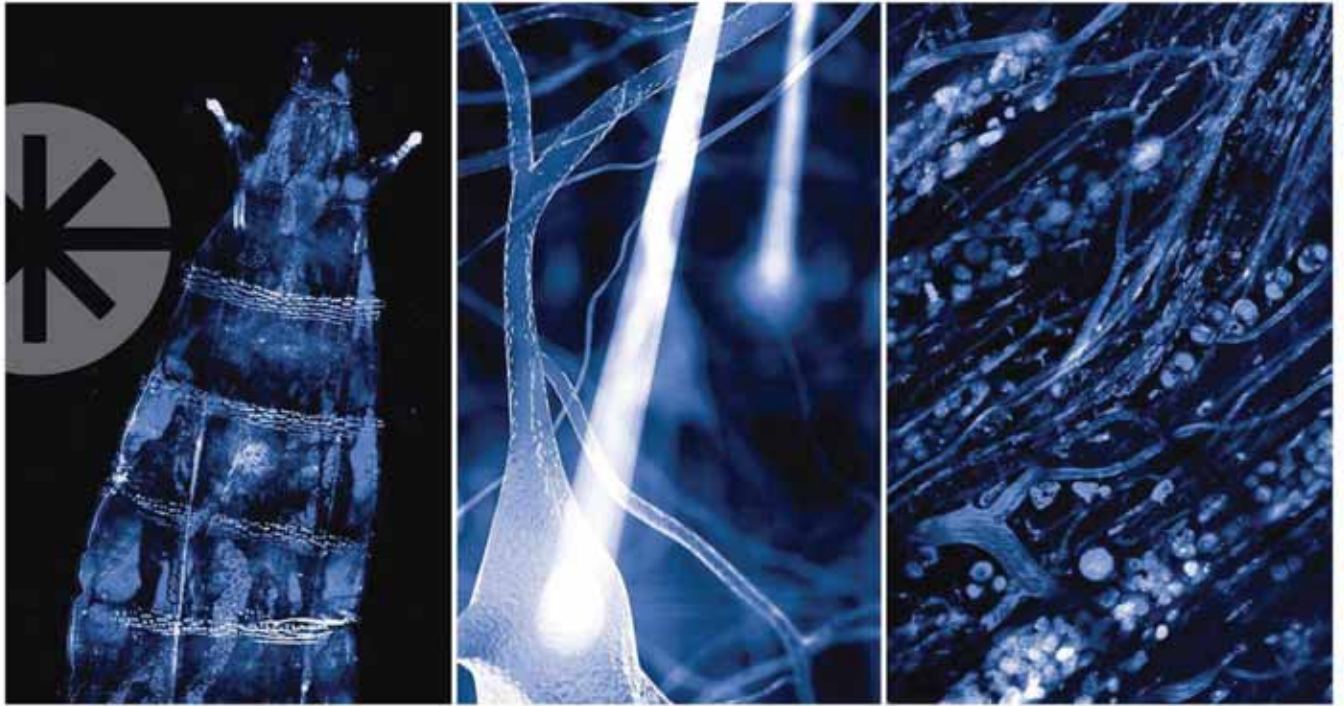


# picoEmerald

CARS, SRS, Label-free Imaging



- Multi-color output
- Perfect temporal & spatial overlap
- 700 ... 1950 nm / 400 ... 9000  $\text{cm}^{-1}$
- Narrowband pulses to cover the entire Raman fingerprint region
- SRS Detection Set



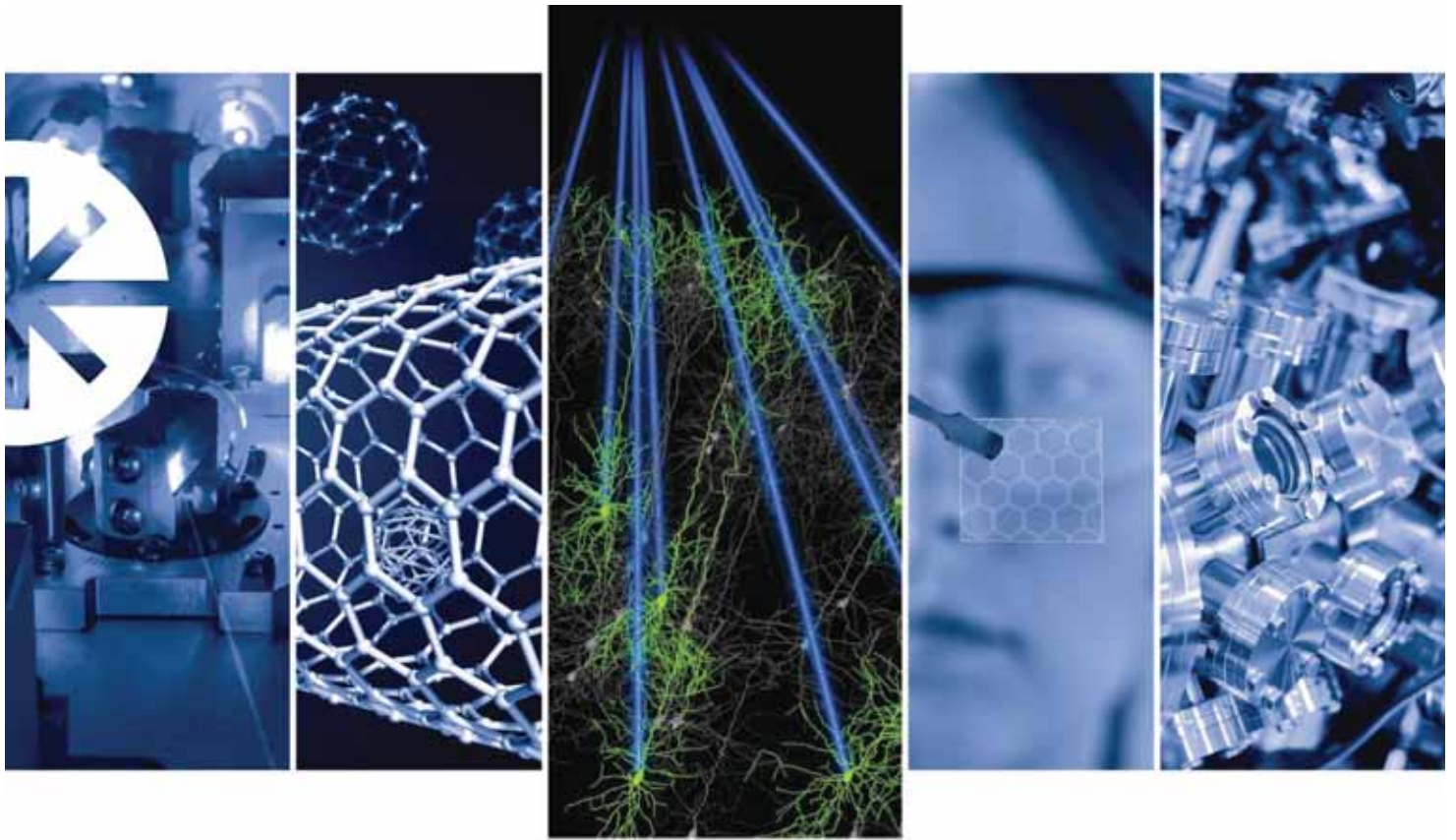
## BRIGHTER, DEEPER, SHARPER MICROSCOPY

The **Chameleon Discovery** with **Total Power Control (TPC)** is the first tunable ultrafast laser for two-photon microscopy to fully integrate **fast power modulation** into the laser. Saving valuable table space and setup costs, TPC guarantees perfect **beam parameters and power** directly into your microscope scanhead for **brighter, deeper, and sharper** imaging performance.

Learn More—[www.coherent.com/Total-Power-Control](http://www.coherent.com/Total-Power-Control)



 **COHERENT**  
Superior Reliability & Performance



# LEADING & INNOVATING TO ACCELERATE YOUR RESEARCH

Whether unlocking the mysteries of matter or mapping brain function, Coherent has the lasers to advance your research. With our unique HALT/HASS reliability protocol, we deliver unmatched laser performance for maximum productivity and improved data quality.

**Attosecond Experiments to Neuroscience, Gravitational Waves to Spectroscopy—**  
Discover More—[coherent.com/industrial-revolution](http://coherent.com/industrial-revolution)





**Femto Easy is a company specialized in ultrafast instrumentation. Strong of its expertise in the production and characterization of high energy ultrashort pulses, the company provides robust and reliable measurement instruments for ultrafast lasers. Femto Easy is the world expert in single shot measurement devices. The company has also developed very valuable and functional devices for spectral and spatial measurements. The current product-line includes single shot autocorrelators, capable of measuring few cycle pulses, innovative SHG single shot FROGs, mini imaging spectrometers and beam profilers.**

**We also develop custom products upon request, vacuum compatible devices, OEM solutions and custom softwares... So please don't hesitate to ask !**



**ROC**

### *Single shot autocorrelator*

ROC stands for Row Optical Correlator. Based on an ultra compact and robust inline setup, the ROC allows the accurate measurement of pulse duration on a single shot basis, and therefore the shot to shot fluctuations. Specifically designed to offer the easiest user experience, they cannot be misaligned and no calibration or tweaking is needed. Also, they are easily transportable. And yes, they are rock-solid! Besides those advantages, the ROC autocorrelators provide excellent technical performances and highly accurate measurements. The ROC autocorrelators are available for different wavelength ranges and several pulse durations.




**BOAR**

### *Autocorrelator with phase retrieval*

BOAR stands for Biprism based Optical Autocorrelation with Retrieval. This new patented technology is based on interferometric single shot autocorrelation, combined with two photons absorption. The chirp is evaluated using the spatial interferogram. Getting rid of the non-linear crystal eliminates the phase matching and polarization issues. It also allows a very broad spectral working range (1200 - 2400 nm) without any tuning.





# A new standard in ultrafast laser measurements

## MISS

### Spatially resolved spectrometer

MISS stands for Mini Imaging Spatial Spectrometer. This innovative spectrometer gives access to the spatially resolved spectrum of your sources. The acquisition can be single shot up to 40 kHz. Being one of the most compact imaging spectrometer, the MISS is easily integrable at different stages of amplified laser systems. It can be used in free space mode to take benefit of the spatial resolution, or with a fiber input, like a regular spectrometer.



## BeamPro

### Beam profiler

Our beam profiler takes advantage of our user friendly software, and provides thorough analysis and statistics of your laser beam. They are suitable for wavelength from 190 to 1100 nm and beams as large as 11 mm.



## FROG

### Fast FROG

FROG stands for Frequency Resolved Optical Gating. The single-shot Fast FROG, based on second harmonic generation is reliable and compact. Key design features, such as the wavefront division technique and the use of our mini imaging spectrometer MISS, make the Fast Frog very easy to use, leading to accurate measurements. Six models are available, covering different pulse duration ranges from sub-5 fs to 10 ps\*, over a broad spectral range. Two designs are available: one for long pulses mainly relying on transmission optics, and one for ultrashort pulses which is completely achromatic.

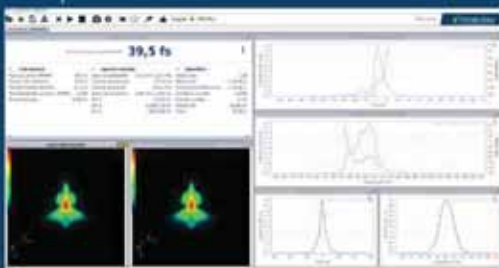
\*: 40 ps measurement available with multi-shot FROG.



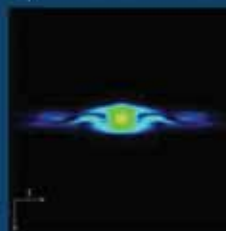
## STAR

STAR stands for Software Technology for Acquisition and Retrieval. User friendly and intuitive, it is touchscreen compatible and provides numerous useful functionalities. It allows remote screen display and remote control of the devices via PC, tablets or smartphones, and can be integrated in more complex environments. Software development is one of the key resources of the company. We can quickly develop and add new functionalities upon request.

The FAST FROG retrieval interface provides all the informations you need about your pulses!



Our retrieval algorithms are capable of retrieving complex spectral and temporal structures in real time.





Dr. Thomas Renner, CEO

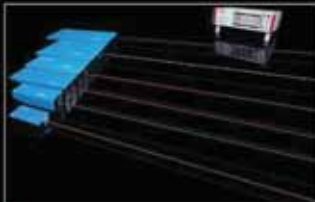
## All Wavelengths.

190 nm - 0.1 THz

TOPTICA's lasers cover a unique wavelength range from 190 nm to 0.1 THz (corresponding to 3 mm) – one of the widest coverage in the laser market. Diode lasers, ultrafast fiber lasers and terahertz sources enable this unique spectral coverage and a multitude of applications in physics, chemistry, biology and industrial metrology or material processing.

Challenge us with your application – at **any wavelength**.

### All Wavelengths @ TOPTICA



▶ Diode Lasers:  
190 - 3500 nm



▶ Ultrafast Fiber Lasers:  
488 nm - 15000 nm



▶ Terahertz Systems:  
0 - 6 (20) THz



[www.toptica.com](http://www.toptica.com)

### Please contact our official authorised distributor:

France

**Opton Laser International**  
29 rue Jean Rostand  
91893 Orsay France  
[www.optonlaser.com](http://www.optonlaser.com)

Phone : +33 1 6941 0405  
Fax : +91-11-26899867 / 26894181  
Email : [contact@optonlaser.com](mailto:contact@optonlaser.com)





EXPERT EN PHOTONIQUE  
DEPUIS 1990

INSTRUMENTATIONS POUR LA SPECTROSCOPIE  
CHIMIE | PHARMACIE | BIOLOGIE



SPECTROSCOPIE RAMAN HAUTE PERFORMANCE



SPECTROSCOPIE RAMAN PORTABLE



SPECTROSCOPIE FTIR



MICROSCOPIE IR & HYPERSPECTRALE



SPECTROMETRE RESOLU EN TEMPS

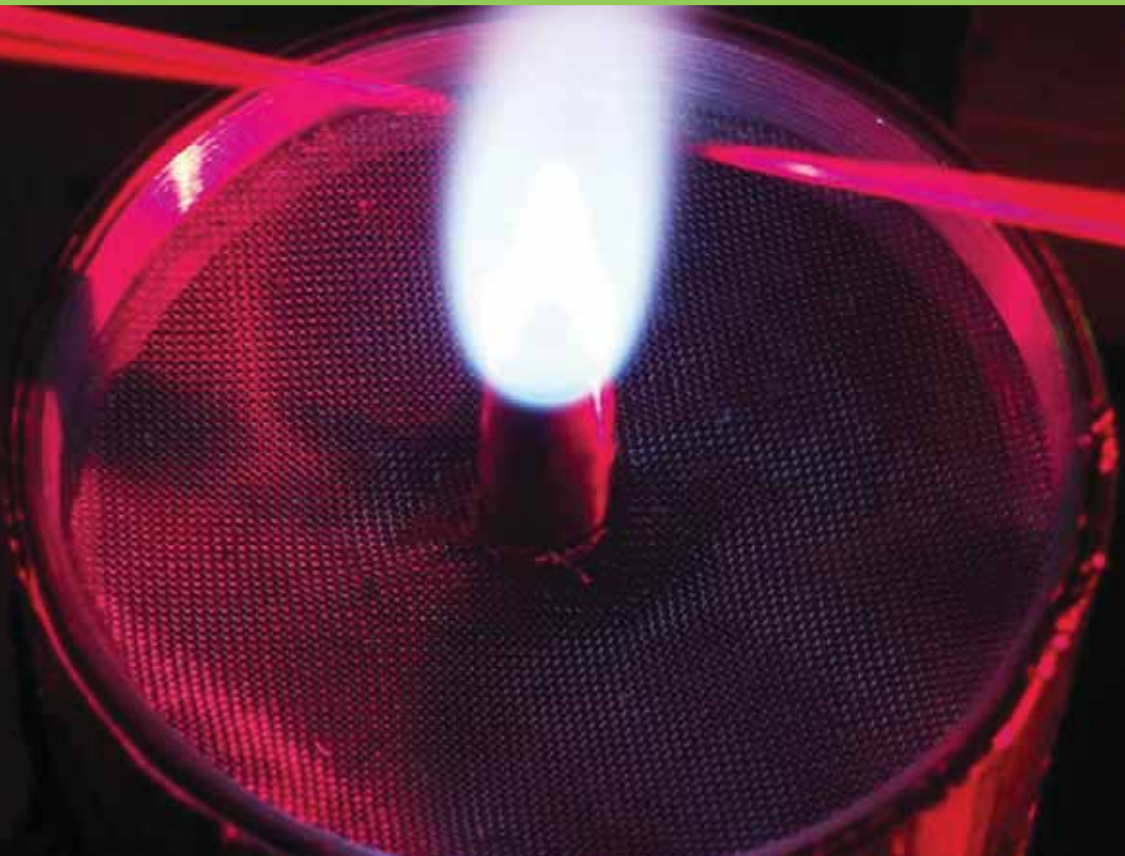


SPECTROMETRE MODULAIRE



**ECONOS**

2019, April 7-10  
CORIA, Rouen, France



**Posters session**

**coRia**  
UMR 6614

# **Shaper based MIR-scanning and multiplex Sum Frequency spectroscopy for nonlinear microscopy**

*Niklas Müller, Tiago Buckup, Marcus Motzkus*

*Physikalisch-Chemisches Institut, Universität Heidelberg, Im Neuenheimer Feld 229, D-69120 Heidelberg, Germany*

# Optimization of supercontinuum generation in a photonic crystal fiber for use as Stokes beam in a single-laser femtosecond micro-CARS setup

*Mauro Falconieri<sup>1</sup>, Michele Marrocco<sup>1</sup>, Caterina Merla<sup>1</sup>, Serena Gagliardi<sup>1</sup>, Flaminia Rondino<sup>2</sup>*

*1. ENEA, C.R. Casaccia, via Anguillarese 301, 00123 Rome, Italy*

*2. ENEA, C.R. Frascati, via E. Fermi 45, 00049 Frascati, Italy*

Supercontinuum generation with ultrashort pulses in photonic crystal fibers (PCF) is an effective way to provide the Stokes beam in single-laser oscillator micro-CARS experiments. In particular, fibers with two near zero-dispersion wavelengths have been proposed for this application thanks to the stability of the emitted supercontinuum spectrum [1], and actually became a dedicated commercial product. However, for proper operation of the CARS setup, the excitation laser working conditions, i.e. wavelength, chirp, and power, must be accurately selected [2]. On this line, fibers with different dispersion properties were recently compared [3], evidencing the importance of selecting proper operating conditions for optimized CARS measurements in terms of signal intensity and stability, and moreover, for multiplex CARS experiments, also in terms of the accessible bandwidth. However, selection of such optimized operating condition requires an extensive amount of experimental work, which could be substantially reduced with the help of a reliable supercontinuum generation model.

Here we present a joint modeling and experimental activity aimed at exploring the dependence of the CARS signal spectrum, intensity and noise, on the operating conditions of a FemtoWHITE CARS photonic crystal fiber (NKT Photonics A/S, Denmark) in a femtosecond single-oscillator micro-CARS setup.

The modeling activity was performed using a recently developed supercontinuum generation model based on a numerical code for the solution of the nonlinear Schroedinger equation for the beam propagation inside the fiber [4]. The original code was modified to account for the laser beam chirp and for the temporal pulse shape, moreover particular care was devoted to the selection of the second-order dispersion input parameters, thus allowing improved match with the experimentally measured supercontinuum spectra with respect to previously published results.

The experimental part was performed on a femtosecond multiplex micro-CARS setup with capability of simultaneous measurements of Stokes and CARS spectra, thus allowing improved analysis of the correlation between them.

## References

- [1] K. M. Hilligsøe, T. V. Andersen, H. N. Paulsen, C. K. Nielsen, and K. Mølmer “Supercontinuum Generation in a Photonic Crystal Fiber with Two Zero Dispersion Wavelengths” *Opt. Express* **12**, 1045 (2004).
- [2] M. Falconieri, M. Marrocco, C. Merla, S. Gagliardi, F. Rondino, M. Ghezelbash, “Characterization of Supercontinuum Generation in a Photonic Crystal Fiber for Uses in Multiplex CARS Micro-Spectroscopy”, submitted to *Journal of Raman Spectroscopy*.
- [3] M. Naji, S. Murugkar, and H. Anis, “Determining optimum operating conditions of the polarization-maintaining fiber with two far lying zero dispersion wavelengths for CARS microscopy”, *Opt. Express* **22**, 10800 (2014).
- [4] J. M. Dudley, J. R. Taylor, eds. *Supercontinuum Generation in Optical Fibers*, (Cambridge University Press, New York, 2010).

# Resolving The Framework Position Of Templating Molecules In Hierarchically Intergrown Zeolites Via Polarized Stimulated Raman Scattering Microscopy

Fleury G.<sup>1</sup>, Steele J.A.<sup>1</sup>, Gerber I.C.<sup>2</sup>, Jolibois F.<sup>2</sup>, Puech P.<sup>3</sup>, Muraoka K.<sup>4</sup>, Keoh S.H.<sup>4</sup>, Chaikittisilp W.<sup>4</sup>, Okubo T.<sup>4</sup>, Roeffaers M.B.J.<sup>1</sup>

<sup>1</sup>KU Leuven, Celestijnenlaan 200F, B-3001 Leuven, Belgium

<sup>2</sup>Université Fédérale de Toulouse Midi-Pyrénées, F-31077 Toulouse, France

<sup>3</sup>Université de Toulouse, F-31055 Toulouse, France

<sup>4</sup>The University of Tokyo, 113-8656 Tokyo, Japan

The preparation of hierarchical zeolites, that is zeolites with at least two different levels of porosity, has proven to be an efficient strategy to enhance the mass transport inside the zeolite particles as well as to slow down their deactivation during catalytic processes. Chaikittisilp et al. recently proposed a synthesis methodology relying on the use of a diquatery ammonium,  $(C_3H_7)_3N^+(CH_2)_5N^+(C_3H_7)_3$  (denoted hereafter Pr<sub>6</sub>-diquat-C<sub>5</sub>), as a templating agent which lead to the formation of hierarchically intergrown silicalite-1 with an unusual morphology consisting of orthogonal silicalite-1 lamellae with a thickness of tens of nanometers [1]. It has been hypothesized that his peculiar morphology is due to the fit of Pr<sub>6</sub>-diquat-C<sub>5</sub> molecules inside the microporous framework of the silicalite-1, which consist of interconnected zigzag and linear micropores running along the crystallographic *a* and *b* axes, respectively. While the crystallographic structure of the lamellae was extensively characterized using HR-TEM [1], the actual location of the Pr<sub>6</sub>-diquat-C<sub>5</sub> molecules inside the micropores remains unknown. As conventional characterization techniques either are not applicable due to the small size of the crystals or hardly provide accurate spatial distribution of the Pr<sub>6</sub>-diquat-C<sub>5</sub> molecules, we use polarized stimulated Raman scattering (SRS) microscopy correlated with SEM imaging and supported by DFT calculations to resolve the position of Pr<sub>6</sub>-diquat-C<sub>5</sub> molecules inside the micropores of the hierarchically intergrown silicalite-1 zeolite.

Analysis of the spontaneous Raman spectrum of Pr<sub>6</sub>-diquat-C<sub>5</sub> occluded in the hierarchically intergrown silicalite-1 in the CH-stretching region reveals that one band at 2884 cm<sup>-1</sup> is well resolved. Simulations of the Raman spectrum of the Pr<sub>6</sub>-diquat-C<sub>5</sub> by DFT calculations indicates that this band corresponds to the contribution of the symmetric stretching of CH<sub>2</sub> groups located on the spacer between the quaternary ammonium centres. Theoretical simulation reveals the high polarization dependence of this mode, which can then be used to resolve the orientation of the Pr<sub>6</sub>-diquat-C<sub>5</sub> in the lamellae of the crystal. Specific vibrational imaging of the mode of interest with a submicrometer diffraction-limited resolution can then be carried out using SRS microscopy. The comparison of the vibrational image of the Pr<sub>6</sub>-diquat-C<sub>5</sub> molecules occluded in the crystal and the SEM image of the latter confirms that SRS microscopy allows to differentiate the main lamellae and the 90° intergrowths. Thus, the polarization dependence of the signal can be assessed in different region of the crystal in a given focal plane. Significant differences in the SRS intensity are clearly observed in different regions of the hierarchically intergrowth crystal. Indeed, the polarization dependence of the signal follow an opposite trend in the main lamella and the lateral lamellae. Considering the crystallographic structure of the main lamella and the simulated polar plots, the polarization-resolved SRS images recorded indicate that Pr<sub>6</sub>-diquat-C<sub>5</sub> molecules are preferentially located in the linear pores of the MFI framework. This preferential localization of Pr<sub>6</sub>-diquat-C<sub>5</sub> should be at the origin of the unusual hierarchically intergrowth morphology of the silicalite-1 crystals. Such insights can be exploited to design new dimeric templating agents that can direct the formation of hierarchically intergrown zeolites by including a similar spacer in in the chemical structure. These results illustrate the strong potential of SRS microscopy for mapping organics located inside zeolite frameworks with a submicrometer resolution.

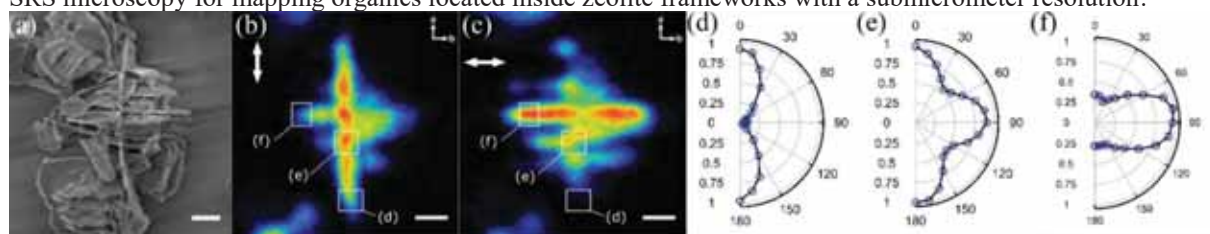


**Fig. 1** (a) SEM image of hierarchical silicalite-1 crystals (scale bar = 1 μm). SRS images of Pr<sub>6</sub>-diquat-C<sub>5</sub> inside the micropores of the crystal using linear polarization (b) parallel to the *a* axis of the main lamella and (c) perpendicular to the *a* axis of the main lamella. (d-f) Polarization dependence of the SRS signal in the three rectangular areas.

## References

[1] W. Chaikittisilp, Y. Suzuki, R.R. Mukti, T. Suzuki, K. Sugita, K. Itabashi, A. Shimojima, T. Okubo, "Formation of Hierarchically Organized Zeolites by Sequential Intergrowth", *Angew. Chem., Int. Ed.*, **52** (12), 3355–3359 (2013)

The work presented in this contribution is based on: *J. Phys. Chem. Lett.*, **9** (7), 1778–1782 (2018)

# Multi-Modulations Schemes in Coherent Raman Microscopy for Spectral or Lateral Multiplexing of the Image Acquisition

Sandro Heuke<sup>1</sup>, Barbara Sarri<sup>1</sup>, Alberto Lombardini<sup>1</sup>, Xavier Audier<sup>1</sup>, Hervé Rigneault<sup>1</sup>

<sup>1</sup>. Aix Marseille Univ, CNRS, Centrale Marseille, Institut Fresnel, Marseille, France.

\* Corresponding author: herve.rigneault@fresnel.fr

For almost a century state of the art cancer diagnosis is based on various staining protocols of tissue section allowing to access important morphological parameters such as the cell density or nucleocytoplasmic ratio. Depending on type of surgery, e.g., tumor resection or point-wise biopsy, the size of tissue removed varies from several centimeter to sub-millimeter. The resected tissue is sliced in steps of 5 to 15  $\mu\text{m}$  resulting into tens tissue sections that will be stained and further evaluated by a trained pathologist. The standard staining procedures, such as the haematoxylin and eosin (H&E) protocol, are time-consuming requiring between 1 h for a frozen section analysis up to several days for embedded tissue blocks. Thus, the development of faster and more efficient diagnostics *in* or *ex vivo* procedures is desirable. Accessing the same information content as conventional histopathology it was recently demonstrated that stimulated Raman scattering (SRS) microscopy can be translated into virtual H&E images without adding any chemical to the sample [1]. For this purpose, two SRS-images at 2850  $\text{cm}^{-1}$  and 2930  $\text{cm}^{-1}$  are required which are ideally acquired within a single scan as drying of fresh samples may compromise the perfect co-registration and, therefore the resolution, in sequential imaging approaches. Furthermore, the total image acquisition time must be optimized to render SRS's efficiency

comparable to chemical staining technology and finally surpass its current limits.

Here, we present 3 approaches using the modulation of the excitation to source in the MHz range to either allow for the simultaneous acquisition of SRS images at distinct Raman shifts or to multiplex the acquisition to 2 or more positions.

(1) Within the first approach two colors serving as pump of a three-color picosecond laser system are modulated at distinct frequencies well above the impact of the  $1/f$  noise [2]. Using a single photo-diode (PD) the third color is demodulated by two separate lock-in amplifiers. Compared to previous implementations of dual-color SRS, no cross-talk between the channels possible, while the complete relevant Raman spectral range, i.e. 500  $\text{cm}^{-1}$  - 5000  $\text{cm}^{-1}$ , can be addressed at power levels that leave enough headroom for further optical equipment in the laser pathway, such as the addition of the following extension.

(2) For the second approach the 2 pump beams modulated at different modulation frequencies are each superimposed by with the Stokes beam [3]. The two beam pairs, i.e. pump and Stokes, are guided separately and coupled into the laser scanning microscope with an angular difference. The latter translates into different lateral position at the sample. Both Stokes beams are separated and detected individually. This dual-focus SRS approach allows to image a sample at distinct lateral or axial positions, i.e. sample planes. Further, it enhances the imaging speed by a factor of 2 while maintaining the signal-to-noise ratio of a single focus approach. Finally, a multi-focus operation is readily obtained using multi-channel modulation and demodulation schemes.

[1] D. A. Orringer et al. Nat. Biomed. Eng. 1 (2017) 0027.

[2] S. Heuke et al. Optics Letters 43 (2018), pp. 3582-3585.

[3] S. Heuke et al. Optics Letters 43 (2018), pp. 4763-4766.



# Quantum beating between N-S-split rotational levels in oxygen: Modelling of the picosecond CARS time domain

J. I. Hölzer<sup>1,2</sup>, C. Meißner<sup>1,2</sup>, T. Seeger<sup>1,2</sup>

1. Engineering Thermodynamics, University of Siegen, Paul-Bonatz-Str. 9-11, 57076 Siegen, Germany

2. Center for Sensor Systems (ZESS), University of Siegen, Paul-Bonatz-Str. 9-11, 57076 Siegen, Germany

Rotational Raman linewidths are an important parameter in the evaluation of temperature and concentration from rotational coherent anti-Stokes Raman scattering studies on combustion and gas phase systems [1–3]. Detailed knowledge of combustion processes is required in order to optimize such processes with respect to fuel consumption and flue gas emissions and to facilitate combination with after treatment technologies like carbon capture and storage (CCS) [4]. Classically Raman linewidths are calculated using scaling law models [3], which rely on empirically determined parameters. These are only sparsely known for the rotational S-branch of many combustion relevant molecules, however, which is why different approaches are considered [5–8]. One of those approaches is the determination from time-resolved experiments, where the signal intensity is recorded as a function of probe pulse delay [5–10]. The collisional dephasing time constant allows direct calculation of the linewidths [6]. This procedure has been demonstrated for nitrogen at elevated temperatures [6] and pressures [5]. For oxygen the temperature dependent time domain CARS study has been published, because its dephasing behavior deviates from the one in nitrogen.

The dephasing behavior depends on the number of collisions, and thereby on temperature and number density, and the molecular properties. For nitrogen the dephasing can be described by a pseudo-first order kinetic arising solely from collisions. The dephasing can be described by a mono-exponential decay function. For oxygen the situation deviates significantly. Because of its triplet ground state, rotational energy levels are split, due to spin-spin- and spin-nuclear angular momentum couplings. Coherent excitation leads to quantum beats in the time regimes of about 16 ps (<sup>S</sup>R-branch) and about 600 ps (<sup>S</sup>S-branch). This necessitates the adaption of the model function, incorporating the rotational transition frequencies, which determine the magnitude of the beating frequency [9,11]. Milner *et al.* and Courtney *et al.* proposed and applied such adapted functions to fs-CARS measurements of optically centrifuged oxygen and oxygen at low pressures (0.04 to 0.4 atm) respectively [9,11]. This work demonstrates the application of a model decay-function for ps-CARS measurements over the combustion relevant temperature range from 297 K to 1900 K at ambient pressure.

## References:

- 1 L. A. Rahn and R. E. Palmer, "Studies of nitrogen self-broadening at high temperature with inverse Raman spectroscopy," *J. Opt. Soc. Am. B*, **3**, 1164 (1986).
- 2 L. Martinsson, P.-E. Bengtsson, M. Aldén, S. Kröll and J. Bonamy, "A test of different rotational Raman linewidth models: Accuracy of rotational coherent anti-Stokes Raman scattering thermometry in nitrogen from 295 to 1850 K," *J. Chem. Phys.*, **99**, 2466 (1993).
- 3 A. C. Eckbreth, *Laser Diagnostics for Combustion Temperature and Species*, 2nd ed., (Gordon and Breach Publishers, Amsterdam, 1996).
- 4 B. Metz and Intergovernmental Panel on Climate Change, Eds., *IPCC special report on carbon dioxide capture and storage*, (University Press, Cambridge, 2005).
- 5 J. D. Miller, S. Roy, J. R. Gord and T. R. Meyer, "Communication: Time-domain measurement of high-pressure N<sub>2</sub> and O<sub>2</sub> self-broadened linewidths using hybrid femtosecond/picosecond coherent anti-Stokes Raman scattering," *J. Chem. Phys.*, **135**, 201104 (2011).
- 6 C. J. Kliewer, A. Bohlin, E. Nordström, B. D. Patterson, P.-E. Bengtsson and T. B. Settersten, "Time-domain measurements of S-branch N<sub>2</sub>→N<sub>2</sub> Raman linewidths using picosecond pure rotational coherent anti-Stokes Raman spectroscopy," *Appl. Phys. B*, **108**, 419 (2012).
- 7 A. Bohlin, E. Nordström, B. D. Patterson, P.-E. Bengtsson and C. J. Kliewer, "Direct measurement of S-branch N<sub>2</sub>-H<sub>2</sub> Raman linewidths using time-resolved pure rotational coherent anti-Stokes Raman spectroscopy," *J. Chem. Phys.*, **137**, 074302 (2012).
- 8 E. Nordström, A. Hosseinnia, C. Brackmann, J. Bood and P.-E. Bengtsson, "Raman linewidth measurements using time-resolved hybrid picosecond/nanosecond rotational CARS," *Optics Letters*, **40**, 5718 (2015).
- 9 A. A. Milner, A. Korobenko and V. Milner, "Coherent spin-rotational dynamics of oxygen superrotors," *New J. Phys.*, **16**, 093038 (2014).
- 10 A. A. Milner, A. Korobenko, J. W. Hepburn and V. Milner, "Effects of Ultrafast Molecular Rotation on Collisional Decoherence," *Phys. Rev. Lett.*, **113**, 043005 (2014).
- 11 T. L. Courtney and C. J. Kliewer, "Rotational coherence beating in molecular oxygen: Coupling between electronic spin and nuclear angular momenta," *J. Chem. Phys.*, **149**, 234201 (2018).

# Micro-SECARS Studies of Organic Molecules on Randomly-Nanostructured SERS-Active Surfaces

V.I. Fabelinsky<sup>1</sup>, D.N. Kozlov<sup>1</sup>, S.N. Orlov<sup>1</sup>, Yu.N. Polivanov<sup>1</sup>, V.V. Smirnov<sup>1</sup>, G.M. Arzumanyan<sup>2</sup>, K.Z. Mamatkulov<sup>2</sup>, K.N. Afanasiev<sup>3</sup>, I.A. Boginskaya<sup>3</sup>, I.A. Ryzhikov<sup>3</sup>, I.A. Budashov<sup>4</sup>, N.L. Nechaeva<sup>5</sup>, H.V. Bandarenka<sup>6</sup>, S.A. Zavatski<sup>6</sup>

1. Prokhorov General Physics Institute of the Russian Academy of Sciences, Vavilov str. 38, 119991 Moscow, Russia

2. Joint Institute for Nuclear Research, Joliot-Curie str. 6, 141980 Dubna, Moscow Region, Russia

3. Institute for Theoretical and Applied Electromagnetics of the Russian Academy of Sciences, Izhorskaya str. 13, 125412 Moscow, Russia

4. Chemistry Department, M.V. Lomonosov Moscow State University, Leninskiye Gory 1-3, 119991 Moscow, Russia

5. N.M. Emanuel Institute of Biochemical Physics, Russian Academy of Sciences, Kosygin str. 4, 119334 Moscow, Russia

6. Belarusian State University of Informatics and Radioelectronics, Brovka str. 6, 220013 Minsk, Belarus

Highly-sensitive detection of biochemically-relevant molecules employing their incoherent or coherent Raman spectroscopy at a plasmonic surface under conditions of electromagnetic (EM) field enhancement is a challenge of a few recent decades [1]. Theoretically, nonlinear Coherent anti-Stokes Raman Scattering (CARS) enhancement by plasmonic nanostructures should be stronger than that of linear spontaneous Raman scattering (RS) due to the larger number of the optical EM fields involved [2]. The aim of this study is an experimental search for the conditions when surface-enhanced (SE) CARS may appear to be a more efficient technique than SERS.

Two types of randomly-nanostructured SERS-active samples representing noble metal surfaces with nanoscale roughness were employed. One is a metamaterial formed by 56-nm diameter gold nanoparticles (Au-NPs) immobilized as single NPs, clusters or islands on a nanostructured CeO<sub>2</sub> faceted dielectric film deposited on a thin Al sublayer [3]. Another is a plasmonic nanostructure representing a quasi-continuous layer of 50-500 nm silver nanoparticles (Ag-NPs) randomly deposited on a porous silicon substrate [4]. As reporters, the molecules of 5-thio(2-nitrobenzoic acid) (TNB) and 4-mercaptophenylboronic acid (MPBA) [5], as well as MPBA-bound glycated albumin have been used. The reporters were being deposited by immersion.

Wavelength-tunable two-color short-pulse high repetition rate ( $\sim 7$  ps, 85 MHz) excitation of a surface in the NIR spectral range, at pump,  $\lambda_p = 690$ -990 nm, and Stokes,  $\lambda_s = 1064$  nm, wavelengths ( $\sim 5$ -7 cm<sup>-1</sup> linewidth each), under Raman-resonant or non-resonant conditions, as well as recording of backward-scattered radiation spectra, were performed using a scanning confocal laser-based micro-CARS spectrometer [5]. The anti-Stokes range plasmon-resonance enhanced spectra, recorded, in a definite spatial point, at given  $\lambda_p$  and  $\lambda_s$ , represent a narrow line of coherent scattered radiation (SECARS) at the wavelength  $\lambda_{as} = \lambda_p / (2 - \lambda_p / \lambda_s)$ , rising above the background of  $\lambda_p$ -excited incoherent scattered radiation. The latter represents a continuum wavelength-dependent spectrum of inelastic light scattering, presumably, by electrons of plasmonic nanostructures [6], overlaid by relatively narrow Raman-resonant anti-Stokes SERS lines of the reporter molecules. Scanning of the 1- $\mu$ m diameter focused laser spot across the surface with  $\mu$ m-scale steps allowed us to obtain a spectrum of scattered radiation in each spatial point and then to calculate a map of the intensity scattered into a preset spectral interval.

We found out the conditions when laser powers do not cause photo-degradation of the reporter/NP conjugates and are still sufficient to generate strong SECARS signals. Using SECARS, at Raman-resonant excitation we acquired the excellent chemical imaging contrast of the reporter molecules employed. The estimated amounts of the reporter molecules as small as  $\sim 20$  in a laser spot could be detected. We spectrally detected glycated albumin, a potential biomarker in diabetes, which is binding with MPBA molecules on the surface. The challenges and the problems of employing the technique are discussed.

## References

- [1] D.V. Voronine, Z. Zhang, A.V. Sokolov, and M.O. Scully, "Surface-enhanced FAST CARS: en route to quantum nano-biophotonics", *Nanophotonics* **7**, 523 (2018).
- [2] C. Steuwe, C.F. Kaminski, J.J. Baumberg, and S. Mahajan, "Surface Enhanced Coherent Anti-Stokes Raman Scattering on Nanostructured Gold Surfaces", *Nano Lett.* **11**, 5339 (2011).
- [3] I.N. Kurochkin, I.A. Ryzhikov, A.K. Sarychev, K.N. Afanasiev, I.A. Budashov, M.V. Sedova, I.A. Boginskaya, S.V. Amitonov, E.V. Korostilev, A.N. Lagarkov, "Enhancement of SERS Signal Using of New Material Based on Cerium Dioxide Facet Dielectric Films", *Moscow University Chemistry Bulletin* **70**, 102 (2015).
- [4] H.V. Bandarenka, K.V. Girel, V.P. Bondarenko, I.A. Khodasevich, A.Yu. Panarin, and S.N. Terekhov, "Formation Regularities of Plasmonic Silver Nanostructures on Porous Silicon for Effective Surface-Enhanced Raman Scattering", *Nanos. Res. Lett.* **11**, 262 (2016).
- [5] V.I. Fabelinsky, D.N. Kozlov, S.N. Orlov, Y.N. Polivanov, I.A. Shcherbakov, V.V. Smirnov, K.A. Vereschagin, G.M. Arzumanyan, K.Z. Mamatkulov, K.N. Afanasiev, A.N. Lagarkov, I.A. Ryzhikov, A.K. Sarychev, I.A. Budashov, N.L. Nechaeva, I.N. Kurochkin, "Surface-Enhanced micro-CARS Mapping of a Nanostructured Cerium Dioxide/Aluminium Film Surface with Gold Nanoparticle-Bound Organic Molecules", *J. Raman Spectrosc.* **49**, 1145 (2018).
- [6] J.T. Hugall and J.J. Baumberg, "Demonstrating Photoluminescence from Au is Electronic Inelastic Light Scattering of a Plasmonic Metal: The Origin of SERS Backgrounds", *Nano Lett.* **15**, 2600 (2015).

# Development of an epi-detected spontaneous Raman and multiplex CARS optical bench for human skin characterisation

Alice Lemarquand<sup>1</sup>, Philippe Leproux<sup>2</sup>, Nicolas Wilkie-Chancellor<sup>1</sup>, Jean-Yves Le Huérou<sup>1</sup>, Stéphane Serfaty<sup>1</sup>

1. SATIE, Université de Cergy-Pontoise, 5 mail Gay Lussac, F-95000 Neuville-sur-Oise, France

2. XLIM, Université de Limoges, 123 avenue Albert Thomas, F-87060 Limoges, France

As a label free, non-invasive and non-destructive technique, spontaneous Raman spectroscopy is a reference skin characterisation tool for *in vitro* and *in vivo* samples, as well as models [1]. Be it in the form of single spectra, depth concentration profile, or spectral mapping, it enables to investigate skin biochemical composition, lipid conformation and protein structure for cosmetic or dermatological applications [2]. Advantages of Raman spectroscopy have been taken to study challenging issues such as the skin barrier function [3], cutaneous aging [4] and interaction with molecules like hyaluronic acid [5]. Lastly, some studies have also been carried out for medical research and cancerous diagnosis [6]. Regarding Coherent Anti-Stokes Raman Scattering (CARS) for skin study, only imaging has been performed so far. It has been used to follow drug delivery process on porcine skin [7] and the penetration pathways for different substances on human skin [8]. Furthermore, CARS microscopy has been combined with other nonlinear optical techniques for diagnosis [9].

In order to explore the potential of coherent spectroscopy for skin characterisation, we intend to record full CARS spectra. To that end, a multiplex nanosecond-pulsed dual output laser source generates directly the two coherent pump and broadband Stokes beams, that have to be spatially overlapped and temporally synchronised [10]. Hence, an instrumental optical bench enabling both spontaneous Raman and multiplex CARS is being developed. The same detection system can be used respectively for the 633 nm spontaneous Raman Stokes shifts and the 1064 pumped CARS Anti-Stokes shifts. The acquisition of spectra from 400 to 4000  $\text{cm}^{-1}$  with a spectral resolution of 0,1 nm should be achieved. Two removable mirrors are installed to switch from one set-up to the other. The focus on samples is made thanks to an epi-detected configuration microscope, which has also been equipped with a motorised stage to further making possible to measure spectral mapping.

Besides assessing the photonic efficiency improvement by using nonlinear optics, this instrumental optical bench will enable to correlate the skin CARS spectra to the numerous studies already existing of spontaneous Raman spectroscopy on skin samples. Once the parameters will be optimised to get non-destructive measurements on *in vitro* samples, spontaneous Raman and CARS signatures from the different cutaneous layers will be compared.

## References

- [1] L. Franzen and M. Windbergs, "Applications of Raman spectroscopy in skin research - From skin physiology and diagnosis up to risk assessment and dermal drug delivery," *Advanced Drug Delivery Reviews*, 2015.
- [2] C. Choe, J. Schleusener, J. Lademann, and M. E. Darvin, "Keratin-water-NMF interaction as a three layer model in the human stratum corneum using *in vivo* confocal Raman microscopy," *Sci. Rep.*, 2017.
- [3] D. Falcone *et al.*, "Microspectroscopic Confocal Raman and Macroscopic Biophysical Measurements in the *in vivo* Assessment of the Skin Barrier: Perspective for Dermatology and Cosmetic Sciences," *Skin Pharmacology and Physiology*, vol. 28, no. 6. pp. 307–317, 2015.
- [4] C. Eklouh-Molinier *et al.*, "In vivo confocal Raman microspectroscopy of the human skin: highlighting of spectral markers associated to aging via a research of correlation between Raman and biometric mechanical measurements," *Anal. Bioanal. Chem.*, 2015.
- [5] M. Essendoubi, C. Gobinet, R. Reynaud, J. F. Angiboust, M. Manfait, and O. Piot, "Human skin penetration of hyaluronic acid of different molecular weights as probed by Raman spectroscopy," *Ski. Res. Technol.*, 2016.
- [6] C. a Lieber, S. K. Majumder, D. Billheimer, D. L. Ellis, and A. Mahadevan-Jansen, "Raman microspectroscopy for skin cancer detection *in vitro*," *J. Biomed. Opt.*, 2012.
- [7] N. A. Belsey *et al.*, "Evaluation of drug delivery to intact and porated skin by coherent Raman scattering and fluorescence microscopies," *J. Control. Release*, 2014.
- [8] X. Chen, S. Grégoire, F. Formanek, J. B. Galey, and H. Rigneault, "Quantitative 3D molecular cutaneous absorption in human skin using label free nonlinear microscopy," *J. Control. Release*, 2015.
- [9] S. Heuke *et al.*, "Detection and Discrimination of Non-Melanoma Skin Cancer by Multimodal Imaging," *Healthcare*, vol. 1, no. 1, pp. 64–83, 2013.
- [10] P. Leproux, V. Couderc, A. De Angelis, M. Okuno, H. Kano, and H. Hamaguchi, "New opportunities offered by compact sub-nanosecond supercontinuum sources in ultra-broadband multiplex CARS microspectroscopy," *J. Raman Spectrosc.*, 2011.

# Measurements of Pressure Broadening and Shifting of the First Rotational Lines of HD in the HD-He Collisional System by Stimulated Raman Spectroscopy.

R. Z. Martínez and D. Bermejo

Instituto de Estructura de la Materia, IEM-CSIC. Serrano 123, 28006 Madrid, Spain

We present measurements of the broadenings and shifts experienced by the first lines of the rotational Raman spectrum of HD,  $S(0)$ ,  $S(1)$  and  $S(2)$ , when He is used as a perturber at different partial pressures. The measurements were conducted at three different temperatures (77, 195 and 300 K).

The experiments were performed using the technique of *quasi-cw* Stimulated Raman spectroscopy, which provides an excellent compromise between the sensitivity and the high resolution necessary to observe these lineshape effects. More specifically, in the configuration used for these experiments [1], the resolution of our setup is limited by the apparatus function, which has a nearly gaussian shape and a width of the order of  $1.8 \times 10^{-3} \text{ cm}^{-1}$  (FWHM). In order to reach the frequency region of the rotational transitions (267, 443 and  $536 \text{ cm}^{-1}$  respectively for  $S(0)$ ,  $S(1)$  and  $S(2)$ ) two single-mode ring dye lasers were used to generate the probe and pump beams.

The measurement procedure consisted, for each spectral line and temperature, in the acquisition of several scans of the line at increasing partial pressures of the perturber molecule. Typically sample pressures were kept under 5 mbar, while He partial pressures were varied between 50 and 900 mbar, depending on the line and temperature.

The obtained line profiles have been analyzed by fitting them with Voigt profiles, which account for the convolution of the apparatus function (gaussian), Doppler width (gaussian) and collisional width (lorentzian). This has allowed the extraction of the collisional contributions to the widths, which, when fitted with an appropriate model (either a linear one or a more complex dependence in the cases where Dicke narrowing is present), have provided us with values for the collisional broadening coefficients.

The collisional shift coefficients have also been obtained in a similar way from the values of the line frequencies at each pressure.

Figure 1 depicts one of the fits used to obtain the collisional broadening coefficient, in this case with a nonlinear model that takes into account the effect of Dicke narrowing.

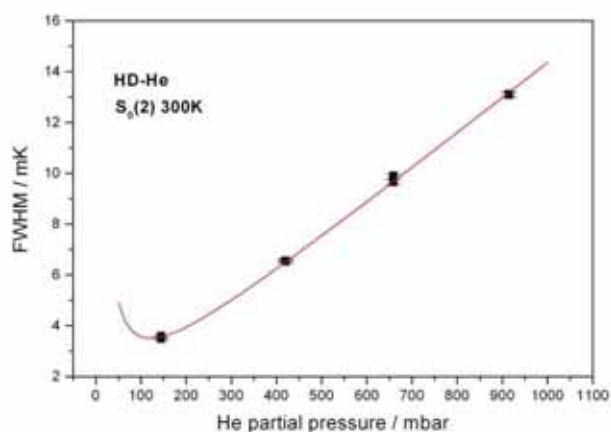


Fig. 1 Nonlinear fit of the experimentally determined collisional widths of the  $S(2)$  line at 300 K.

We are currently in the process of comparing our collisional broadening and shift coefficients with those obtained from an *ab initio* quantum scattering calculation [2].

## References

- [1] R. Z. Martínez, D. Bermejo, F. Thibault and P. Wcislo, "Testing the *ab initio* quantum-scattering calculations for the  $D_2$ -He benchmark system with stimulated Raman spectroscopy", *J. Raman Spectrosc.* **49**, 1339 (2018).
- [2] R.Z. Martínez, D. Bermejo, F. Thibault and P. Wcislo, *in preparation*.

# Determination of Raman linewidths from picosecond rotational CARS spectroscopy

Christian Meißner<sup>1,2</sup>, Jonas Hölzer<sup>1,2</sup>, Thomas Seeger<sup>1,2</sup>

1. University of Siegen, Paul-Bonatz-Str. 9-11, 57076 Siegen, Germany

2. Center for Sensor Systems (ZESS), University of Siegen, Paul-Bonatz-Str. 9-11, 57076 Siegen, Germany

Laser-based measurement techniques such as coherent anti-Stokes Raman spectroscopy (CARS) are well established tools for combustion diagnostics. A main advantage of pure rotational coherent anti-Stokes Raman spectroscopy (RCARS) is the possibility to probe several combustion relevant species from one single-shot RCARS spectrum. Therefore a broadband dye laser is used for the pump and Stokes beams to probe S-branch rotational Raman transitions. The population density and therewith the transition probability follows Boltzmann's distribution. The resulting strong temperature dependence of the RCARS signal's spectral shape allows to detect even small changes in temperature with high accuracy. These and other advantages of the RCARS technique lead to several technical relevant applications which have been presented in the last years [1,2].

For CARS temperature and species concentration determination experimental spectra are usually compared to a library of calculated spectra. The calculation of theoretical CARS spectra is commonly done by empirical scaling law models like the modified energy gap law (MEG) [3]. For accurate evaluation of the CARS signal these scaling law models require precise knowledge of molecule data such as the Raman linewidth. Since the Raman linewidth depends critically on the rotational quantum number  $J$  [4] and the major collision partners which are present in the probe volume [5], the linewidth has to be determined depending on these parameters and even temperature and pressure. Previous studies showed that collision partners like  $H_2$  or  $H_2O$  have a strong influence on the RCARS temperature evaluation, when using inappropriate S-branch Raman linewidth [5,6].

Linewidths determination can be done by measuring coherence decays and subsequently calculating Raman linewidths from the coherence decay time constants [4,7,8]. Therefore picosecond laser pulses are required, due to the picosecond coherence lifetimes of the excited states of small molecules like  $N_2$  and  $O_2$  [4,7].

Since  $N_2$  is often the first choice as probe molecule for RCARS in air-fed combustion processes and  $O_2$  can be a major collision partner it is close to investigate the effect of  $N_2$ - $O_2$  collisions on the S-branch  $N_2$  Raman linewidth. Until now, only the effect of  $N_2$  perturbing  $O_2$  Q-branch Raman linewidths has been investigated [9]. Taking the influence of  $O_2$  on  $N_2$  S-branch Raman linewidths into account and including the new linewidths into the scaling law models may improve the accuracy of RCARS thermometry when probing nitrogen.

## References

- [1] S. P. Kearney, and D. R. Gueldenbecher, "Temperature measurements in metalized propellant combustion using hybrid fs/ps coherent anti-Stokes Raman scattering," *Appl. Opt.* **55**, 4958 (2016).
- [2] S. R. Engel, A. F. Koegler, Y. Gao, D. Kilian, M. Voigt, T. Seeger, W. Peukert and A. Leipertz, "Gas phase temperature measurements in the liquid and particle regime of a flame spray pyrolysis process using  $O_2$ -based pure rotational coherent anti-Stokes Raman scattering," *Appl. Opt.* **51**, 6063 (2012).
- [3] L. A. Rahn, and R. E. Palmer, "Studies of nitrogen self-broadening at high temperature with inverse Raman spectroscopy," *JOSA B* **3**, 1164 (1986).
- [4] C. J. Kliewer, A. Bohlin, E. Nordström, B. D. Patterson, P.-E. Bengtsson, and T. B. Settersten, "Time-domain measurements of S-branch  $N_2$ - $N_2$  Raman linewidths using picosecond pure rotational coherent anti-Stokes Raman spectroscopy," *Appl. Phys. B* **108**, 419 (2012).
- [5] A. Bohlin, and P.-E. Bengtsson, "Rotational CARS thermometry in diffusion flames: On the influence of nitrogen spectral line-broadening by  $CH_4$  and  $H_2$ ," *Proc. Combust. Inst.* **33**, 823 (2011).
- [6] A. Bohlin, E. Nordström, H. Carlsson, X.-S. Bai, and P.-E. Bengtsson, "Pure rotational CARS measurements of temperature and relative  $O_2$ -concentration in a low swirl turbulent premixed flame," *Proc. Combust. Inst.* **34**, 3629 (2013).
- [7] Y. Gao, A. Bohlin, T. Seeger, P.-E. Bengtsson, and C. J. Kliewer, "In situ determination of  $N_2$  broadening coefficients in flames for rotational CARS thermometry," *Proc. Combust. Inst.* **34**, 3637 (2013).
- [8] C. J. Kliewer, Y. Gao, T. Seeger, J. Kiefer, B. D. Patterson, and T. B. Settersten, "Picosecond time-resolved pure-rotational coherent anti-Stokes Raman spectroscopy in sooting flames," *Proc. Combust. Inst.* **33**, 831 (2011).
- [9] G. Millot, R. Saint-Loup, J. Santos, R. Chauv, H. Berger, and J. Bonamy, "Collisional effects in the stimulated Raman Q branch of  $O_2$  and  $O_2$ - $N_2$ ," *J. Chem. Phys.* **96**, 961 (1992).

# Coherent Raman micro-spectrometry

Vasyl Shynkar<sup>1</sup>, Sébastien Vergnole<sup>1</sup>, Sébastien Legendre<sup>1</sup>, Catalina David<sup>1</sup>, Alberto Lombardini<sup>2</sup>, Hervé Rigneault<sup>2</sup>, Philippe De Bettignies<sup>1</sup>

1. HORIBA FRANCE, Villeneuve d'Ascq, Nord, France

2. Aix-Marseille Univ, CNRS, Centrale Marseille, Institut Fresnel, Marseille, France

Last decades have seen the blossom of coherent Raman spectroscopy and microscopy [1] due to research performed in this field and to tremendous progress done in the photonics technologies development, namely building new pulsed lasers and highly sensitive detectors. From application point of view, more and more attention is brought to coherent Raman microscopy (CRM) [2, 3], a technique complementary to classical (spontaneous) Raman micro-spectrometry. CRM permits to overcome the main drawbacks of classical Raman microscopy. One of them is the extremely low Raman scattering cross-section, of about  $10^{-30}$  cm<sup>2</sup>, which requires long exposure time to construct a Raman image, which makes observation of living or moving specimen difficult. Another drawback of Raman scattering is that observable samples are limited to non-fluorescent samples since strong fluorescence emission typically overlaps the weak Raman signal. All these drawbacks are solved using CRM that provides a coherent excitation of all the vibrational bonds, resulting in a  $10^6$  enhancement of the Raman signal. Additionally, CRM provides a 3D sectioning capability with a spatial resolution below 1  $\mu$ m.

One of the CRM process is coherent anti-Stokes Raman scattering (CARS) that can be implemented in a multiplex scheme known as M-CARS using a narrow band and a broadband lasers pulses [4]. This scheme permits to build versatile Raman imaging systems that give access to the full vibration spectral range. The advantage is significant especially in the observation of living sample, where molecules distribution and conditions change with time to express biological activities. M-CARS permits also to observe fluorescent samples because light detected in CARS microscope has a shorter wavelength than that of the incident light. We demonstrate herein the combination of M-CARS spectrometer with near-field atomic force microscope which permits further enhance the spatial resolution up to 10 nm range.

The other CRM process is stimulated Raman scattering (SRS) that has additional advantages over CARS such as to be free of a non-resonant background that is inherent to CARS. SRS has proved to be useful for biomedical imaging where water represents the predominant source of CARS non-resonant background. The absence of the non-resonant background makes also the SRS spectra identical to Raman spectra that ease the interpretation and permits to use the existing data bases for molecular fingerprints.

HORIBA FRANCE is building custom-made CRM systems based on HORIBA basic micro-spectrometers and proposes CARS and SRS micro-spectrometers. Herein we present our devices built for M-CARS and SRS detection. In addition, we present a novel technology called Stimulated Raman Gain and Opposite Loss Detection (SRGOLD) [5] that can be integrated into our SRS systems to further increase the SRS signal and reduce the noise (Figure).

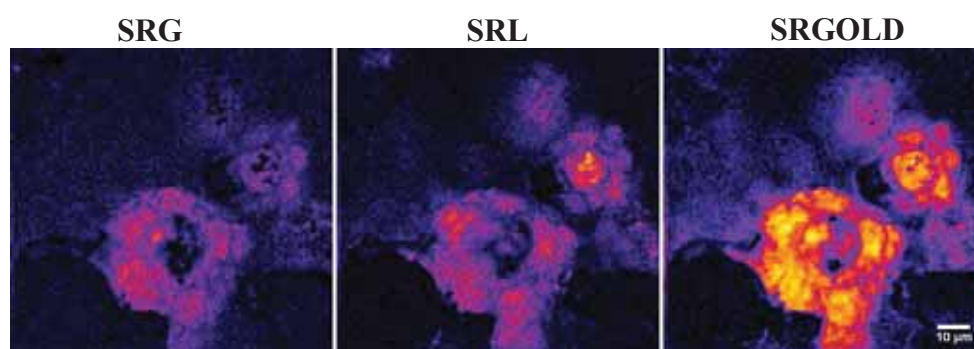


**Figure** The adipocytes images obtained in different modes of stimulated Raman scattering detection at 1440 cm<sup>-1</sup>: SRG for stimulated Raman gain, SRL for stimulated Raman loss and SRGOLD (the noise is reduced, and the signal is enhanced by a factor of two).

## References

- [1] Arnaud Zoubir, *Raman Imaging*, (Springer – Verlag, Berlin, 2012).
- [2] Ji-Xin Cheng, Xiaoliang Sunney Xie, *Coherent Raman Scattering Microscopy*, (Taylor & Francis Group, Boca Raton, 2013).
- [3] H. Rigneault, and P. Berto, "Tutorial: Coherent Raman light matter interaction processes," *APL Photonics* **3**, 091101 (2018).
- [4] E. Capitaine, N. O. Moussa, C. Louot, S. M. Bardet, H. Kano, L. Duponchel, P. Lévêque, V. Couderc, and P. Leproux, "Fast epi-detected broadband multiplex CARS and SHG imaging of mouse skull cells", *Biomed. Opt. Express* **9**, 245 (2018).
- [5] P. Berto, E. R. Andresen, and H. Rigneault, "Background-Free Stimulated Raman Spectroscopy and Microscopy", *Phys. Rev. Lett.* **112**, 053905 (2014).

# Lipid droplets formation in endothelial cells and hepatocytes studied by means of Raman and CARS microscopy

Ewelina Szafraniec<sup>1,2</sup>, Aleksandra Dorosz<sup>1,2</sup>, Marko Rodewald<sup>3</sup>, Tobias Meyer<sup>4</sup>, Stefan Chlopicki<sup>5,2</sup>, Michael Schmitt<sup>3</sup>, Jürgen Popp<sup>3,4</sup>, Malgorzata Baranska<sup>1,2</sup>

1. Faculty of Chemistry, Jagiellonian University, Gronostajowa 3, 30-387 Krakow, Poland

2. Jagiellonian Centre for Experimental Therapeutics (JCET), Jagiellonian University, Bobrzynskiego 14, 30-348 Krakow, Poland

3. Institute of Physical Chemistry (IPC) and Abbe Center of Photonics(ACP), Friedrich-Schiller-University, Helmholtzweg 4, Jena, Germany

4. Leibniz Institute of Photonic Technology e.V. Jena Albert-Einstein-Str. 9, Jena, Germany

5. Chair of Pharmacology, Jagiellonian University Medical College, Grzegorzeczka 16, 31-531 Krakow, Poland

Lipid droplets (LDs) are now understood as being complex and dynamic organelles, playing a central role in the regulation of lipid homeostasis. LDs usually serve as a storage of energy substrates for membrane synthesis and production of essential lipid-derived molecules such as lipoproteins or hormones. However, LDs found e.g. in leukocytes, eosinophils and neutrophils play also a role as intracellular sites for lipids further used in inflammatory responses. In this context, recent studies showed, that LDs are formed also in endothelial cells as a result of fatty acid stimulation as well as the response to an inflammatory agent (TNF- $\alpha$ ), however their exact role in the endothelium is still not well understood.[1,2]

Next to adipose tissue, liver has the greatest capacity to store lipids in LDs. In basal conditions, hepatocytes accumulate only small amounts of triacylglycerols in LDs, however as a result of an unhealthy life style, the liver can hold massive amounts of lipids that is described as liver steatosis. Noteworthy, the main source of the hepatic lipids originates from fatty acids circulating in the bloodstream. Since the endothelium is in constant contact with blood, it is obvious that, high concentration of lipids also affects the endothelial cells lining the liver sinusoids – the capillary bed of the liver. Excess lipids both in the circulation and at the tissue level contribute to endothelial dysfunction that underlies much of the pathophysiology of both metabolic syndrome, including obesity, diabetes and their cardiovascular complications. Therefore, it is desirable to gain knowledge of how endothelial cells handle the overabundance of lipids, that is closely related to formation of LDs.

We previously reported the characterization of LDs of different size and origin comparing the LDs formed after stimulation of aortic endothelial cells with arachidonic acid, with hepatocytes in a steatotic liver.[3] Here, we present the first results of a study aiming to characterize the formation of LDs in sinusoidal endothelial cells and hepatocytes (TSEC and AML-12 cell line, respectively) as a response to the identical conditions, namely, the stimulation with oleic and palmitic acids. In the next step we investigated the changes in the composition of LDs associated with its metabolism and degradation. These goals are addressed by the utilizing the full chemical specificity of Raman spectroscopy, and the high-speed of single band CARS imaging at the CH<sub>2</sub> Raman resonance at 2850 cm<sup>-1</sup> (Fig. 1). In doing so, we are able to characterize the diversity in the formation of LDs in endothelium as compared to hepatocytes. Moreover, we characterized the differences in the formation of LDs and degradation manner with respect to used fatty acid.

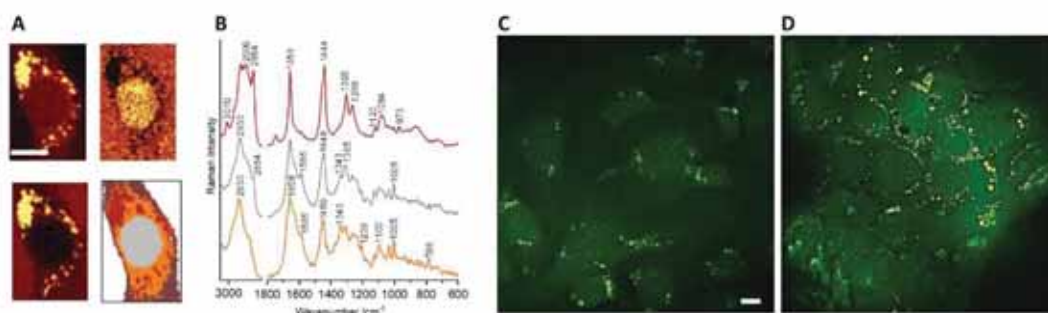


**Fig. 1** Raman images and *k-means* cluster analysis false color image of TSEC cell stimulated with oleic acid (A) together with corresponding Raman spectra (B) and CARS images of TSEC (C) and AML-12 cells (D) stimulated with oleic acid recorded at the CH<sub>2</sub> stretch vibration at 2850 cm<sup>-1</sup> indicative for lipids. Scale bar equals 10 μm.

This work was supported by Polish National Science Centre grant No. UMO-2016/22/M/ST4/00150.

## References

- [1] A. Kuo, M. Y. Lee, W. C. Sessa, "Lipid droplet biogenesis and function in the endothelium", *Circ. Res.* **120**, 1289-1297 (2017)
- [2] K. Czamara, K. Majzner, A. Selmi, M. Baranska, Y. Ozaki, A. Kaczor, "Unsaturated lipid bodies as a hallmark of inflammation studied by Raman 2D and 3D microscopy", *Sci. Rep.*, **7**, 40889 (2017)
- [3] K. Majzner, K. Kochan, N. Kachamakova-Trojanowska, E. Maslak, S. Chlopicki, M. Baranska, "Raman imaging providing insights into chemical composition of lipid droplets of different size and origin: in hepatocytes and endothelium", *Anal. Chem.* **86**, 6666-74 (2014)

# Peculiarities of Micro Raman Spectra of Blood Neutrophils Transformed during NETosis as a Possible Marker of Sepsis Mortality

G.M. Arzumanyan<sup>1</sup>, A.S. Gur'ev<sup>2</sup>, D.E. Kravtsunova<sup>3</sup>, K. Z. Mamatkulov<sup>1</sup>, A.S. Marchenko<sup>1</sup>,  
K.A. Vereshchagin<sup>4</sup>, A.Yu. Volkov<sup>2</sup>.

1. Joint Institute for Nuclear Research, Joliot-Curie str. 6, 141980 Dubna, Moscow Region, Russia

2. Medtechnopark LTD, Moscow, Russian Federation

3. Moscow Chemical Lyceum

4. A.M. Prokhorov General Physics Institute, Russian Academy of Sciences, Vavilov str. 38, 119991 Moscow, Russia

Recently there is an increasing interest in complex subcellular structures in immunology that implement important immune functions. Control over the formation of such structures is an important bio-medical task. Examples of such structures are neutrophil extracellular traps (NETs) arising in the life cycle of human neutrophils as a result of NETosis [1]. Neutrophil extracellular traps are composite DNA complexes and neutrophil proteins transformed in the NETosis process.

The search for standard methods for assessing the level of NETotic transformed neutrophils in the blood is going on intensively. These methods can be divided into 2 groups - specific and nonspecific. Recently it was shown that the non-specific method [2] allows one to reliably predict a lethal outcome in septic conditions. Specific methods may be more informative, however, the developed immunological techniques are complex and rarely used in clinical practice. Therefore, the search for a direct specific spectroscopic method for assessing the level of NETotic neutrophils is relevant.

This work is devoted to solving the problem of direct specific detection of NETotic transformed neutrophils components in the blood using micro Raman spectroscopy.

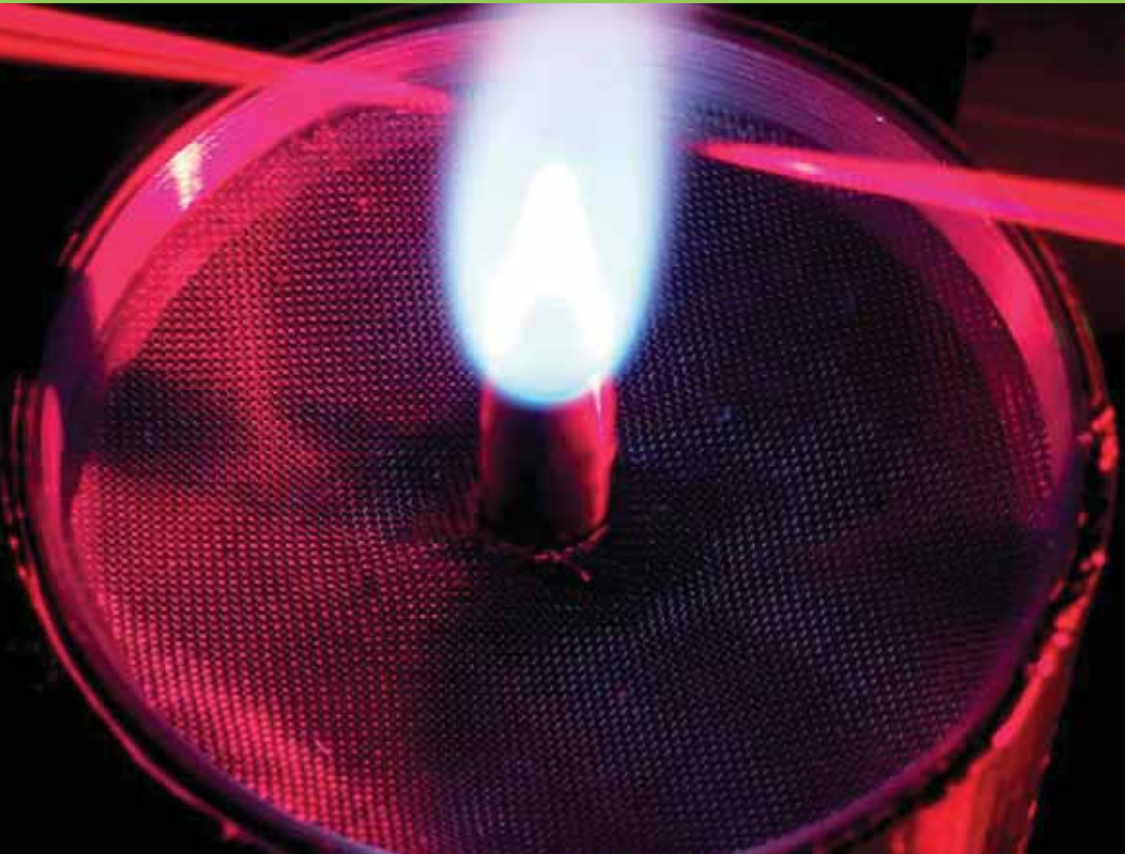
We expect that there are significant differences in the Raman spectra of untransformed and transformed neutrophils, caused by remarkable modifications of the cell contents during the NETotic transformation. A comparison of the micro Raman spectra of neutrophils from the patient's blood with the standard (reference) spectra of neutral and activated neutrophils will make it possible to establish a NETotic transformation at an early stage.

The paper discusses approaches to the construction of neutrophil spectral images (standard spectra) based on the registered micro Raman spectra both with and without subtraction of the luminescent "lining". Based on methods similar to EMSC [3], reference spectra of samples of transformed and untransformed neutrophils are constructed. The features of the spectral images of transformed and untransformed neutrophils are considered. NETosis markers based on the features of low-frequency segments of the Raman spectrum of citrulline are proposed.

## References

- [1]. Boeltz, S., Amini, P., Anders, H. J., Andrade, F. A., Bilyy, R., Chatfield, S., Herrmann, M. "To NET or not to NET: current opinions and state of the science regarding the formation of neutrophil extracellular traps". Cell death and differentiation. (2019).
- [2]. Darya V Mosalskaya, Alexander S Gur'ev, Andrey F Lopatin, "Prognostic value of DNA-traps level in blood smears from patients with sepsis", Intensive Care Medicine Experimental, 6 (Suppl 1), p. 7-8 (2018).
- [3]. Nils Kristian Afseth, Achim Kohler. "Extended multiplicative signal correction in vibrational spectroscopy, a tutorial". Chemometrics and Intelligent Laboratory Systems, 117, pp.92-99 (2012).





# List of participants

ABDELMONEM Ahmed  
Karlsruhe Institute of Technology (KIT)  
ahmed.abdelmonem@kit.edu

ALBERT Anne  
Opton Laser International  
contact@optonlaser.com

ATTAL-TRETOU Brigitte  
DPHY  
btretout@onera.fr

BARANSKA Malgorzata  
Raman Imaging Group/Faculty of Chemistry  
baranska@chemia.uj.edu.pl

BARROS Joanna  
DPHY  
joanna.barros-ext@onera.fr

BARVIAU Benoît  
CORIA - UMR 6614  
benoit.barviau@coria.fr

BAUDISCH Matthias  
APE Angewandte Physik &  
matthias\_baudisch@ape-berlin.de

BAZ Assaad  
THORLAB S  
abaz@thorlabs.com

BEAUREPAIRE Emmanuel  
Lab for optics and biosciences  
emmanuel.beaurepaire@polytechnique.edu

BECHEKER Rezki  
CORIA - UMR 6614  
becheker@coria.fr

BENGTSSON Per-Erik  
Combustion Physics  
per-erik.bengtsson@forbrf.lth.se

BERMEJO Dionisio  
Instituto de Estructura de la Materia (IEM)  
dbermejo@iem.cfmac.csic.es

BERNHARD Philippe  
Teledyne - Princeton Instruments  
pbernhard@princetoninstruments.com

BERTHILIER Frédéric  
COHERENT  
Frederic.Berthillier@coherent.com

BOHLIN Alexis  
Faculty of Aerospace Engineering  
G.A.Bohlin@tudelft.nl

BOIVIN Gilles  
MICRO-CONTROLE SPECTRA-PHYSICS (NEWPORT MKS)  
gilles.boivin@newport.com

BOOD Joakim  
Div . of Combustion Physics  
joakim.bood@forbrf.lth.se

BRINKMANN Maximilian  
Institute of Applied Physics, University of Muenster  
brinkmannmax@wwu.de

BUCKUP Tiago  
Universität Heidelberg  
tiago.buckup@pci.uni-heidelberg.de

DING Pengji  
Division of Combustion  
pengji.ding@forbrf.lth.se

DOROSZ Aleksandra  
Raman Imaging Group  
aleksandra.dorosz@doctoral.uj.edu.pl

DUBROUIL Antoine  
Femto Easy  
info@femtoeasy.eu

DURAND Aurelia  
Amplitude  
aurelia.durand@amplitude-laser.com

FALCONIERI Mauro  
FSN-TECFIS  
mauro.falconieri@enea.it

FALLNICH Carsten  
Optical Technologies  
fallnich@wwu.de

FLAQUIERE Guy  
MICRO-CONTROLE SPECTRA-PHYSICS (NEWPORT MKS)  
guy.flaquiere@Spectra-Physics.com

FLEURY Guillaume  
Centre for Surface Chemistry and Catalysis  
guillaume.fleury@kuleuven.be

FRADET Florence  
CORIA - UMR 6614  
florence.fradet@coria.fr

GILLIOT Pierre  
IPCMS  
pierre.gilliot@ipcms.unistra.fr

GODIN Thomas  
CORIA - UMR 6614  
thomas.godin@coria.fr

GOZHYK Iryna  
Surface du Verre et Interfaces UMR125  
iryna.gozhyk@saint-gobain.com

GRISCH Frédéric  
CORIA - UMR 6614  
frederic.grisch@coria.fr

HEUKE Sandro  
Institut Fresnel  
sandro.heuke@fresnel.fr

HIDEUR Ammar  
CORIA - UMR 6614  
ammar.hideur@coria.fr

HOELZER Jonas Immanuel  
Engineering Thermodynamics  
jonas.hoelzer@uni-siegen.de

HOSSEINNIA Ali  
Combustion Physics  
ali.hosseinnia@forbrf.lth.se

IDLAHCEN Saïd  
CORIA - UMR 6614  
idlahcen@coria.fr

JOSSENT Mathieu  
NOVAE  
m.jossent@novae-laser.com

JOUBERT Pierre  
Institut UTINAM  
pierre.joubert@univ-fcomte.fr

KOZLOV DIMITRII  
Optical spectroscopy  
dnk@kapella.gpi.ru

KULATILAKA Waruna  
Texas A&M University  
waruna.kulatilaka@tamu.edu

KUMAR Vikas  
Fakultät für Chemie (PC)  
vikas.kumar@uni-due.de

LEGROS Sylvain  
CORIA - UMR 6614  
sylvain.legros@coria.fr

LEMARQUAND Alice  
SATIE  
alice.lemarquand@u-cergy.fr

LETAILLEUR Christophe  
CORIA - UMR 6614  
christophe.letailleur@coria.fr

LIU Hanqin  
Ozeki Lab  
liuhanqin.elec@gmail.com

MARROCCO Michele  
DTE-PCU  
michele.marrocco@enea.it

MARTINEZ-TORRES Raul  
Departemento de Física Molecular  
raul@iem.cfmac.csic.es

MEISSNER Christian  
Engineering Thermodynamics  
christian.meissner@uni-siegen.de

MERLA Caterina  
ENEA  
caterina.merla@enea.it

MILLE Bruno  
CORIA - UMR 6614  
bruno.mille@coria.fr

NAFA Malik  
LENS / Non-linear optics and precision spectroscopy  
nafa@lens.unifi.it

OBRAZTSOVA Elena  
Nanomaterials Spectroscopy Laboratory  
elobr@mail.ru

POLLI Dario  
VIBRA lab - Physics Department  
dario.polli@polimi.it

POTMA Eric  
University of California Irvine  
epotma@uci.edu

RADI Peter  
Photon Science Department  
peter.radi@psi.ch

RAN Yang  
Institut für Angewandte Physik  
yang.ran@uni-jena.de

ROEFFAERS Maarten  
Centre for Surface Chemistry and Catalysis  
maarten.roeffaers@kuleuven.be

RUCHKINA Maria  
Combustion Physics  
maria.ruchkina@forbrf.lth.se

SANTAGATA Rosa  
DPHY  
rosa.santagata@onera.fr

SCHERMAN Michael  
DPHY/SLM  
michael.scherman@onera.fr

SEDARSKY David  
Chalmers University of Technology  
sedarsky@chalmers.se

SEEGER Thomas  
Technische Thermodynamik  
thomas.seeger@uni-siegen.de

SHOU Jingwen  
Ozeki Lab  
shou\_jingwen@outlook.com

SHYNKAR Vasyl  
HORIBA R & amp  
vasyl.shynkar@horiba.com

SZAFRANIEC Ewelina  
Raman Imaging Group  
ewelina.szafraniec@uj.edu.pl

SZMYGEL Ester  
Laboratoire Interdisciplinaire Carnot de Bourgogne  
info@femtoeasy.eu

TANAIS Jocelyn  
ACAL BFI FRANCE  
anne.stiegler@acalbfi.fr

TAPIE Jean-Luc  
Coherent  
jean-luc.tapie@coherent.com

VELLA Angela  
Groupe de Physique des Matériaux  
angela.vella@univ-rouen.fr

VERESHCHAGIN Alexey  
Photonics Dpt.,  
iofan.fe@mail.ru

VERESHCHAGIN Konstantin  
Department of Optical Spectroscopy  
stin57@mail.ru

VERGNOLE Sebastien  
HORIBA  
sebastien.vergnole@horiba.com

WUERTHWEIN Thomas  
Institute of Applied Physics  
t.wuerthwein@uni-muenster.de

XAVIER Pradip  
CORIA - UMR 6614  
xavierp@coria.fr

ZHANG Haisu  
Laboratoire Interdisciplinaire Carnot de Bourgogne  
Haisu.Zhang@u-bourgogne.fr

ZHOU Zhen  
CORIA - UMR 6614  
zhen.zhou@coria.fr



Under the patronage of



organised by

